

https://researchcommons.waikato.ac.nz/

Research Commons at the University of Waikato

Copyright Statement:

The digital copy of this thesis is protected by the Copyright Act 1994 (New Zealand).

The thesis may be consulted by you, provided you comply with the provisions of the Act and the following conditions of use:

- Any use you make of these documents or images must be for research or private study purposes only, and you may not make them available to any other person.
- Authors control the copyright of their thesis. You will recognise the author's right to be identified as the author of the thesis, and due acknowledgement will be made to the author where appropriate.
- You will obtain the author's permission before publishing any material from the thesis.

Structural performance of cold-formed steel wall systems incorporating sustainable composite sheathing

Kang Huang



Supervised by

Dr Ray Hudd

Associate Prof. Krishanu Roy

Prof. James B.P. Lim

A thesis submitted in fulfilment of the requirements for the degree of Doctor of Philosophy in Engineering, The University of Waikato, 2026

Abstract

Cold-formed steel (CFS) wall systems are widely adopted in low- and mid-rise buildings due to their high strength-to-weight ratio and construction efficiency. The structural behaviour of these systems is governed by the interaction between thin-walled steel framing, sheathing materials and mechanical fasteners. In recent years, sustainable composite boards manufactured from recycled packaging and plastics—commercially available in New Zealand under the name SaveBOARD—have been proposed as alternative sheathing materials; however, their structural performance in load-bearing CFS walls has not been systematically investigated in peer-reviewed research.

This thesis presents a multi-scale experimental investigation into the structural performance of CFS wall systems incorporating sustainable composite sheathing (SaveBOARD). The research integrates material characterisation, connection-level testing, full-height single-stud wall subassembly tests under axial compression, and full-scale wall tests under quasi-static cyclic lateral loading. Key parameters include sheathing type, stud thickness, screw spacing configuration and axial load interaction.

The results demonstrate that sustainable composite boards can provide effective restraint against local and distortional buckling within the tested configurations. In the axial subassembly tests, the gypsum-sheathed specimen increased ultimate axial resistance by 36.8% relative to the bare frame, while the PIL- and EPL-sheathed specimens achieved increases of 36.5% and 27.0%, respectively. Under cyclic loading, the tested composite-sheathed walls exhibited reduced pinching and more stable hysteretic behaviour than the gypsum reference specimens, primarily because the response was governed by progressive bearing deformation at screw connections rather than abrupt brittle panel fracture. Screw spacing is identified as a primary structural parameter, with diminishing returns observed under excessive densification. A stability–connection coupling interpretation is developed to explain the interaction between connection degradation and global wall response.

Overall, the findings support the structural feasibility of using sustainable composite sheathing in CFS wall systems within the tested configurations and provide a mechanistic basis for performance-informed design considerations and future analytical modelling.

Preface

This thesis is submitted to the University of Waikato, New Zealand in fulfilment of the requirement for the degree of Doctor of Philosophy. The work contained in this thesis has not been previously submitted for a degree or diploma in any other higher educational institution. To the best of my knowledge and belief, the thesis contains no material previously published or written by another person except where due reference is made.

Publications

Journals

1. **Huang K.**, Roy K*, Hudd R, Wang W, Lim JBP. Structural behaviour of sustainable composite board and cold-formed steel connections: Experimental study. *Journal of Building Engineering*. 2025; 111:113383. (JCR Q1, Published)

2. **Huang K**, Roy K*, Hudd R, Wang W, Lim JBP. (2025). Axial and cyclic behaviour of cold-formed steel stud walls sheathed with sustainable composite boards. *Engineering Structures*. (JCR Q1, under review)

3. **Huang K**, Roy K*, Hudd R, Wang W, Lim JBP. (2025). Cyclic lateral behaviour of cold-formed steel walls sheathed with sustainable composite boards. *Thin-Walled Structures*. (JCR Q1, under review)

Acknowledgements

I would like to express my sincere gratitude to my **chief supervisor, Dr. Ray Hudd**, for his continuous guidance, patience, and support throughout the course of this research. His thoughtful feedback and constructive suggestions consistently helped me refine my research ideas, improve the quality of my work, and overcome the many challenges encountered during my doctoral journey. I am particularly grateful for the freedom and trust he gave me to explore different research directions while always being available to provide guidance when needed. His commitment to academic excellence and rigorous approach to research have had a profound influence on my development as an independent researcher. Beyond his academic supervision, his understanding, encouragement, and support during difficult periods gave me the confidence and motivation to continue moving forward.

I am also deeply grateful to my other supervisor **Associate Prof. Krishanu Roy**, for his close and continuous involvement in the supervision of this work. His hands-on guidance, day-to-day supervision, detailed technical insights, constructive feedback, and consistent engagement, particularly in designing the experimental programme and interpreting the results were central to the development and strengthening of this thesis. His technical insight, support in securing funding, and instrumental role in organising the experimental facilities, test rig, and materials were fundamental to the successful execution of this research. In addition, his rigorous analytical approach, and exceptional attention to detail have significantly strengthened the quality, depth, and overall rigour of this work.

My sincere thanks are extended to **Prof. James B. P. Lim** for his guidance, academic encouragement, and valuable comments during different stages of this research, which helped to improve both the quality and clarity of the thesis.

I would also like to acknowledge **SaveBoard Ltd., Hamilton, New Zealand**, and **Mr. Paul Charteris** for their generous provision of materials and practical support, which made the experimental programme possible.

Finally, I would like to sincerely thank my fellow postgraduate students and the technical staff of the laboratory at the **University of Waikato** for their invaluable assistance during specimen preparation and testing.

Declaration of Gen AI

GenAI tools were used to assist with language editing, including grammar and improvements to writing clarity and style. All research ideas, original drafting, design, experimental work, data analysis, interpretation of results, and conclusions are the author's own. All GenAI outputs were critically reviewed, verified, and revised by the author to ensure they accurately reflected the intended meaning and the evidence presented in this thesis.

Table of contents

Chapter 1 Background 1
1.1. Cold-formed steel wall systems in structural practice 1
1.2. Shear walls in framed structures: timber and CFS systems 4
1.3. Seismic and wind performance requirements of CFS wall systems 6
1.4. Sheathing–frame interaction and connection mechanics 7
1.4.1. Local connection behaviour 7
1.4.2. Influence of screw spacing and detailing 8
1.4.3. Sheathing restraint and axial–lateral coupling 9
1.4.4. Material-dependent failure hierarchy 9
1.5. Sustainable composite boards in New Zealand: the case of SaveBOARD 10
1.5.1. Product description and material characteristics 10
1.5.2. Structural implications and research gap 13
1.6. Identified knowledge gaps and research questions 14
1.6.1. Established knowledge 14
1.6.2. Limitations in current knowledge 15
1.6.3. Research gap 16
1.6.4. Research questions 16
1.7. Chapter summary 18
Chapter 2 Research objectives and methodological framework 20
2.1. Research philosophy and approach 20
2.2. Overall research structure 21
2.3. Material characterisation 22
2.3.1. CFS section 23
2.3.2. Sheathing materials 24
2.4. Connection behaviour investigation 25
2.5. Wall-level axial behaviour 25
2.6. Wall-level cyclic behaviour 26
2.7. Summary of experimental details and data reduction 28
2.8. Experimental matrix and variable isolation strategy 31
2.9. Numerical modelling methodology and scope 31
2.9.1. Modelling objective 31
2.9.2. Geometry and element formulation 32
2.9.3. CFS material properties 33

2.9.4. SaveBOARD material model 33
2.9.5. Damage representation 34
2.9.6. Contact formulation 35
2.9.7. Boundary conditions and loading 35
2.9.8. Mesh sensitivity and numerical convergence 36
2.9.9. Numerical outcome and limitations 36
2.10. Analytical interpretation and synthesis 37
2.11. Link between research questions and thesis chapters 38
2.12. Chapter summary 38
Chapter 3 Local in-plane behaviour of screw connections between SaveBOARD and CFS members 40
3.1. Role of connection behaviour in sheathed CFS wall systems 40
3.2. Experimental programme and specimen configuration 41
3.2.1. Test setup 42
3.2.2. Materials and specimen details 43
3.2.3. Fastener specification 44
3.2.4. Loading protocol and instrumentation 46
3.3. Experimental results and failure mechanisms 47
3.3.1. Load–displacement behaviour 47
3.3.2. Ultimate strength and stiffness comparison 48
3.3.3. Failure modes 50
3.3.4. Influence of edge distance 51
3.4. Analytical interpretation of connection strength 52
3.4.1. Bearing-dominated strength mechanism 52
3.4.2. Post-peak behaviour and progressive crushing 53
3.4.3. Edge distance sensitivity 54
3.4.4. Implications for wall-level behaviour 55
3.4.5. Practical edge distance implications and friction effects 55
3.5. Chapter summary 58
Chapter 4 Axial compression behaviour of SaveBOARD-sheathed CFS walls 60
4.1. Role of sheathing in axial stability of CFS walls 60
4.2. Experimental programme and specimen matrix 61
4.2.1. Specimen configuration 61
4.2.2. Sheathing types 63

4.2.3. Framing thickness 63
4.2.4. Loading arrangement and boundary conditions 64
4.2.5. Instrumentation 65
4.3. Axial load–displacement behaviour 65
4.3.1. Comparison with bare frame 66
4.3.2. Influence of sheathing type 68
4.3.3. Effect of stud thickness 69
4.4. Buckling mode and composite restraint mechanism 70
4.4.1. Bare frame behaviour 75
4.4.2. Sheathing-restrained behaviour 75
4.4.3. Interaction between connection stiffness and stability 76
4.4.4. Implications for design 76
4.5. Structural interpretation and effectiveness of SaveBOARD sheathing 77
4.6. Chapter summary 79
Chapter 5 Cyclic lateral behaviour and axial–cyclic interaction of SaveBOARD-sheathed CFS walls 81
5.1. Role of connection mechanics in cyclic wall behaviour 81
5.2. Subassembly-level cyclic reference programme 82
5.2.1. Purpose and specimen configuration 82
5.2.2. Loading protocol and data reduction 82
5.2.3. Cyclic response and failure mechanisms 83
5.2.4. Role of the subassembly tests in the full-scale programme 84
5.3. Experimental programme and test matrix 84
5.3.1. Test setup 84
5.3.2. Loading protocol 85
5.3.3. Sheathing and framing variables 86
5.3.4. Screw spacing configuration 86
5.3.5. Axial load condition 87
5.3.6. Instrumentation and data collection 87
5.3.7. EEEP idealisation and characteristic parameters 88
5.4. Hysteretic behaviour and load–displacement response 89
5.4.1. Global hysteresis characteristics 90
5.4.2. Envelope curves 91
5.4.3. Energy dissipation 93

5.5. Influence of screw spacing and densified-edge configuration 94
5.5.1. Effect of uniform screw spacing 94
5.5.2. Densified-edge configuration 96
5.5.3. Mechanistic interpretation 96
5.5.4. Design implications 97
5.6. Axial–cyclic interaction effects 97
5.6.1. Global hysteretic response under combined loading 97
5.6.2. Damage localisation and failure mode transition 98
5.6.3. Mechanistic interpretation 100
5.6.4. Implications for design and seismic performance 100
5.7. Quantitative justification of key cyclic performance statements 101
5.8. Chapter summary 104
Chapter 6 Synthesis of experimental findings and design implications 106
6.1. Introduction 106
6.2. Hierarchy of structural mechanisms governing sheathed CFS walls 108
6.2.1. Connection behaviour as the primary nonlinear trigger 109
6.2.2. Sheathing restraint as axial stability modifier 110
6.2.3. Framing slenderness as amplifier 110
6.2.4. Unified hierarchical model 111
6.3. Stability–connection coupling mechanism 112
6.3.1. Axial restraint depends on connection rotational stiffness 112
6.3.2. Cyclic loading progressively reduces rotational stiffness 113
6.3.3. Coupling under combined axial and cyclic loading 114
6.3.4. Unified coupling interpretation 115
6.4. Normalised performance and structural efficiency interpretation 116
6.4.1. Need for normalisation 117
6.4.2. Thickness-normalised strength 117
6.4.3. Stiffness-normalised mobilisation efficiency 118
6.4.4. Energy efficiency index 119
6.4.5. Integrated efficiency interpretation 120
6.4.6. Implications of normalised interpretation 120
6.5. Design implications for load-bearing CFS wall systems with sustainable composite sheathing 121
6.5.1. Connection detailing as a primary design parameter 122

6.5.2. Axial load-bearing applications 123
6.5.3. Cyclic and seismic performance considerations 125
6.5.4. Combined axial–cyclic loading 127
6.5.5. Material selection and sustainability considerations 128
6.5.6. Scope of application 130
6.5.7. Methodological implications 130
6.6. Original contribution of the synthesis 131
6.7. Chapter summary 131
Chapter 7 Conclusions 134
7.1. Overview and research context 134
7.2. Conclusions in relation to the research questions 135
7.3. Contributions of the thesis 138
7.4. Limitations and future research 139
7.5. Closing statement 143

List of Figures

Figure 3-1 Experimental setup. 42
Figure 3-2 Screw geometry (adapted from Huang et al., 2025). 45
Figure 3-3 Representative load–displacement curves for screw connection specimens with different horizontal and vertical edge distances 47
Figure 3-4 Effect of edge distance on connection strength (adapted from Huang et al., 2025). 51
Figure 4-1 Axial compression test setup. 65
Figure 4-2 Representative axial load–displacement curves for bare, gypsum- and SaveBOARD-sheathed wall panels. 66
Figure 4-3 Representative local and distortional buckling modes observed in bare and sheathed axial compression specimens. 74
Figure 5-1 Cyclic lateral loading test setup. 85
Figure 5-2 Experimental envelope curves derived from the measured cyclic hysteresis loops. 92
Figure 5-3 Energy dissipation comparison between sheathing types. 94
Figure 5-4 Backbone curves for different uniform screw spacing configurations. 95
Figure 5-5 Representative damage progression observed in the cyclic-only and combined axial–cyclic PIL wall specimens. 99

List of Tables

Table 1-1 Summary of candidate sheathing material properties considered in this thesis. 12
Table 1-2 Summarises how the research questions are addressed within the thesis..... 18
Table 2-1 Summary of the measured steel properties. 24
Table 2-2 Summary of experimental programme and measured response quantities. ... 29
Table 2-3 Summary of the link between research questions, thesis chapters and evidence type..... 38
Table 3-1 Measured material properties of sheathing materials used in the screw connection tests (adapted from Huang et al., 2025). 43
Table 3-2 Summary of screw connection test parameters 44
Table 3-3 Representative screw connection results showing the influence of edge distance. 48
Table 4-1 Comparison of axial stiffness and ultimate load for all wall configurations. . 67
Table 5-1 Summary of cyclic wall specimens and test parameters. 87
Table 5-2 Representative cyclic performance parameters for selected wall specimens. 89
Table 6-1 Key experimental results used for synthesis and cross-scale interpretation. 107
Table 6-2 Synthesis of experimental evidence and governing mechanisms across scales. 108

Chapter 1 Background

1.1. Cold-formed steel wall systems in structural practice

Cold-formed steel (CFS) wall systems are widely adopted in low- and mid-rise construction due to their high strength-to-weight ratio and compatibility with industrialised framing systems. In structural terms, this high strength-to-weight ratio means that relatively thin and lightweight steel members can provide considerable load-carrying capacity while reducing material use, transportation demand and construction handling effort. However, the same thin-walled geometry that enables this efficiency also makes CFS studs sensitive to local, distortional and global buckling under compression. Therefore, the practical performance of CFS wall systems depends not only on steel material strength, but also on how effectively the wall assembly restrains instability through sheathing panels and discrete screw connections. This interaction is particularly important when alternative sheathing materials are introduced. A lower-stiffness board may not provide restraint in the same manner as conventional plywood or gypsum sheathing, but it may still contribute structurally if the screw–panel interface can sustain bearing deformation and maintain distributed load transfer (Schafer, 2002; Schafer, 2008). This consideration provides the basis for evaluating SaveBOARD sheathing as a recycled composite material within CFS wall systems. Component-based modelling frameworks and system-level databases have further advanced understanding of framing–sheathing interaction mechanisms in CFS wall assemblies (Peterman et al., 2014).

Unlike hot-rolled steel members, CFS studs are highly susceptible to local, distortional and global buckling because the cold-forming process produces thin plate elements with high width-to-thickness ratios, open cross-sectional geometry and limited torsional rigidity (Hancock and Rasmussen, 1995; Schafer, 2002). Under axial compression,

individual plate elements may deform locally, flange–lip assemblies may rotate in a distortional mode, and the member may also experience overall flexural or flexural–torsional instability. This stability sensitivity is therefore a direct consequence of the thin-walled geometry rather than material weakness alone. Consequently, system-level behaviour cannot be inferred solely from isolated member capacity, because the effective compression resistance of a CFS stud depends strongly on the restraint provided to its flanges, lips and web along the member length. The presence of sheathing panels fundamentally alters the structural response by providing lateral and rotational restraint to stud flanges and webs, thereby enhancing axial stability and modifying failure modes (Vieira and Schafer, 2012; Fülöp and Dubina, 2004). In this context, sheathing panels are not only surface linings but also restraint elements that can modify the effective boundary conditions of slender studs by limiting flange out-of-plane displacement and rotation at discrete screw locations. This mechanism provides the basis for the axial compression investigation presented later in this thesis. Early experimental investigations also demonstrated that sheathing restraint substantially enhances axial stability and modifies buckling hierarchy in thin-walled members (Telue and Mahendran 2004). Thus, the key structural challenge in CFS wall design is to retain the material efficiency associated with lightweight thin-walled steel members while controlling the instability mechanisms that arise from their slender geometry.

Experimental investigations have demonstrated that sheathing attachment can significantly increase both stiffness and strength of CFS wall panels under axial compression (Tian et al. 2004). The degree of enhancement depends on panel stiffness, fastener density and framing thickness (Peterman et al., 2014; Abeysiriwardena et al.,

2021). This indicates that CFS walls behave as composite systems in which framing–sheathing interaction governs global response.

Under lateral loading, sheathed CFS walls function as shear walls. Numerous cyclic studies have shown that hysteretic response is typically governed by connection slip, screw bearing and progressive panel edge damage rather than by yielding of steel framing members (Fülöp and Dubina, 2004; Zhang and Xu, 2016; Ringas and Becque, 2023). Pinching behaviour and stiffness degradation are closely linked to fastener deformation and panel-to-frame interaction (Peterman et al., 2014; Ibarra et al., 2005).

Although current standards such as AISI S213 (AISI S213, 2020) provide empirical design guidance for lateral performance, the quantitative contribution of sheathing to axial restraint and cyclic degradation remains only partially codified. Much of the design framework is based on experimental databases dominated by gypsum, wood-based panels and steel sheets (Brière et al., 2018; Pehlivan et al., 2025; CFSEI, 2008). The applicability of these assumptions to emerging alternative sheathing materials requires careful reassessment.

Accordingly, CFS wall systems should be understood across three interrelated scales. At the material scale, the mechanical properties of the steel framing and sheathing panels provide the baseline for interpreting structural response, including the properties measured or characterised using GB/T 228.1-2021, ASTM D3500-20 and ASTM D790. At the connection scale, screw bearing, pull-through and slip behaviour govern how forces are transferred between the sheathing and the CFS framing (Peterman et al., 2014; Wu et al., 2020; Abeysiriwardena et al., 2021). At the system scale, the combined interaction between material properties and connection behaviour determines the global

axial and cyclic wall response (Fülöp and Dubina, 2004; Zhang and Xu, 2016). This multi-scale perspective provides the foundation for evaluating both conventional and sustainable sheathing systems within CFS structural practice.

1.2. Shear walls in framed structures: timber and CFS systems

Shear walls have long been established as primary lateral force-resisting elements in timber construction. In timber systems, global racking behaviour is typically governed by nail slip and bearing deformation within wood fibres (Filiatrault and Folz, 2002; FEMA, 2000; FEMA, 2005). Analytical models such as SAWS (Folz and Filiatrault, 2001) and deterioration models (Ibarra et al., 2005) have been widely used to capture hysteretic behaviour.

CFS shear walls share conceptual similarities with timber systems in that global resistance arises from panel-to-frame fastener behaviour. However, the mechanical differences between timber and thin-walled steel framing introduce important distinctions. Timber framing does not experience local or distortional buckling in the same manner as CFS members, whereas thin-walled steel studs are highly stability-sensitive (Hancock and Rasmussen, 1996; Schafer, 2002).

Experimental studies have confirmed that cyclic performance of CFS shear walls is strongly governed by sheathing–frame interaction (Fülöp and Dubina, 2006a; Peterman et al., 2014). Screw spacing has been shown to significantly affect stiffness, peak strength and pinching behaviour (Xu and Martinez, 2006; DaBreo and Rogers, 2014; Ringas and Becque, 2023). Increasing screw density enhances initial stiffness but may lead to diminishing returns due to concentrated bearing damage (Serrette et al., 1998; Schafer, 2002). Large-scale experimental databases have corroborated this diminishing-return

behaviour across various sheathing materials and detailing configurations (Zhang et al., 2024).

Comparative investigations of gypsum, wood-based panels and steel sheets have demonstrated material-dependent cyclic characteristics. Gypsum provides moderate stiffness due to its relatively high in-plane rigidity; however, it exhibits brittle cracking under pull cycles because tensile stresses localise around fastener holes, leading to sudden loss of load transfer (Zhang et al., 2016; Wu et al., 2020). Wood-based panels offer improved ductility through progressive embedment and bearing deformation around screw connections, but their mechanical properties may degrade under elevated moisture conditions, potentially affecting long-term stiffness and strength (Dujmović et al., 2021; AS 1720.1-2010). Steel sheathing delivers high strength and stiffness owing to its elastic–plastic capacity; however, its high rigidity can transfer significant forces to boundary studs and hold-downs, resulting in demand concentration in framing members (Pehlivan et al., 2025; AISI, 2020).

More recent research has explored centre-sheathed configurations and multi-panel systems, highlighting the importance of connection detailing and deformation redistribution (Brière et al., 2018; Wu et al., 2020). However, the majority of available databases focus on conventional sheathing materials, while alternative or recycled composite panels have only been examined in limited experimental programmes and remain insufficiently represented in structural performance datasets.

When alternative composite boards are introduced, differences in elastic modulus, tensile capacity and crushing behaviour may fundamentally alter failure hierarchy. Studies on composite laminated joints—such as fibre-reinforced or layered composite panels

connected by mechanical fasteners—have demonstrated progressive bearing-dominated failure rather than brittle rupture (Li et al., 2016; Chen and Tay, 2017). These mechanisms differ from traditional gypsum cracking or plywood splitting responses (Dujmović et al., 2021).

Despite extensive research on conventional sheathing materials, peer-reviewed full-scale experimental studies on SaveBOARD-sheathed CFS wall systems remain unavailable in the published literature. In particular, the interaction between screw spacing, framing thickness and axial load under cyclic loading has not been comprehensively quantified for this material system.

1.3. Seismic and wind performance requirements of CFS wall systems

CFS wall systems are widely used in low- and mid-rise buildings as both gravity load-bearing and lateral load-resisting elements. In seismic regions, these systems must sustain significant cyclic drift demands without premature loss of strength, stiffness, or stability (Landolfo et al., 2006; Fiorino et al., 2012). Under wind loading, although the deformation amplitudes may be smaller than in severe seismic events, repeated load reversals and sustained service-level actions can still induce progressive connection degradation and stiffness deterioration (Peck et al., 2012; AISI S213, 2020).

Extensive experimental research on gypsum-, wood- and steel-sheathed CFS shear walls has demonstrated that global lateral performance is governed not only by peak strength, but also by hysteretic stability, energy dissipation capacity, and resistance to pinching (Boudreault et al., 2017; Shamim and Rogers, 2013; Zhang et al., 2024). In particular, screw connection behaviour, local tearing or crushing of sheathing materials, and

degradation of composite action strongly influence cyclic performance and drift capacity (DaBreo and Rogers, 2014; Ringas and Becque, 2023).

Therefore, understanding the cyclic lateral behaviour of sheathed CFS walls is essential for evaluating their structural suitability in regions subjected to seismic and wind-induced loading demands. This broader performance context underpins the experimental investigation presented in the subsequent chapters.

1.4. Sheathing–frame interaction and connection mechanics

The structural behaviour of sheathed CFS wall systems is fundamentally governed by the interaction between thin-walled steel framing members and attached sheathing panels through discrete mechanical fasteners. Unlike monolithic structural elements, sheathed CFS walls derive their global stiffness and strength from distributed connection behaviour, making fastener mechanics a critical determinant of system response (Peterman et al., 2014; Abeysiriwardena et al., 2021).

1.4.1. Local connection behaviour

Component-level investigations of CFS stud-to-sheathing connections have demonstrated nonlinear load–deformation behaviour characterised by an initial elastic phase followed by progressive bearing deformation and post-peak softening (Peterman et al., 2014; Wu et al., 2020). Governing failure modes typically include bearing deformation of the sheathing, screw tilting and bending, pull-through, and local panel tearing or crushing. Similar nonlinear connection characteristics have been reported across a range of CFS shear wall systems with different sheathing materials (Li et al., 2016; Chen et al., 2015).

The relative dominance of these mechanisms depends on panel modulus, thickness, edge distance and steel thickness (Abeysiriwardena et al., 2021; Li et al., 2017). Wood-based panels exhibit fibre crushing and splitting (Dujmović et al., 2021), whereas steel-sheet sheathing often shifts demand towards connection yielding or boundary elements (Pehlivan et al., 2025). These findings highlight that connection response provides the primary link between material-scale behaviour and wall-scale performance.

1.4.2. Influence of screw spacing and detailing

Screw spacing has been identified as a key parameter influencing lateral capacity, stiffness and pinching behaviour (Xu and Martinez, 2006; DaBreo and Rogers, 2014; Ringas and Becque, 2023). Denser screw layouts generally enhance initial stiffness and peak strength, but with diminishing returns beyond certain density thresholds (Schafer, 2002).

Reported test programmes have employed a wide range of fastener spacings; for example, a steel-sheathed CFS shear wall programme investigated fastener spacings of 50, 75, 100 and 150 mm across multiple wall aspect ratios and framing thicknesses (Rizk, 2018). Other recent experimental work on steel-sheathed CFS walls has also adopted perimeter fastener spacing on the order of ~150 mm, with larger spacings (e.g., ~300 mm) along intermediate studs in multi-panel configurations (Mourad et al., 2026).

Numerical models incorporating explicit fastener behaviour have confirmed that accurate representation of screw slip and bearing response is essential for predicting global hysteretic degradation (DaBreo and Rogers, 2014). Experimental studies further demonstrate that non-uniform screw arrangements, such as densified-edge layouts, improve restraint in regions of high connection demand (Ringas and Becque, 2023). Thus,

global wall behaviour is strongly influenced by the spatial distribution of discrete fasteners rather than by intrinsic panel strength alone.

1.4.3. Sheathing restraint and axial–lateral coupling

Beyond shear resistance, sheathing panels provide lateral and rotational restraint to slender CFS studs under axial compression. Experimental research has shown that attached panels can significantly delay local and distortional buckling and enhance axial capacity (Kyvelou et al., 2017; Wu et al., 2020). This stabilising effect aligns with distortional buckling scaling principles described by Hancock and Rasmussen (1996) and Schafer (2002).

Composite interaction between framing and sheathing therefore influences both axial and lateral performance. Analytical and numerical studies have further emphasised the need to capture axial–lateral interaction effects when modelling CFS wall assemblies (Nguyen et al., 2017; Peterman et al., 2014). Under combined loading conditions, redistribution of deformation demand between framing and sheathing becomes critical, as axial compression in the studs modifies framing stiffness and stability, thereby altering the proportion of lateral deformation accommodated by fastener slip, panel deformation and global instability (DaBreo and Rogers, 2014). However, systematic full-scale experimental data examining axial–cyclic interaction across different sheathing materials remain limited.

1.4.4. Material-dependent failure hierarchy

Extensive databases exist for gypsum-, wood-based and steel-sheathed CFS walls (Brière et al., 2018; Pehlivan et al., 2025; Zhang and Xu, 2016). Conventional sheathing materials exhibit distinct failure characteristics, with gypsum panels typically governed by brittle

tensile cracking, wood-based panels by progressive withdrawal and fibre crushing, and steel sheets by high in-plane stiffness with increased force transfer to boundary framing members (Wu et al., 2020; Dujmović et al., 2021; AISI, 2020).

In contrast, the sustainable composite board investigated in this study (SaveBOARD), manufactured from recycled packaging and polymer matrices, exhibits comparatively lower elastic modulus but may demonstrate progressive bearing-dominated connection behaviour governed by localised screw embedment and matrix deformation. Such mechanisms differ from brittle gypsum cracking or plywood splitting and may influence the stability of cyclic hysteresis.

For SaveBOARD-sheathed CFS wall systems, the key uncertainty is not simply whether the board can provide sheathing resistance, but how its lower elastic modulus and progressive screw-bearing response modify the failure hierarchy of the overall wall system. In particular, the interaction between material stiffness, connection behaviour, screw spacing and framing slenderness has not yet been systematically quantified for this type of recycled composite sheathing.

1.5. Sustainable composite boards in New Zealand: the case of SaveBOARD

1.5.1. Product description and material characteristics

The increasing emphasis on sustainable construction and circular economy principles has driven the development of alternative sheathing materials derived from recycled composite waste streams. SaveBOARD is the registered trade mark for a composite board manufactured in New Zealand from recycled beverage cartons—comprising layered paperboard, polyethylene and aluminium foil—and post-consumer soft plastics. Rather than separating these materials through conventional recycling processes, the production

method involves shredding and thermally compressing mixed packaging waste into consolidated rigid panels. This upcycling approach retains the multi-layered structure of the original materials and converts heterogeneous waste streams directly into building products without reprocessing into virgin raw constituents (saveBOARD, 2022; saveBOARD, 2024).

Product documentation indicates that SaveBOARD panels are marketed for use as internal wall and ceiling linings, rigid air barriers and pre-cladding substrates within timber and steel framing systems (saveBOARD, 2022; saveBOARD, 2024; Mulford Plastics, 2023). Environmental Product Declarations (EPDs) published by EcoChoice Aotearoa (2025) report reduced embodied carbon relative to conventional plasterboard, reflecting both recycled material content and diversion of packaging waste from landfill.

In this thesis, three commercially available SaveBOARD product variants are examined:

SaveBOARD Exposed (EPL): a pre-finished internal wall and ceiling lining designed for residential and commercial applications, featuring a transparent facing that reveals the compressed composite core and eliminates the need for additional plaster finishing.

SaveBOARD Paperfaced Internal Lining (PIL): a paintable internal wall and ceiling lining with recycled paper facings bonded to the composite core, positioned as an alternative to traditional plasterboard.

SaveBOARD betterBRACE Rigid Air Barrier (RAB): a structural rigid air barrier panel intended for use behind external cladding systems, providing bracing capacity and moisture resistance within framed wall assemblies.

To provide material context for the subsequent experimental chapters, the principal candidate sheathing materials considered in this thesis are summarised in Table 1-X. The

comparison highlights the large stiffness difference between conventional wood-based sheathing and the recycled composite boards, while also showing that material stiffness alone is not sufficient to predict wall-scale behaviour. In connection-dominated CFS wall systems, screw-bearing response, local crushing behaviour and deformation compatibility are also expected to influence axial restraint and cyclic hysteresis.

Table 1-1 Summary of candidate sheathing material properties considered in this thesis.

Material	Abbreviation	Nominal thickness (mm)	Tensile modulus (MPa)	Tensile strength (MPa)	Flexural strength (MPa)	Bending modulus (MPa)	Maximum bending deflection (mm)	Role in this thesis
Gypsum plasterboard	GYP	10	2230	1.87	6.84	2270	7.1	Conventional reference sheathing
Plywood	PLY	12	7992.36	56.71	/	/	/	Conventional wood-based reference sheathing
SaveBOARD betterBRACE Rigid Air Barrier	RAB1	12	131.60	6.41	/	/	/	Sustainable composite rigid air barrier board
SaveBOARD betterBRACE Rigid Air Barrier	RAB2	7	125.02	6.05	/	/	/	Sustainable composite rigid air barrier board with reduced thickness
SaveBOARD Paperfaced Internal Lining	PIL	10	106.03	7.62	9.51	398	25.3	Sustainable composite internal lining board
SaveBOARD Exposed Lining	EPL	10	103.51	7.47	8.10	346	29.6	Sustainable composite exposed internal lining board

Note: Material properties reported in this table comprise experimentally measured values from the research programme and, where direct testing was not undertaken within the corresponding wall-test series, values adopted from the associated experimental studies used in this thesis. These properties are used to support interpretation of material, connection and wall behaviour. They should not be interpreted as design values.

As shown in Table 1-1, SaveBOARD panels differ mechanically from conventional gypsum and plywood sheathing. Their elastic modulus is substantially lower than that of plywood, indicating that they should not be treated simply as stiffness-based

replacements for wood-based panels. However, the boards exhibit measurable tensile resistance and progressive local crushing behaviour around screw connections, suggesting that their structural contribution may arise from deformation compatibility and sustained screw-bearing resistance rather than elastic rigidity alone. This distinction provides the basis for the connection-level and wall-level investigations presented in Chapters 3 to 5.

While bracing capacities and installation guidelines are provided in product literature (saveBOARD, 2024), publicly available documentation is primarily limited to compliance statements, installation manuals and summary test data. To the author's knowledge, no peer-reviewed wall-scale experimental studies on SaveBOARD-sheathed CFS systems have been reported in the published literature.

1.5.2. Structural implications and research gap

Given that global CFS wall behaviour is highly sensitive to sheathing stiffness, connection response and screw spacing configuration (Peterman et al., 2014; Ringas and Becque, 2023), the introduction of a composite board with distinct mechanical characteristics raises several important structural questions. First, it is necessary to examine whether the lower elastic modulus of the composite board reduces global wall stiffness, or whether the wall response is governed primarily by connection behaviour. Second, the influence of progressive bearing-dominated failure on cyclic hysteresis stability needs to be clarified. Third, it is important to determine whether the restraint provided by composite sheathing can effectively delay local and distortional buckling in slender CFS studs. Finally, the interaction between screw spacing optimisation and composite material behaviour must be investigated, because detailing rules developed for conventional sheathing materials may not be directly transferable to recycled composite

boards. These questions are particularly relevant in the New Zealand context, where CFS framing is widely adopted and sustainable material alternatives are increasingly promoted.

The motivation for focusing on SaveBOARD is not limited to the absence of peer-reviewed wall-scale experimental data. SaveBOARD was selected because it represents a commercially available New Zealand recycled composite board that is already promoted for use in framed wall construction, while its structural role in load-bearing CFS wall systems remains insufficiently understood. Its recycled fibre–polymer composition, lower elastic modulus, and potential for progressive bearing deformation around screw connections distinguish it from conventional gypsum and plywood sheathing. These characteristics create both an opportunity and a design uncertainty: the board may contribute to sustainable construction and provide stable connection-dominated deformation, but its effect on axial restraint, cyclic hysteresis, screw spacing efficiency and wall-level failure hierarchy cannot be inferred directly from existing conventional sheathing databases. Therefore, addressing this gap requires a systematic multi-scale investigation across material, connection, axial and cyclic loading levels.

1.6. Identified knowledge gaps and research questions

1.6.1. Established knowledge

The existing body of research provides a well-established understanding of the behaviour of gypsum-, wood-based and steel-sheathed CFS wall systems under axial and cyclic loading. Previous studies have shown that sheathing attachment can enhance axial capacity by restraining local and distortional buckling (Kyvelou et al., 2017; Wu et al., 2020). Under cyclic loading, global wall response is predominantly governed by screw connection behaviour rather than framing yielding, with screw bearing, slip and

degradation playing a central role in hysteretic performance (Fülöp and Dubina, 2006b; Peterman et al., 2014). Existing research has also demonstrated that screw spacing and edge detailing significantly influence stiffness, strength and pinching behaviour (Xu and Martinez, 2006; Ringas and Becque, 2023). Although material stiffness affects lateral capacity, hysteretic stability is strongly controlled by connection degradation and damage progression (Zhang and Xu, 2016; Pehlivan et al., 2025). These findings collectively confirm that sheathed CFS walls are connection-dominated structural systems in which material properties, fastener mechanics and framing slenderness interact to define global response.

1.6.2. Limitations in current knowledge

Despite this extensive foundation, several limitations remain evident in the current literature. First, most available experimental databases are based on conventional sheathing materials, including gypsum, plywood, OSB and steel sheets (Brière et al., 2018; AISI, 2020). Consequently, the transferability of these datasets to alternative composite boards with different elastic moduli, crushing characteristics and failure progression remains uncertain.

A further limitation concerns the integration of behaviour across different structural scales. Although connection-level studies and wall-scale tests have been conducted separately, relatively few investigations explicitly link connection hysteresis to wall-level cyclic stability within a unified experimental framework (Peterman et al., 2014; Abeysiriwardena et al., 2021). As a result, the mechanistic relationship between component-level response and system-level behaviour remains insufficiently developed.

In addition, axial–cyclic interaction remains comparatively underexplored. While the effects of sheathing restraint under monotonic axial compression have been investigated (Kyvelou et al., 2017), systematic experimental evidence examining combined axial compression and cyclic lateral loading for alternative sheathing systems remains limited (DaBreo and Rogers, 2014).

Finally, the optimisation of screw spacing for recycled composite sheathing has not been sufficiently established. Existing recommendations regarding screw density are derived largely from gypsum- and wood-based panel systems (Xu and Martinez, 2006), and it remains uncertain whether these detailing principles provide an appropriate or optimal basis for composite boards with different local bearing and deformation characteristics.

1.6.3. Research gap

The central research gap is therefore the absence of an integrated structural assessment linking the material characteristics of sustainable composite sheathing to connection behaviour, axial restraint and cyclic wall performance. Existing design knowledge derived from conventional gypsum, timber-based and steel sheathing cannot be assumed to transfer directly to SaveBOARD because its lower elastic stiffness and progressive screw-bearing response produce a different interaction between panel deformation, connection degradation and CFS framing stability. This thesis addresses this gap through a multi-scale experimental programme spanning material, connection, axial-subassembly and cyclic wall behaviour.

1.6.4. Research questions

In response to the identified gaps, this thesis addresses the following research questions. Each question is linked to a specific experimental scale and evidence type so that the

progression from material behaviour to connection response and wall-level performance is explicit. RQ1 is addressed primarily through axial compression tests on bare, gypsum-sheathed and SaveBOARD-sheathed CFS wall specimens. RQ2 is addressed through both component-level screw connection tests and wall-level cyclic tests, allowing the link between local bearing behaviour and global hysteretic response to be examined. RQ3 is addressed through cyclic wall tests with different screw spacing configurations, including densified-edge layouts. RQ4 is addressed through the combined axial–cyclic test programme and the synthesis of damage progression and deformation capacity.

RQ1. How does SaveBOARD sheathing influence the axial compression behaviour and buckling restraint of full-height single-stud CFS wall subassemblies compared with conventional sheathing systems?

RQ2. To what extent is the cyclic lateral response of SaveBOARD-sheathed CFS walls governed by connection behaviour, and how does this compare with conventional sheathing materials?

RQ3. How does screw spacing configuration, including densified-edge detailing, interact with composite board properties to influence strength, stiffness and energy dissipation?

RQ4. Within SaveBOARD-sheathed CFS wall systems, how does the combination of axial compression and cyclic lateral loading affect damage progression and deformation capacity?

Table 1-2 Summarises how the research questions are addressed within the thesis.

Research question	Main chapter(s)	Main evidence used
RQ1 – Axial restraint and buckling behaviour	Chapter 4	Axial compression tests on bare, gypsum-sheathed and SaveBOARD-sheathed CFS wall specimens; comparison of peak load, initial stiffness and observed buckling modes.
RQ2 – Connection-governed cyclic mechanism	Chapter 3 and Chapter 5	Screw connection load–displacement response, failure modes and edge-distance sensitivity in Chapter 3; cyclic hysteresis, pinching and damage progression in Chapter 5.
RQ3 – Screw spacing and densified-edge detailing	Chapter 5	Cyclic wall tests with different screw spacing configurations; comparison of strength, stiffness, energy dissipation and damage localisation.
RQ4 – Axial–cyclic interaction	Chapter 5 and Chapter 6	Combined axial compression and cyclic lateral loading test; comparison with cyclic-only behaviour; synthesis of damage progression, deformation capacity and design implications.

Note: This mapping is used throughout the thesis to maintain traceability between the research questions, experimental evidence and design-oriented interpretation.

1.7. Chapter summary

This chapter established the structural context and research motivation for investigating cold-formed steel wall systems incorporating sustainable composite sheathing. Existing research demonstrates that the behaviour of sheathed CFS walls is governed by the interaction between thin-walled framing instability, sheathing restraint and discrete screw connections. Although conventional gypsum-, wood- and steel-sheathed systems have been studied extensively, the transferability of this knowledge to recycled composite boards remains uncertain because their stiffness, local crushing behaviour and screw-bearing response differ from those of conventional sheathing materials.

SaveBOARD was identified as a relevant case study because it represents a commercially available recycled composite board used in New Zealand framed construction, while its structural contribution to load-bearing CFS wall systems has not been comprehensively established. The literature review showed that four aspects remain particularly important:

the ability of the board to provide axial restraint to slender CFS studs, the role of connection deformation in cyclic response, the influence of screw spacing and edge detailing, and the interaction between axial compression and cyclic lateral loading.

These gaps lead directly to the research questions defined in Section 1.6.4 and establish the rationale for the multi-scale methodology adopted in this thesis. The subsequent investigation therefore progresses from material characterisation and local screw-connection behaviour to axial subassembly response and full-scale cyclic wall behaviour, allowing the global structural response to be interpreted through identifiable component-level mechanisms.

Chapter 2 Research objectives and methodological framework

2.1. Research philosophy and approach

The research presented in this thesis is grounded in an experimental, mechanics-based approach aimed at establishing a physically interpretable understanding of sheathing–frame interaction in CFS wall systems.

Rather than relying solely on empirical bracing capacities or code-based classifications, this study adopts a hierarchical framework that links material behaviour, connection response and wall-scale performance. In this framework, the mechanical properties of the steel framing and sheathing materials provide the basis for interpreting connection behaviour. The connection response then governs how forces are transferred between the sheathing and the CFS framing, which in turn controls the global axial and cyclic response of the wall system. By interpreting wall-scale behaviour through these lower-scale mechanisms, the study links observed global performance trends directly to identifiable local mechanisms and enables rational interpretation rather than purely descriptive comparison.

The research is hypothesis-driven and is developed from the literature review presented in Chapter 1. The first hypothesis is that cyclic wall performance is governed more strongly by screw connection behaviour than by intrinsic panel stiffness alone. This hypothesis is important because SaveBOARD has a substantially lower elastic modulus than plywood, yet its progressive bearing behaviour around screw connections may still allow stable load transfer under cyclic loading. The second hypothesis is that screw

spacing optimisation is material-dependent, and that detailing rules developed for gypsum or wood-based panels may not be directly transferable to recycled composite boards. The third hypothesis is that axial load modifies damage distribution and deformation capacity, but does not necessarily change the basic connection-dominated failure hierarchy of the wall system.

The experimental programme was therefore designed to test these hypotheses through a sequence of material characterisation, screw connection testing, axial compression testing and cyclic wall testing. This sequence allowed local material and connection mechanisms to be linked progressively to wall-scale axial and lateral behaviour.

2.2. Overall research structure

The investigation is organised into three sequential but interlinked experimental levels. The first level consists of material characterisation, which establishes the mechanical properties of the CFS framing members and candidate sheathing boards. These properties provide the baseline data required to interpret differences in connection stiffness, bearing resistance and wall-level response. The second level examines screw connection behaviour, because the transfer of force between the sheathing and CFS framing occurs through discrete mechanical fasteners. The third level evaluates wall-system response under axial compression and quasi-static cyclic lateral loading.

This hierarchical structure was selected because sheathed CFS walls do not behave as isolated steel studs or isolated panels. Instead, their response depends on the interaction between material properties, screw connection deformation and framing stability. By

progressing from material scale to connection scale and then to wall scale, the methodology allows the observed global behaviour to be interpreted mechanistically rather than only described empirically.

2.3. Material characterisation

Material characterisation establishes the baseline mechanical parameters governing structural response. Similar hierarchical experimental strategies have been adopted in previous CFS wall investigations to ensure consistency between material, connection and system-scale interpretation (Peterman et al., 2014).

The test standards used in this thesis were selected according to the specific material property or structural response being measured. Because the experimental programme covered steel coupons, recycled composite board coupons, screw connections, axial compression subassemblies and cyclic wall specimens, no single New Zealand standard provided a complete test framework for all stages. Therefore, recognised international standards were adopted where they were most appropriate for the specimen type and loading condition. GB/T 228.1-2021 was used for steel coupon testing because it provides a standardised method for determining metallic material properties. ASTM D3500-20 and ASTM D790 were used for sheathing board tensile and flexural characterisation because these standards are suitable for board-type and wood/composite sheet materials. ASTM E2126-19 was used for quasi-static cyclic wall testing because it is widely adopted for evaluating the lateral performance of sheathed wall systems and provides a consistent basis for hysteresis, envelope and energy dissipation evaluation.

Although these standards originate from different jurisdictions, they were used to obtain reproducible material and structural response parameters rather than to claim direct compliance with a specific New Zealand design standard. This approach is appropriate for the present research because the objective was to establish comparative structural behaviour and mechanistic interpretation for a New Zealand-manufactured recycled composite board within CFS wall systems.

2.3.1. CFS section

The mechanical properties of the CFS framing members were determined through uniaxial tensile coupon tests conducted in accordance with GB/T 228.1-2021. The coupon tests were used to determine the yield strength, ultimate tensile strength, elastic modulus and elongation of the steel used in the wall experimental programmes.

Two distinct CFS framing series were used in the experimental programme. The full-height single-stud subassembly programme used 0.80 mm and 0.85 mm thick steel sections, whereas the full-scale cyclic wall programme used nominal stud thicknesses of 0.75 mm and 1.05 mm. These framing series correspond to separate experimental programmes and are therefore reported independently rather than interpreted as nominal and measured values of the same steel sections.

The measured steel properties used to characterise the two experimental programmes are summarised in Table 2-1.

Table 2-1 Summary of the measured steel properties.

Experimental programme	Series	Thickness (mm)	Yield strength (MPa)	Tensile strength (MPa)	Elastic modulus (MPa)	Elongation (%)
Single-stud subassembly	S1	0.80	441.52	489.92	187,500	14.2
Single-stud subassembly	S2	0.85	490.38	550.18	188,500	13.3
Full-scale cyclic wall	S1	0.75	461.6	511.8	186,000	14.8
Full-scale cyclic wall	S2	1.05	487.1	514.7	192,000	13.1

2.3.2. Sheathing materials

The sheathing materials investigated in this study included gypsum plasterboard, plywood and three SaveBOARD variants, namely Exposed Lining (EPL), Paperfaced Internal Lining (PIL) and Rigid Air Barrier (RAB). Their tensile and flexural properties were determined in accordance with ASTM D3500-20 and ASTM D790 to quantify stiffness and strength differences between conventional and composite boards. Uniaxial tensile tests on the sustainable composite boards were conducted under displacement control at 2 mm/min using a 100 kN universal testing machine. Specimens were prepared in accordance with ASTM D3500-20. Three-point bending tests were conducted in accordance with ASTM D790 using 340 mm × 50 mm specimens and a span-to-depth ratio of 16:1, also at a displacement rate of 2 mm/min.

The objective at this stage was not to rank materials by intrinsic strength, but to establish mechanical parameters necessary for interpreting connection and wall behaviour.

2.4. Connection behaviour investigation

Given the connection-dominated nature of sheathed CFS systems (Peterman et al., 2014; Ringas and Becque, 2023), detailed screw connection testing was conducted. Previous component-level investigations have emphasised the nonlinear load–deformation characteristics and progressive bearing behaviour of screw connections in CFS wall systems (Li et al., 2016; Chen et al., 2016; Wu et al., 2020).

The objectives of this stage were to identify the governing failure modes of the screw connections, including bearing deformation, pull-through and shear-related failure; to quantify the corresponding load–deformation characteristics; to examine the influence of edge distance on connection response; and to establish trends in connection stiffness and ductility. This stage therefore provides the mechanistic bridge between material properties and wall-scale behaviour.

Importantly, connection testing allows the response of different sheathing materials to be distinguished in terms of failure mechanism. In particular, it enables comparison between brittle fracture-dominated behaviour and progressive bearing-dominated behaviour, which later informs the interpretation of cyclic hysteresis stability at the wall scale.

2.5. Wall-level axial behaviour

Full-height single-stud wall subassemblies were tested under monotonic axial compression. Each specimen consisted of a CFS stud connected to top and bottom tracks, with sheathing attached to one face of the framing. These specimens are referred

to as wall subassemblies rather than complete multi-stud walls, because they were designed to isolate the axial restraint provided by the sheathing–screw system to an individual slender stud. Previous axial compression studies have demonstrated that attached sheathing can significantly enhance buckling restraint and modify axial failure modes in slender CFS members (Telue and Mahendran 2004).

The axial compression programme was designed to quantify the restraint provided by sheathing to slender CFS studs and to determine whether SaveBOARD panels could delay local and distortional buckling in a manner comparable to conventional sheathing materials. Bare CFS specimens were included as the baseline condition, while gypsum- and SaveBOARD-sheathed specimens were tested to evaluate the contribution of panel restraint. Framing thickness was varied to examine the sensitivity of the restraint effect to stud slenderness, since thinner CFS members are expected to benefit more from lateral and rotational restraint provided by attached sheathing.

This stage directly addresses RQ1. The use of wall-scale specimens, rather than isolated material coupons, allowed the axial restraint mechanism to be evaluated under realistic load transfer conditions involving steel framing, sheathing panels and screw connections. The results also provide a bridge between the connection behaviour investigated in Chapter 3 and the wall-level stability response discussed in Chapter 4.

2.6. Wall-level cyclic behaviour

Quasi-static reversed cyclic tests were conducted in accordance with ASTM E2126-19. Extensive cyclic experimental programmes have established baseline hysteretic

characteristics of CFS shear walls under similar loading protocols (Serrette and Wan, 1992; Rogers et al., 1998; Dubina et al., 2004).

The cyclic wall programme was designed to evaluate the lateral performance of SaveBOARD-sheathed CFS walls under quasi-static reversed cyclic loading. The main response parameters considered were initial stiffness, peak strength, deformation capacity, hysteretic loop shape, pinching behaviour and cumulative energy dissipation. These parameters were selected because they describe not only the maximum lateral resistance of the wall, but also the stability of load transfer and damage accumulation under repeated load reversals.

The test matrix varied sheathing type, stud thickness, screw spacing configuration and axial load condition. Sheathing type was varied to compare SaveBOARD with conventional reference materials. Stud thickness was included to assess whether the influence of sheathing restraint changes with framing slenderness. Screw spacing was selected as a primary design variable because fastener density directly controls the distribution of shear transfer along the panel edges. A combined axial–cyclic specimen was also included to provide preliminary evidence of how gravity load may influence cyclic damage progression and deformation capacity.

Screw spacing was selected as a primary cyclic wall variable because lateral load transfer in sheathed CFS walls occurs through discrete fasteners along the sheathing perimeter. A 200 mm screw spacing was used as the reference configuration because it represents a practical spacing level commonly adopted in sheathed light-frame wall

construction and provides a baseline for comparing material effects. Reduced spacings of 150 mm and 100 mm were included to examine whether increasing fastener density improves strength, stiffness and energy dissipation, and whether the improvement remains proportional as spacing becomes closer. The densified-edge configuration was included to investigate whether additional fasteners concentrated near high-demand edge regions could improve restraint efficiency without uniformly increasing fastener density across the entire wall.

A constant axial load of 12 kN was applied to one specimen to provide a preliminary and indicative assessment of axial–cyclic interaction. Only one axial load level was investigated; therefore, the test was not intended to establish a general relationship between axial load ratio and cyclic wall performance. The intention was not to cover the full range of possible axial load ratios, but to examine whether the presence of sustained compression modifies cyclic damage progression, deformation capacity and connection degradation.

This stage addresses RQ2 to RQ4 by linking local connection mechanics to wall-level hysteretic response, screw spacing efficiency and axial–cyclic interaction.

2.7. Summary of experimental details and data reduction

To improve reproducibility and to clarify the relationship between the different experimental stages, the key details of the test programme are summarised in Table 2-2. The table identifies the specimen type, main dimensions, investigated variables, loading protocol, number of specimens or replicates, and the principal response

quantities extracted from each test series. More detailed drawings, specimen labels and individual test results are provided in the relevant experimental chapters and appendices.

Table 2-2 Summary of experimental programme and measured response quantities.

Experimental stage	Specimen type and dimensions	Main variables	Loading protocol	Reported configurations / specimens	Main measured or derived quantities
Material characterisation	CFS tensile coupons and sheathing board coupons prepared according to the relevant test standards. Sheathing tensile coupons were prepared for ASTM D3500-20 testing, and flexural coupons were prepared for ASTM D790 testing.	Steel section properties; sheathing type; board product variant, including gypsum plasterboard, plywood, EPL, PIL and RAB.	Tensile testing in accordance with GB/T 228.1-2021 and ASTM D3500-20; flexural testing in accordance with ASTM D790.	Replicate numbers are not separately reported in the current thesis text; the material properties are reported as representative values used for interpreting connection and wall behaviour.	Elastic modulus, yield or tensile strength, flexural strength, bending modulus and material-specific deformation characteristics.
Screw connection tests	Single-shear screw connection specimens consisting of one sheathing coupon connected to a CFS member using one self-drilling screw. The schematic connection test length shown in the setup is 200 mm. The fastener had a nominal shank diameter of 3.6 mm and a head diameter of 8 mm.	Sheathing type; horizontal edge distance H; vertical edge distance V; panel type; screw–panel bearing condition.	Monotonic in-plane shear loading under displacement control. No additional screw pre-tension control was applied beyond standard screw installation torque.	Mean results are reported for 17 RAB edge-distance configurations, 15 PIL edge-distance configurations and 5 plywood edge-distance configurations in Appendix A. Individual replicate numbers for each configuration are not separately stated in the current thesis text.	Load–displacement response, mean tensile displacement, mean connection strength, initial connection stiffness, post-peak softening and failure mode.
Axial compression tests	Full-height single-stud CFS wall subassemblies consisting of one CFS stud connected to top and bottom tracks, with an intermediate transverse nogging at mid-height. Sheathing was attached to one face only. Appendix C shows an axial wall specimen geometry of 600 mm × 2400 mm.	Bare frame versus sheathed frame; sheathing type, including gypsum, EPL and PIL; stud thickness; sheathing restraint condition.	Monotonic axial compression under displacement control until failure. Boundary conditions were configured to represent track restraint while preventing unrelated global out-of-plane instability.	Four axial configurations are reported in Table 4-1: bare frame, gypsum-sheathed frame, EPL-sheathed frame and PIL-sheathed frame. Replicate numbers are not separately reported in the current thesis text.	Ultimate axial resistance, initial axial stiffness, percentage strength increase relative to the bare frame, local flange deformation, out-of-plane displacement, buckling initiation location and observed local/distortional buckling modes.
Cyclic lateral tests	Full-scale CFS wall specimens with sheathing attached to the framing. Appendix D shows cyclic wall specimen geometry of 1200 mm × 2400 mm. The bottom track was anchored to a rigid foundation beam, and cyclic displacement was applied at the top track.	Sheathing type, including GYP, PLY, RAB1, RAB2, PIL and EPL; nominal cyclic wall stud thickness of 0.75 mm and 1.05 mm; screw spacing; densified-edge detailing; axial load condition.	Quasi-static reversed cyclic loading under displacement control in accordance with ASTM E2126-19. A free-top boundary condition was adopted, allowing the top track to translate laterally and rotate in-plane without diaphragm restraint.	Fourteen cyclic wall specimens are reported in Appendix H: S1-PIL-DE, S1-PIL-100, S1-PIL-150, S1-PIL-200, S1-PIL-200-V, S1-RAB1-200, S1-RAB2-200, S1-EPL-200, S1-GYP-200, S1-PLY-200, S2-PIL-200, S2-RAB1-200, S2-RAB2-200 and S2-EPL-200. Among these, S1-PIL-200-V was the single combined axial–cyclic specimen subjected to 12 kN axial load.	Hysteresis loops, envelope curves, initial lateral stiffness, peak lateral strength, energy dissipation, ductility factor, equivalent elastic–plastic idealisation parameters, pinching behaviour and damage progression.

The experimental data were reduced using consistent procedures across the test programme. For monotonic material, connection and axial compression tests, the peak load was taken as the maximum recorded load, while the initial stiffness was calculated from the initial linear portion of the load–displacement response. Failure modes were classified from direct visual observations and post-test photographs, with emphasis on bearing deformation, screw tilting, pull-through, local tearing, panel cracking and local or distortional buckling.

For cyclic wall tests, the measured load–displacement histories were used to derive hysteresis loops and envelope curves. The envelope curve was obtained by connecting the peak load points reached at each displacement level in the positive and negative loading directions. Energy dissipation was calculated as the area enclosed by each hysteresis loop, and cumulative energy dissipation was obtained by summing the loop areas over successive cycles. Ductility and equivalent elastic–plastic idealisation parameters were calculated from the envelope response and are summarised in Appendix F and Appendix H.

Comparisons between specimens were made using both absolute and relative response measures. Absolute measures included peak load, initial stiffness, deformation capacity and energy dissipation. Relative measures included strength increase compared with the bare frame, stiffness or strength variation between sheathing types, screw spacing effects relative to the 200 mm reference spacing, and the influence of the 12 kN axial load relative to the corresponding cyclic-only specimen. This approach allowed

material effects, connection-density effects, framing-slenderness effects and axial-load interaction effects to be interpreted separately.

2.8. Experimental matrix and variable isolation strategy

The experimental matrix was designed to isolate the influence of key structural variables while maintaining sufficient realism for practical CFS wall construction. The primary independent variables were sheathing type, stud thickness, screw spacing and axial load condition. These variables were selected because they correspond to the main mechanisms identified in Chapter 1: material-dependent connection behaviour, framing slenderness, fastener-density effects and axial–lateral interaction.

To ensure that differences in response could be attributed to these variables, other parameters were kept consistent wherever possible. These included wall geometry, fastener type, boundary condition and loading protocol. Maintaining these controlled conditions allowed material-driven effects, connection-density effects, framing-slenderness effects and axial-load interaction effects to be interpreted separately. At the same time, the test specimens retained the essential components of practical sheathed CFS wall systems, including steel studs, tracks, sheathing panels and screw connections.

2.9. Numerical modelling methodology and scope

2.9.1. Modelling objective

Numerical modelling was undertaken in Abaqus/Standard to support interpretation of the experimentally observed interaction between the CFS framing, sustainable composite sheathing and screw fasteners. The numerical investigation focused

primarily on the axially loaded wall/subassembly configuration and was intended to examine deformation transfer, local contact behaviour and framing instability mechanisms that could not be quantified directly from the experimental observations.

The numerical model was developed as a supporting mechanistic tool rather than as an independently validated design model. Particular attention was therefore given to representation of the three-dimensional geometry, discrete fasteners, contact interfaces, material directionality and geometric nonlinearity. As discussed subsequently, the high degree of contact and material nonlinearity prevented completion of a fully converged wall-scale solution, and no numerical prediction of ultimate capacity is therefore used as primary evidence in this thesis.

2.9.2. Geometry and element formulation

The CFS framing, SaveBOARD sheathing and screw fasteners were represented as three-dimensional deformable bodies. Eight-node linear brick elements with reduced integration (C3D8R) were adopted for the solid components. This element formulation was selected to permit explicit representation of local contact, screw–board interaction and through-thickness deformation while limiting the computational cost associated with the large three-dimensional model.

The screw fasteners were represented explicitly rather than by idealised spring or connector elements. This approach enabled local interaction between the screws, sheathing and CFS framing to be represented directly, but substantially increased the

number of contact interfaces and consequently the computational cost and convergence difficulty of the analysis.

2.9.3. CFS material properties

The CFS framing was represented using an isotropic elastic–plastic material model. The steel properties were assigned using the measured tensile-coupon results corresponding to the relevant framing series. For the 0.80 mm steel series, the measured yield strength, ultimate tensile strength and elastic modulus were 441.52 MPa, 489.92 MPa and 187.5 GPa, respectively. For the 0.85 mm series, the corresponding values were 490.38 MPa, 550.18 MPa and 188.5 GPa. A Poisson's ratio of 0.30 was adopted.

2.9.4. SaveBOARD material model

The SaveBOARD sheathing was represented using an equivalent orthotropic elastic formulation to account for the directional response of the recycled composite board. Abaqus defines the orthotropic constitutive relationship through nine independent stiffness coefficients, D_{1111}, D_{1122}, D_{2222}, D_{1133}, D_{2233}, D_{3333}, D_{1212}, D_{1313} and D_{2323}. These coefficients were derived from the corresponding engineering constants using the standard orthotropic elasticity relationships implemented in Abaqus.

During verification of the numerical model, the original stiffness-matrix entries were found to contain a unit-scaling inconsistency. The original values corresponded to engineering moduli expressed approximately 1000 times larger than the experimentally measured MPa-scale board properties. Because the model uses an N–mm unit system, material stiffness must be specified directly in MPa (N/mm²). The orthotropic

formulation has therefore been revised so that the elastic constants are expressed consistently with the experimentally measured material properties.

The nominal density of the RAB SaveBOARD material was taken as 850 kg/m³, corresponding to 8.5×10^{-10} tonne/mm³ in the adopted N–mm–tonne unit system. This value is consistent with the manufacturer's nominal density for saveBOARD betterBRACE rigid air barrier products.

2.9.5. Damage representation

A maximum-principal-stress damage initiation criterion was explored for the sustainable composite board, together with energy-based linear damage evolution and a small viscous stabilisation parameter to assist numerical convergence. The maximum-principal-stress criterion is tension-driven and therefore was intended to represent initiation of tensile cracking rather than compressive crushing.

Verification of the original numerical model identified that the preliminary damage-initiation value was not consistent with the measured tensile strength of the board. Accordingly, the damage parameters are not treated as experimentally validated material properties in this thesis. The measured tensile strengths provide the appropriate experimental basis for future calibration of the damage-initiation criterion, while the fracture-energy parameters require independent calibration against post-peak or fracture-response data.

A damage-stabilisation viscosity coefficient of 1×10^{-5} was used as a numerical regularisation parameter. This value is a solution-stabilisation parameter rather than a physical material property.

2.9.6. Contact formulation

Surface-to-surface contact was defined between the interacting framing, sheathing and fastener surfaces. Hard contact was adopted in the normal direction to prevent interpenetration while permitting separation after loss of contact. No independently calibrated friction coefficient was introduced in the preliminary model; therefore, the tangential interaction was treated as frictionless in accordance with the default Abaqus contact formulation. This assumption was adopted to focus the analysis on geometric contact, fastener bearing and material deformation rather than uncertain frictional resistance.

2.9.7. Boundary conditions and loading

The numerical boundary conditions were selected to reproduce the displacement-controlled axial compression test. The bottom support region was restrained against translation in all three global directions. At the top of the model, horizontal translations were restrained while a prescribed vertical displacement of 30 mm was applied downward.

A Static, General analysis procedure was adopted with geometric nonlinearity activated through the NLGEOM option. Displacement-controlled loading was selected rather

than force-controlled loading because it allowed the post-elastic deformation response to be traced more robustly as instability and local contact changes developed.

2.9.8. Mesh sensitivity and numerical convergence

A nominal global element seed size of 10 mm was adopted for the final model configuration. Local refinement was introduced around screw holes, contact interfaces and other regions in which high local deformation or stress concentration was expected.

Mesh sensitivity was assessed qualitatively using both coarser and finer discretisations. Coarser meshes produced excessively diffuse deformation patterns and were unable to represent localised interaction around the fastener and contact regions adequately. Finer meshes provided similar qualitative deformation patterns in the regions that converged but substantially increased the number of elements, contact calculations and overall computational demand. On this basis, the 10 mm global seed with local refinement was selected as a compromise between local deformation resolution and computational feasibility.

2.9.9. Numerical outcome and limitations

The full three-dimensional model became increasingly difficult to solve as deformation progressed. The principal sources of numerical difficulty were the large number of surface-to-surface contact interactions, explicit representation of the screw fasteners, geometric nonlinearity, localised contact-state changes and attempted progressive damage of the sustainable composite sheathing. These mechanisms generated severe convergence difficulties and substantially increased computational demand.

Consequently, a complete converged load–displacement response and reliable numerical ultimate capacity were not obtained. The FE modelling is therefore reported as a documented numerical development and mechanistic investigation rather than as a validated predictive analysis. No numerical capacity values are used to support the principal conclusions of the thesis, which remain based on the experimental results.

Representative numerical deformation patterns are retained in Appendix I to illustrate the modelling approach and the types of local interaction observed during the converged stages of the analysis. These results are interpreted qualitatively only. Future numerical work should use experimentally calibrated orthotropic and damage parameters, simplified connection representations where appropriate, and staged multi-scale validation to reduce the computational burden associated with explicit three-dimensional contact modelling.

2.10. Analytical interpretation and synthesis

Although primarily experimental, the research incorporates simplified analytical interpretation to discuss backbone curves, stiffness degradation and idealised force–displacement response, drawing on established seismic performance and hysteretic response frameworks (FEMA 440, 2005; Ibarra et al., 2005; Schafer, 2002). Direct strength and component-based modelling concepts further inform the interpretation of stiffness enhancement and buckling restraint mechanisms in sheathed systems (Moen and Schafer, 2008; Schafer, 2008).

The objective is not to develop a comprehensive predictive model, but rather to provide physically interpretable relationships between key parameters, to support the interpretation of observed experimental trends, and to inform design-oriented assessment of the tested wall systems.

2.11. Link between research questions and thesis chapters

Table 2-3 Summary of the link between research questions, thesis chapters and evidence type.

Research question	Primary chapter(s)	Evidence type and purpose
RQ1 – Axial restraint and buckling behaviour	Chapter 4	Axial compression tests are used to quantify the influence of SaveBOARD sheathing on peak load, stiffness enhancement and local/distortional buckling restraint compared across bare, gypsum-, EPL- and PIL-sheathed subassemblies.
RQ2 – Connection-governed cyclic mechanism	Chapter 3 and Chapter 5	Chapter 3 provides component-level evidence through screw connection tests, including load–displacement response, bearing deformation and failure modes. Chapter 5 provides wall-level evidence through cyclic hysteresis, pinching behaviour and damage progression.
RQ3 – Screw spacing and densified-edge detailing	Chapter 5	Cyclic wall tests with different screw spacing configurations are used to evaluate the influence of fastener density on strength, stiffness, energy dissipation and damage localisation.
RQ4 – Axial–cyclic interaction	Chapter 5 and Chapter 6	The combined axial–cyclic test provides indicative evidence of axial load interaction, while Chapter 6 synthesises the implications for deformation capacity, failure hierarchy and design interpretation.

This mapping establishes traceability between the identified research gaps, research questions, experimental evidence and design-oriented synthesis. It also clarifies that RQ2 is addressed at both the connection scale and the wall scale, rather than only in the cyclic wall chapter.

2.12. Chapter summary

This chapter established the methodological framework used to address the research questions identified in Chapter 1. The investigation adopts a multi-scale experimental

approach in which material characterisation provides the mechanical basis for interpreting screw-connection behaviour, connection response provides the mechanism for understanding sheathing–frame load transfer, and wall-level axial and cyclic tests determine how these local mechanisms influence structural performance.

The experimental programme separates the principal variables of sheathing type, framing thickness, screw spacing and axial-load condition while maintaining consistent specimen geometry, fastener type, boundary conditions and loading procedures wherever practicable. This structure enables the effects of material behaviour, connection density, framing slenderness and axial–lateral interaction to be interpreted systematically rather than through isolated specimen comparisons.

The chapter also defines the procedures used for material testing, experimental data reduction, cyclic response evaluation and numerical interpretation. The numerical modelling is used as supporting mechanistic evidence rather than as an independently calibrated design model. Together, these methods establish the evidence framework used in Chapters 3–5 and provide traceability between the research questions, experimental observations and the synthesis developed later in the thesis

Chapter 3 Local in-plane behaviour of screw connections between SaveBOARD and CFS members

3.1. Role of connection behaviour in sheathed CFS wall systems

This chapter investigates the local in-plane behaviour of screw connections between SaveBOARD composite boards and CFS members. As shown in Chapter 1, the global behaviour of sheathed CFS wall systems is strongly governed by connection mechanics rather than by framing yielding alone. Understanding connection-level behaviour is therefore essential for interpreting both axial restraint mechanisms (Chapter 4) and cyclic lateral response (Chapter 5).

The work presented in this chapter is partly based on the published journal article by Huang et al. (2025) in the *Journal of Building Engineering*. The content has been reorganised and condensed to align with the integrated research framework of this thesis, with emphasis placed on the mechanistic linkage between connection behaviour and wall-level performance.

Previous studies on CFS screw connections have primarily focused on gypsum and wood-based panels (Peterman et al., 2014; Wu et al., 2020). Similar nonlinear load–deformation characteristics have also been reported across a range of CFS shear wall configurations with alternative sheathing materials (Li et al., 2016; Chen et al., 2015). However, SaveBOARD differs from conventional sheathing materials in material composition, exhibiting a multi-layer structure comprising recycled fibre and polymer

matrices. These differences may influence local bearing behaviour, shear resistance, and tearing mechanisms around screw holes.

Accordingly, this chapter addresses Research Question RQ2 at the component level by identifying the governing failure modes of the screw connections, quantifying their load–displacement characteristics, examining the influence of screw edge distance, and establishing a simplified analytical interpretation of connection strength. These findings provide the mechanistic foundation for the wall-level investigations presented in subsequent chapters.

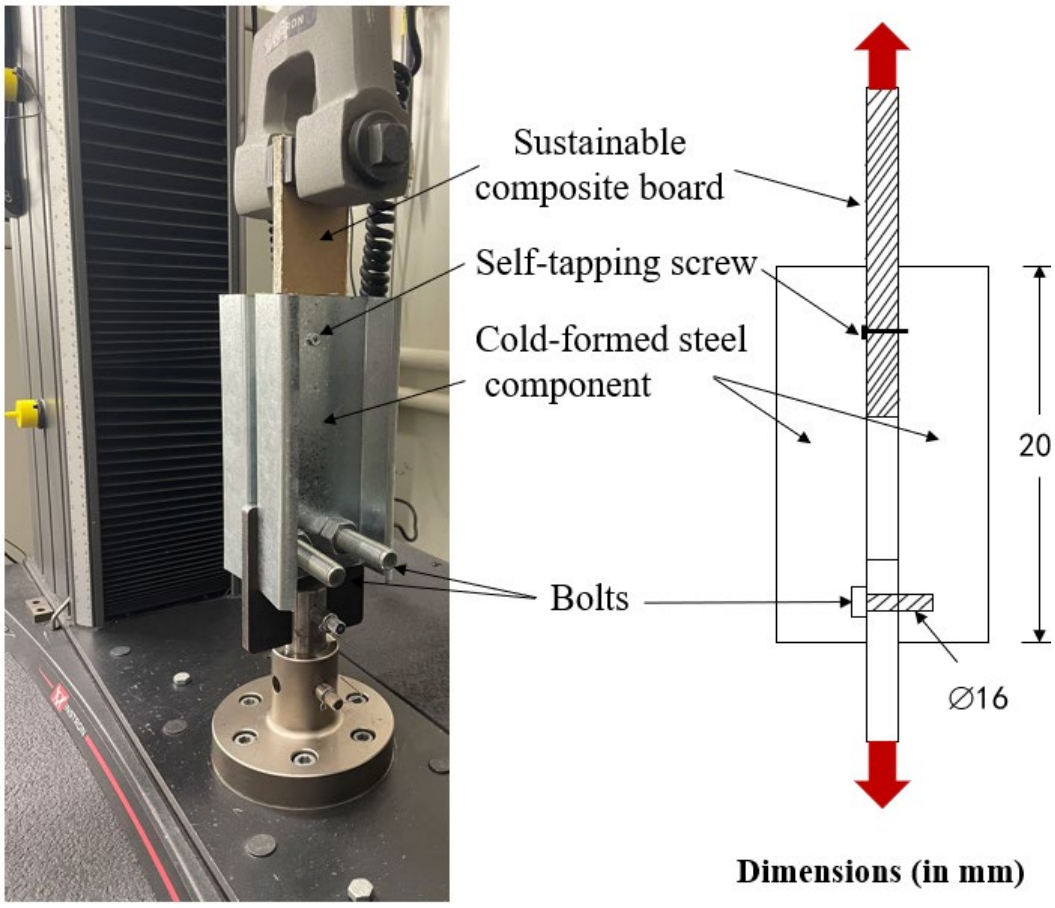
3.2. Experimental programme and specimen configuration

To characterise the local in-plane behaviour of screw connections between SaveBOARD panels and CFS members, a controlled component-level experimental programme was conducted. The objective of this stage was to isolate individual fastener behaviour under monotonic in-plane shear loading, independent of global wall-scale instability effects. Such component-level isolation testing has been widely adopted in prior shear wall investigations to decouple connection mechanics from system-level instability (Rogers & Fülöp 2006).

The configuration was designed to replicate realistic stud–sheathing attachment conditions while maintaining experimental simplicity and repeatability. The connection geometry, fastener type and material combinations were kept consistent with those later adopted in the full-scale wall tests described in Chapters 4 and 5. This ensures direct mechanistic linkage between connection-level response and system-level performance.

3.2.1. Test setup

The connection tests employed a single-shear configuration in which a sheathing coupon was attached to a CFS stud segment using a single self-drilling screw. Load was applied in-plane to simulate shear demand along the stud–panel interface.



(a) Photograph of the actual experiment. (b) Schematic diagram with dimensions.

Figure 3-1 Experimental setup.

The loading arrangement was configured to minimise bending effects and ensure that deformation was concentrated in the screw–sheathing interface. This approach allows direct measurement of bearing deformation, screw tilting and post-peak softening.

3.2.2. Materials and specimen details

The CFS members used in the connection tests corresponded to the framing grades and thicknesses adopted in the wall-scale experiments. The connection-level programme examined SaveBOARD RAB and PIL panels, because these products were selected to represent recycled composite sheathing materials with different facing and application characteristics. Plywood was included as a conventional wood-based reference material. Gypsum is discussed in this thesis as a conventional wall-level reference material, but gypsum connection data are not included in the connection-test dataset presented in this chapter. Therefore, direct connection-level comparisons in this chapter are limited to RAB, PIL and plywood.

The CFS material properties were determined by tensile coupon testing in accordance with GB/T 228.1-2021, while the tensile and flexural properties of the sheathing materials were characterised in accordance with ASTM D3500-20 and ASTM D790, respectively, as described in Chapter 2. These parameters provide the mechanical basis for interpreting connection stiffness and failure progression. Specimen geometry and key parameters are summarised in Table 3-1.

Table 3-1 Measured material properties of sheathing materials used in the screw connection tests (adapted from Huang et al., 2025).

Specimen	Tensile Modulus (MPa)	Tensile strength (MPa)	Compressive Strength (MPa)	Shear Strength (MPa)
RAB- sustainable composite board	131.60	6.41	27.51	5.03
PIL- sustainable composite board	106.03	7.62	27.51	5.71
Plywood	7992.36	56.71	23.91	13.20

Note: The tensile modulus and tensile strength values are reported for the sheathing materials used in the connection-level tests. These values should not be interpreted as screw connection parameters; the connection response is reported separately through load–displacement behaviour, peak connection load and failure mode.

To avoid confusion between material properties and connection-test variables, the main screw connection test parameters are summarised separately in Table 3-2.

Table 3-2 Summary of screw connection test parameters

Parameter	Value / configuration used	Purpose
Sheathing materials	RAB, PIL and plywood	To compare recycled composite boards with a conventional wood-based reference material
CFS member	Cold-formed steel stud segment corresponding to the wall-scale framing material	To maintain consistency between connection tests and wall tests
Fastener type	Self-drilling screw	To represent practical sheathing-to-CFS attachment
Screw shank diameter	3.6 mm	Primary fastener geometry controlling local bearing area
Screw head diameter	8 mm	Relevant to pull-through and local bearing behaviour
Loading type	Monotonic in-plane single-shear loading	To isolate local screw–sheathing load transfer behaviour
Primary variable	Horizontal and vertical edge distance	To examine bearing area, tearing sensitivity and edge-distance effects
Measured response	Load–displacement curve, peak load, displacement capacity and failure mode	To link connection behaviour to wall-scale axial and cyclic response

3.2.3. Fastener specification

The fasteners were self-drilling screws with a nominal shank diameter of 3.6 mm, a head diameter of 8 mm and an overall length of 24.5 mm. No pre-drilling was employed.

No pre-drilling was employed.

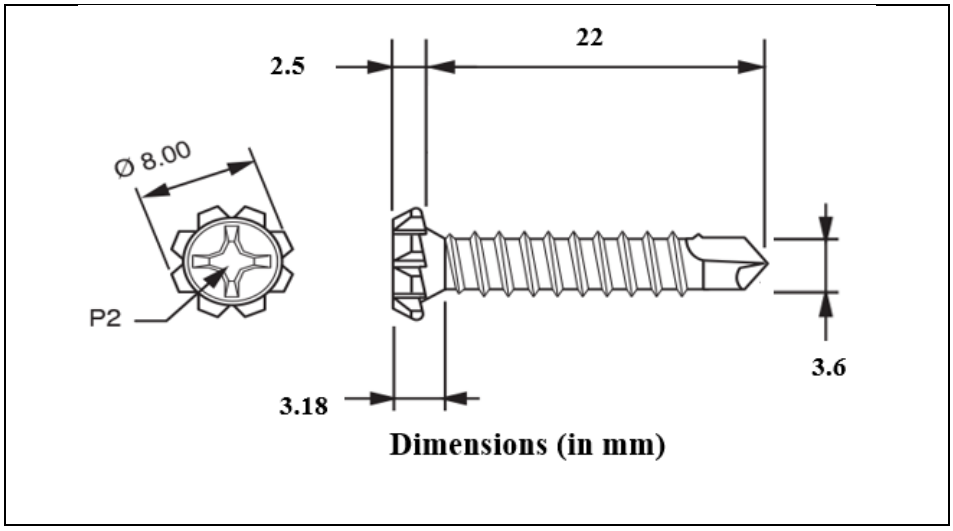


Figure 3-2 Screw geometry (adapted from Huang et al., 2025).

Edge distance was selected as a primary variable because it directly controls the local load-transfer region around the screw. A smaller edge distance reduces the effective bearing area between the screw and the sheathing material and increases stress concentration near the loaded edge, which may promote premature pull-through, local tearing or edge rupture. A larger edge distance provides a greater surrounding material area for bearing deformation and stress redistribution, but the improvement is expected to reduce once the connection response becomes governed by local crushing around the screw hole rather than edge failure.

Previous studies have shown that insufficient edge distance can lead to premature pull-through or panel splitting (Abeysiriwardena et al., 2021; Li et al., 2017), and comparable edge-distance sensitivity has also been observed in CFS shear wall databases incorporating different panel materials (Serrette et al., 1998). By systematically varying this parameter, the present study evaluates whether SaveBOARD composite panels exhibit a similar failure transition to conventional

sheathing materials, or whether their recycled fibre–polymer matrix allows more progressive bearing deformation before edge tearing occurs.

3.2.4. Loading protocol and instrumentation

Monotonic in-plane shear loading was applied under displacement control. The loading rate was selected to minimise dynamic effects while allowing stable capture of post-peak softening behaviour.

Load and displacement were continuously recorded. Connection stiffness was defined as the slope of the initial linear portion of the load–displacement curve. Ultimate strength was taken as the peak load. Post-peak deformation capacity and failure mode were documented.

Failure modes were classified according to the dominant local deformation or damage mechanism observed around the screw–panel interface. The main categories included bearing-dominated deformation, screw tilting and bending, pull-through, and local tearing or crushing of the panel material.

These classifications provide essential mechanistic context for interpreting cyclic pinching behaviour observed at wall scale in Chapter 5, where pinching refers to the reduction in hysteretic loop width and force recovery during load reversal due to slip and local damage accumulation at the connections.

3.3. Experimental results and failure mechanisms

3.3.1. Load–displacement behaviour

Representative load–displacement curves for the tested specimens are presented in Figure 3-3. The specimen notation used in Figure 3-3 follows the format Hx-Vy, where H denotes the horizontal edge distance from the screw centre to the side edge of the board, and V denotes the vertical edge distance from the screw centre to the loaded edge. For example, H25-V10 represents a specimen with a horizontal edge distance of 25 mm and a vertical edge distance of 10 mm.

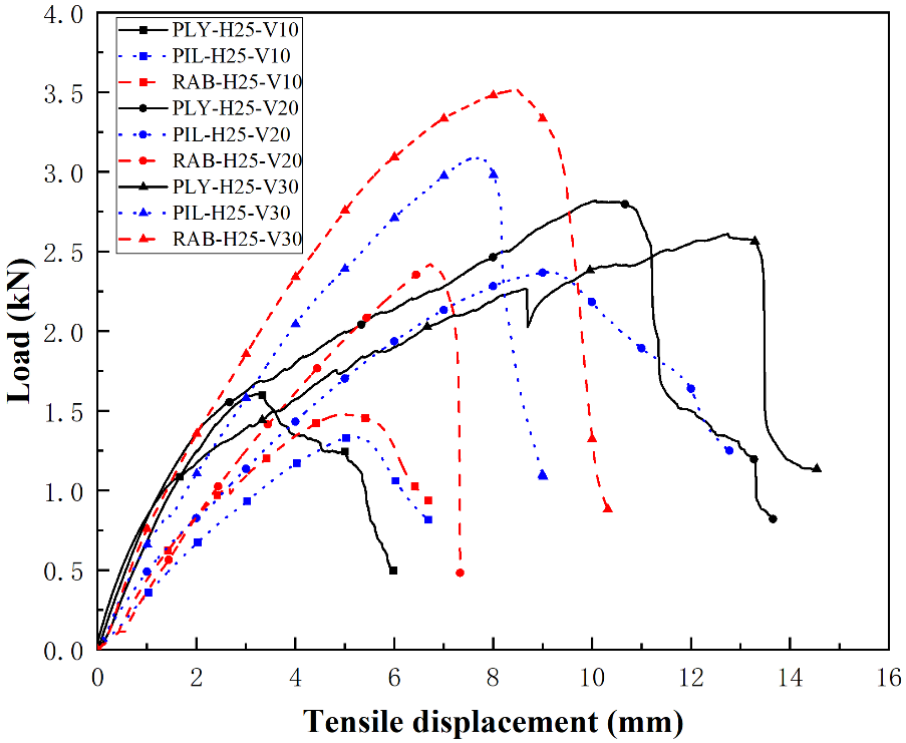


Figure 3-3 Representative load–displacement curves for screw connection specimens with different horizontal and vertical edge distances (adapted from Huang et al., 2025). (The notation Hx-Vy denotes horizontal edge distance H = x mm and vertical edge distance V = y mm.)

The curves generally exhibit three stages:

1. Initial linear elastic response
2. Nonlinear bearing-dominated deformation
3. Post-peak softening and strength degradation

Compared with the plywood reference specimens, the SaveBOARD connections showed lower tensile modulus and lower absolute material strength, but they demonstrated progressive bearing deformation and gradual post-peak degradation around the screw hole. The contrast with gypsum behaviour is discussed at wall scale in Chapter 5, where gypsum-sheathed specimens were included as cyclic reference specimens.

3.3.2. Ultimate strength and stiffness comparison

The detailed connection results for all edge-distance configurations are provided in Appendix A, while representative results are summarised in Table 3-3 to show the main strength trends directly in the chapter. For both RAB and PIL boards, increasing edge distance generally increased mean connection strength and displacement capacity. For example, the RAB connection strength increased from 1.64 kN at H = 25 mm and V = 10 mm to 4.69 kN at H = 60 mm and V = 60 mm. Similarly, PIL increased from 1.64 kN at H = 25 mm and V = 10 mm to 4.07 kN at H = 60 mm and V = 50 mm.

Table 3-3 Representative screw connection results showing the influence of edge distance.

Material	Horizontal edge distance H (mm)	Vertical edge distance V (mm)	Mean displacement at peak / characteristic displacement (mm)	Mean connection strength (kN)	Interpretation
RAB	25	10	5.21	1.64	Small edge distance; early local damage and limited bearing area
RAB	25	40	10.13	3.30	Improved vertical edge distance; increased bearing resistance

Table 3-3 Representative screw connection results showing the influence of edge distance.

Material	Horizontal edge distance H (mm)	Vertical edge distance V (mm)	Mean displacement at peak / characteristic displacement (mm)	Mean connection strength (kN)	Interpretation
RAB	60	60	19.20	4.69	Largest tested edge-distance combination; highest reported RAB strength
PIL	25	10	5.12	1.64	Small edge distance; limited connection capacity
PIL	25	35	11.25	3.51	Improved vertical edge distance; higher deformation capacity
PIL	60	50	20.17	4.07	Large horizontal edge distance; highest reported PIL strength in the selected series
Plywood	25	10	3.29	1.67	Small edge distance; limited displacement capacity
Plywood	25	20	8.74	2.81	Higher connection strength with increased edge distance
Plywood	25	30	15.59	2.57	Large displacement capacity but no proportional strength increase

These results show that edge distance affects both strength and deformation capacity. However, the relationship is not purely linear, particularly when different materials are compared. For the composite boards, the increase in strength with larger edge distance is associated with a larger effective bearing area around the screw and a reduced tendency for premature edge tearing. The plywood results show that increased displacement capacity does not always translate directly into higher strength, indicating that material-specific failure progression also influences connection response.

The key implication is that screw connection strength in sheathed CFS systems is governed by the combined effect of edge distance, local bearing resistance and material damage progression. Therefore, the connection response cannot be predicted from panel elastic modulus alone. This observation provides the basis for the wall-level interpretation in Chapters 4 and 5.

3.3.3. Failure modes

The detailed photographic failure classification is provided in Appendix B, while the dominant failure observations are summarised here because they are central to the interpretation of wall-level behaviour. Four failure mechanisms were observed: bearing-dominated deformation around the screw hole, screw tilting and bending, pull-through failure, and local tearing or crushing of the panel material.

For the SaveBOARD specimens, failure generally initiated as localised bearing deformation around the screw hole, followed by progressive crushing and tearing of the recycled fibre–polymer matrix. This produced gradual post-peak degradation rather than sudden load loss. In contrast, brittle sheathing materials such as gypsum tended to exhibit more abrupt cracking and localised fracture near the fastener line. Plywood developed higher strength in some configurations, but its response was also influenced by local splitting and material-direction effects.

This distinction is structurally important because the local failure mode controls how connection degradation is transferred to the wall scale. Progressive bearing deformation allows load redistribution among adjacent fasteners and may reduce the severity of hysteretic pinching. Abrupt panel cracking or edge tearing can cause local connection loss, reducing the effective shear transfer length and accelerating stiffness degradation in cyclic wall response.

3.3.4. Influence of edge distance

The influence of edge distance on strength and deformation capacity is illustrated in Figure 3-4.

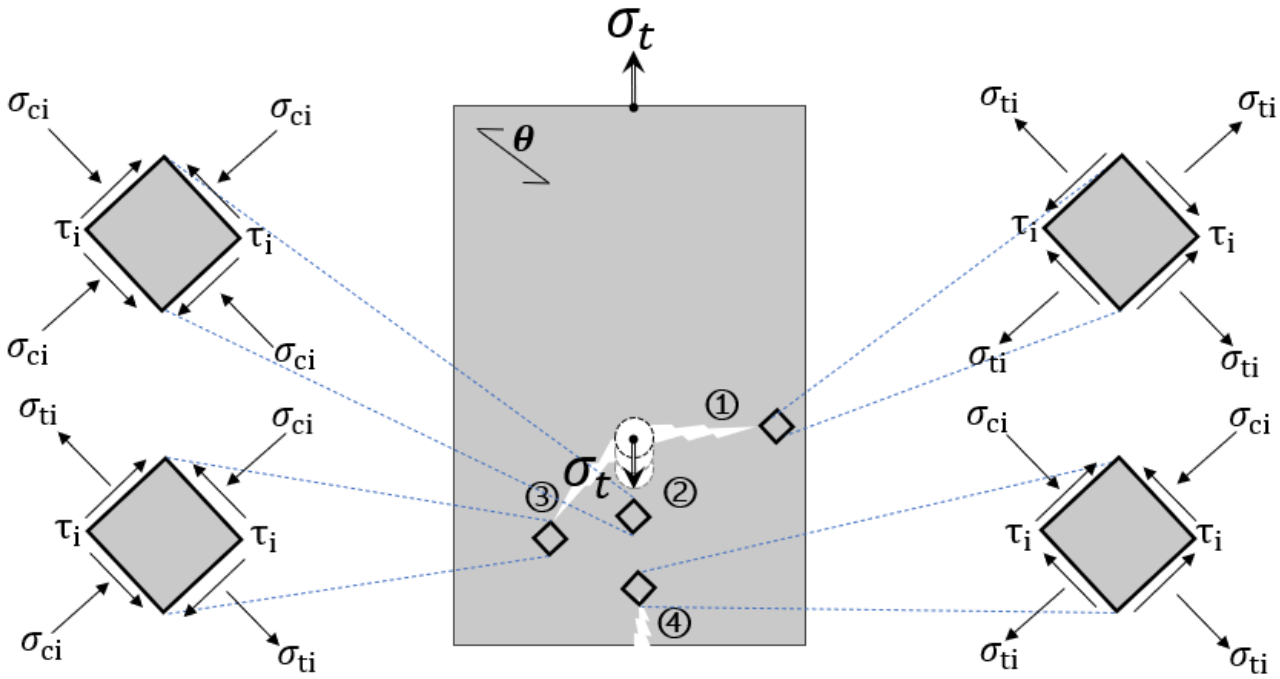


Figure 3-4 Effect of edge distance on connection strength (adapted from Huang et al., 2025).

Specimens with reduced edge distance exhibited earlier pull-through or tearing initiation. However, SaveBOARD specimens showed less abrupt failure transition compared to gypsum panels at equivalent edge distance.

This suggests that composite boards may be less sensitive to edge detailing than brittle gypsum systems, although sufficient edge distance remains essential for optimal performance.

3.4. Analytical interpretation of connection strength

The experimental results presented in Section 3.3 demonstrate that connection strength and deformation capacity vary with sheathing type and edge distance. To interpret these observations mechanistically, a simplified analytical framework is adopted based on bearing-dominated connection behaviour.

3.4.1. Bearing-dominated strength mechanism

For screw connections in thin sheathing panels attached to steel framing, ultimate strength is commonly governed by bearing resistance of the panel material rather than by shear failure of the screw (Peterman et al., 2014; Abeysiriwardena et al., 2021). In the present study, this concept is used to support mechanistic interpretation of the test results. The following simplified expression is therefore introduced as an explanatory bearing-based relationship, not as a calibrated design equation:

$$P_u \approx k\, f_b\, t\, d \tag{1}$$

Where, f_b= effective bearing strength of panel material, t= panel thickness, d= screw diameter, k= coefficient representing the influence of stress distribution, edge distance, local embedment and deformation mode.

This relationship suggests that connection strength is expected to scale with panel thickness, screw diameter and local bearing resistance, rather than elastic modulus alone. However, the coefficient (k) is not calibrated in this thesis because the purpose of the connection programme was to identify failure mechanisms and edge-distance sensitivity, rather than to develop a statistically validated design equation. The tested

configurations involved different sheathing materials, edge distances and failure progressions, which would require a larger and more systematically replicated dataset for reliable coefficient calibration.

The experimental results indicate that although SaveBOARD panels exhibit substantially lower tensile modulus than plywood, their screw connection response was not governed by elastic modulus alone. The composite boards developed connection resistance through progressive local bearing and crushing around the screw hole, which allowed stable load transfer and post-peak deformation despite their lower material stiffness.

3.4.2. Post-peak behaviour and progressive crushing

Unlike brittle gypsum cracking, SaveBOARD panels exhibited gradual strength degradation following peak load. This behaviour indicates progressive crushing and redistribution of stress around the screw hole rather than sudden fracture.

The load–displacement curves (Figure 3-4) show extended deformation capacity beyond peak load, suggesting that local damage accumulation does not immediately lead to catastrophic loss of load-carrying capacity. The relationship between connection-level degradation and wall-scale hysteretic stability has been emphasised in recent cyclic performance reviews (Ringas and Becque, 2023).

This progressive mechanism is significant for cyclic behaviour because it allows connection stiffness to degrade more gradually, reduces the likelihood of an abrupt post-peak strength drop, and may mitigate severe pinching during load reversal.

Thus, connection-level behaviour provides an explanation for wall-scale hysteresis stability observed in Chapter 5.

3.4.3. Edge distance sensitivity

From the simplified bearing expression, reduced edge distance decreases the effective resisting area and increases stress concentration. This explains the experimentally observed reduction in ultimate strength for specimens with smaller edge distances.

However, composite boards demonstrated less abrupt strength transition with decreasing edge distance compared to gypsum panels. This suggests that the multi-layer structure of SaveBOARD may allow stress redistribution across composite layers before local tearing propagates.

This behaviour implies that optimal detailing rules derived for brittle gypsum systems may not be directly transferable to composite boards.

The wall-scale significance of this observation is that edge-distance-controlled connection failure can alter the distribution of load transfer along panel boundaries. If local edge tearing occurs early, individual fasteners may lose effective resistance and transfer additional demand to adjacent screws, increasing damage localisation and hysteretic pinching. In contrast, bearing-dominated deformation allows load redistribution to occur more gradually, which can help maintain distributed sheathing–frame interaction during cyclic loading. Therefore, edge distance is not only a local detailing parameter but also a mechanism that influences wall-level damage progression.

3.4.4. Implications for wall-level behaviour

The analytical interpretation presented here establishes three important implications. First, connection strength is governed primarily by bearing resistance rather than panel stiffness alone. Second, progressive crushing mechanisms can provide enhanced deformation capacity by allowing gradual local deformation around the screw–panel interface. Third, edge distance affects stress concentration, but its influence depends on the ductility and local bearing behaviour of the sheathing material. These insights are critical for understanding both the axial restraint mechanisms discussed in Chapter 4 and the cyclic hysteresis behaviour and screw spacing optimisation examined in Chapter 5.

It should be emphasised that the simplified bearing expression is not used in this thesis to predict design strength or to propose a codified connection capacity equation. Its role is to explain why materials with lower elastic modulus may still mobilise meaningful screw connection resistance if local bearing deformation and stress redistribution can be sustained. A calibrated predictive equation would require additional replicate tests, direct measurement of material bearing strength, and systematic separation of edge-distance, panel-thickness and failure-mode effects. This is therefore identified as a direction for future connection-level research.

3.4.5. Practical edge distance implications and friction effects

The experimental results indicate that edge distance significantly influences connection strength and failure mode. In practical sheathed CFS wall construction, screw

placement is constrained by panel edge-clearance requirements, stud flange width, screw head size and installation tolerance. Therefore, increasing edge distance indefinitely is not a practical design solution. Although larger edge distance can increase the available bearing area and reduce the likelihood of premature edge tearing, excessively large edge distance may move the fastener away from practical framing locations or reduce fastening efficiency.

In typical sheathed wall construction, screws are installed through the sheathing into CFS studs or tracks, and the available placement width is limited by the supporting steel member. This means that the optimum edge distance must balance structural performance with constructability. An edge distance that is too small may cause early edge tearing or pull-through, while an edge distance that is unnecessarily large may not provide proportional strength improvement and may be difficult to achieve consistently on narrow CFS flanges.

The test observations suggest a transition in failure hierarchy as edge distance changes. When sufficient surrounding material is available, the connection response is dominated by progressive bearing deformation around the screw hole. When the edge distance is reduced, the failure mode shifts toward combined bearing and pull-through. At very small edge distances, edge tearing or local rupture becomes more likely. This transition is important because bearing-dominated behaviour allows gradual load redistribution, whereas edge tearing can cause sudden loss of local connection capacity and accelerate wall-level stiffness degradation.

At wall scale, connection failure mode directly influences hysteretic pinching, damage localisation and energy dissipation. Connections governed by progressive bearing are more likely to maintain distributed restraint along the stud height and panel boundary. Conversely, premature edge tearing may cause localised connection loss, reducing the effective shear transfer length and increasing demand on neighbouring fasteners. Thus, maintaining adequate edge distance is essential not only for local connection strength but also for preserving global deformation stability under cyclic loading.

Friction and clamping effects were also considered. In practical construction, screw fastening produces clamping between the sheathing and steel framing, which may generate some frictional resistance under in-plane shear loading. In the present single-shear tests, screw installation torque and pre-tension were not measured or controlled. The screws were installed using standard practical installation procedures, and no additional pre-tension was intentionally applied. Therefore, the measured resistance may include a minor contribution from clamping friction, but the test configuration was designed so that the dominant response was governed by bearing deformation and mechanical interaction at the screw–sheathing interface.

This interpretation is supported by the observed failure modes, which were characterised by bearing deformation, screw tilting, pull-through and local tearing rather than frictional slip alone. Accordingly, friction is acknowledged as a secondary effect and a source of experimental variability, but it is not treated as the primary resistance mechanism. Future studies could control screw installation torque or directly

measure screw pre-tension to separate frictional resistance from bearing-dominated connection behaviour more precisely.

3.5. Chapter summary

This chapter investigated the local in-plane behaviour of screw connections between SaveBOARD composite panels and CFS members. Given the connection-dominated nature of sheathed CFS wall systems established in Chapter 1, understanding component-level behaviour is essential for interpreting global structural response.

The experimental results demonstrated that connection behaviour is governed primarily by bearing resistance of the sheathing material rather than by screw shear failure. SaveBOARD panels exhibited progressive bearing-dominated deformation, resulting in gradual post-peak softening rather than abrupt brittle fracture. This contrasts with the more sudden cracking behaviour observed in gypsum specimens.

Edge distance was shown to influence ultimate strength and failure mode through its effect on effective bearing area, stress concentration and edge-tearing susceptibility. The SaveBOARD specimens exhibited progressive bearing and crushing before local tearing, suggesting that detailing optimisation for recycled composite boards should consider both local connection capacity and wall-scale damage redistribution. Screw torque and pre-tension were not measured in this study; therefore, frictional clamping is acknowledged as a possible secondary effect, while the observed response is interpreted primarily as bearing-dominated mechanical interaction.

The simplified analytical interpretation indicates that connection strength is governed by the effective bearing capacity of the panel material, which is influenced by panel thickness and local embedment behaviour, rather than by elastic modulus alone. This interpretation, consistent with the experimentally observed load–displacement responses, suggests that composite boards with lower in-plane stiffness may still achieve comparable connection capacity if sufficient bearing resistance is mobilised.

The findings of this chapter indicate that connection behaviour governs deformation stability more strongly than intrinsic panel stiffness alone. The progressive crushing mechanisms observed in the composite boards may enhance cyclic deformation capacity by allowing more gradual local damage development around the screw–panel interface. In addition, detailing parameters such as screw spacing and edge distance interact with material behaviour and therefore need to be evaluated at the wall scale rather than interpreted only from isolated material properties. These insights form the mechanistic basis for the wall-level investigations presented in the following chapters. Chapter 4 examines how sheathing restraint influences axial buckling behaviour, while Chapter 5 evaluates how connection mechanics translate into cyclic hysteresis response.

Chapter 4 Axial compression behaviour of SaveBOARD-sheathed CFS walls

4.1. Role of sheathing in axial stability of CFS walls

As discussed in Chapter 1, CFS wall systems are highly sensitive to local and distortional buckling due to the slenderness of thin-walled members (Hancock and Rasmussen, 1996; Schafer, 2002). In practical construction, sheathing panels are attached to framing members and may provide lateral and rotational restraint that delays instability.

Previous experimental investigations have demonstrated that conventional sheathing materials, such as gypsum and wood-based panels, can significantly enhance axial capacity by restraining local and distortional buckling modes (Kyvelou et al., 2017). Similar axial enhancement effects have been reported in earlier studies on sheathed CFS wall panels, confirming the stabilising influence of attached panels on local and distortional buckling behaviour (Telue and Mahendran 2004). However, no published peer-reviewed studies have quantified the full-height single-stud wall subassemblies restraint contribution of SaveBOARD sheathing in CFS wall systems.

This chapter addresses Research Question RQ1:

How does SaveBOARD sheathing influence the axial compression behaviour and buckling restraint of full-height single-stud CFS wall subassemblies compared with conventional sheathing systems?

The work presented here forms the second level of the multi-scale framework introduced in Chapter 2. Whereas Chapter 3 established the component-level connection behaviour, the present chapter evaluates the axial response of full-height single-stud CFS wall subassemblies incorporating SaveBOARD sheathing.

The primary objectives of this chapter are to quantify the axial strength enhancement provided by sheathing relative to bare CFS frames, evaluate stiffness differences between different sheathing types, identify the governing buckling modes, and interpret the composite restraint mechanisms developed through sheathing–frame interaction. The findings provide insight into how attached sheathing modifies the stability behaviour of thin-walled steel wall systems.

4.2. Experimental programme and specimen matrix

To evaluate the axial compression behaviour of SaveBOARD-sheathed CFS wall subassemblies, a series of full-height monotonic compression tests was conducted. The experimental programme was designed to quantify the influence of sheathing type and framing thickness on axial capacity and buckling restraint.

The subassembly specimens were designed to represent a repeated stud–sheathing–fastener unit in light-gauge steel-framed wall construction. All panels were tested under displacement-controlled monotonic axial compression until failure.

4.2.1. Specimen configuration

The axial compression specimens were full-height single-stud CFS wall subassemblies rather than complete multi-stud wall panels. Each specimen was designed to isolate the

restraint effect of one sheathing panel attached to one CFS stud through screw connections. This configuration allowed the influence of sheathing type on local and distortional buckling restraint to be examined without the additional complexity of load sharing between multiple studs.

The purpose of using a single-stud subassembly was not to reproduce the global diaphragm action of a complete multi-bay wall system, but to provide a controlled configuration for evaluating the local and member-level interaction between the CFS stud, sheathing board and screw fasteners. In practical light-gauge steel-framed buildings, the structural performance of a sheathed wall is governed by the cumulative contribution of repeated stud–sheathing–fastener units. The present specimen represents one such full-height vertical strip, allowing the influence of sheathing material and stud characteristics to be isolated without the additional complexity introduced by boundary studs, hold-downs and multi-bay load redistribution.

Therefore, the axial results are most directly applicable to comparative assessment of sheathing restraint and stud buckling behaviour rather than direct prediction of the axial capacity of a complete multi-stud wall.

Sheathing panels were attached on one face only, while the opposite face remained unsheathed. The vertical edges of the stud were not laterally restrained by adjacent studs, resulting in open-edge boundary conditions.

The specimen therefore represents a single-stud wall subassembly with intermediate bracing, rather than a complete multi-stud wall system. This configuration was

intentionally adopted to isolate the stabilising contribution of sheathing restraint on an individual compression member under controlled boundary conditions.

Mechanical fasteners identical to those used in the connection tests (Chapter 3) were employed to ensure consistency between component-level and wall-level investigations.

The overall geometry and boundary configuration of the specimens are illustrated in Appendix C.

4.2.2. Sheathing types

The axial compression programme investigated four specimen configurations: a bare CFS frame used as the reference specimen, a gypsum plasterboard-sheathed subassembly used as the conventional comparison case, and sustainable composite board subassemblies sheathed with EPL and PIL. The inclusion of the bare specimen allowed the restraint contribution provided by sheathing attachment to be directly quantified, while the gypsum specimen provided a conventional reference for evaluating the axial restraint effectiveness of EPL and PIL.

4.2.3. Framing thickness

The axial compression specimens were grouped according to the relevant light-gauge CFS framing thickness used in the test programme. The single-stud axial subassembly programme used two CFS framing series with steel thicknesses of 0.80 mm and 0.85 mm. These sections formed part of a distinct subassembly-level experimental programme and were different from the 0.75 mm and 1.05 mm framing series used in

the full-scale cyclic wall tests. These values are treated as measured specimen thicknesses within the axial compression programme.

Increasing stud thickness reduces susceptibility to local and distortional buckling, allowing assessment of whether sheathing restraint becomes less significant as framing stiffness increases. To avoid ambiguity, the axial compression results in this chapter are interpreted using the reported specimen thicknesses for the tested axial configurations, while cross-chapter comparisons are made using the broader thin-gauge versus thicker-gauge framing distinction.

This variable directly addresses the stability sensitivity discussed in Chapter 1.

4.2.4. Loading arrangement and boundary conditions

Monotonic axial compression was applied using a hydraulic actuator under displacement control. Boundary conditions were configured to represent realistic track restraint while preventing global out-of-plane instability unrelated to stud behaviour. Axial compression was applied under displacement control using a servo-controlled testing machine with a nominal capacity of 1000 kN. A constant loading rate of 2 mm/min was maintained until a clear post-peak reduction in load and significant lateral deformation were observed. The initial axial stiffness was calculated as the slope of the load–displacement response between 10% and 40% of the peak load, while the ultimate axial resistance was defined as the maximum recorded axial load.

The loading setup is illustrated in Figure 4-1.



(a) S1 CFS stud wall panel

(b) CFS stud wall panels sheathed with gypsum boards

Figure 4-1 Axial compression test setup.

4.2.5. Instrumentation

Axial load and vertical displacement were recorded continuously throughout each test. In addition, local flange deformation, out-of-plane displacement and the location of buckling initiation were monitored to identify the governing instability modes and to correlate these modes with the restraint provided by the sheathing.

4.3. Axial load–displacement behaviour

The axial load–displacement responses of the tested wall specimens are presented in Figure 4-2.

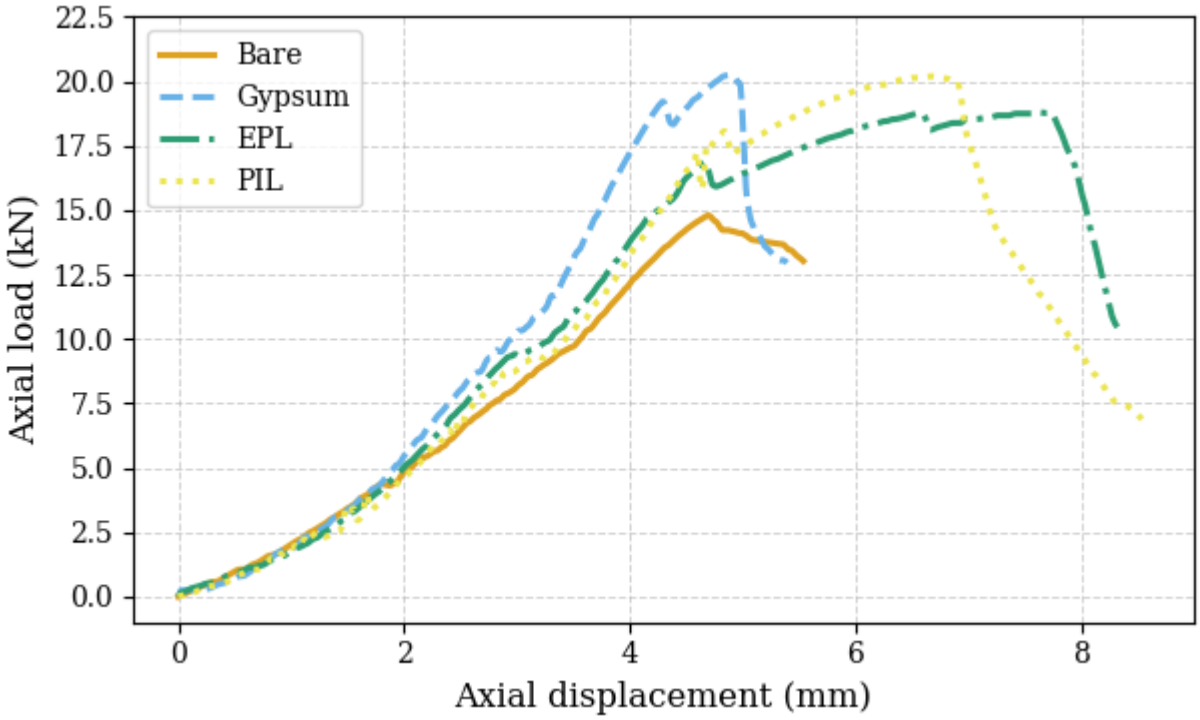


Figure 4-2 Representative axial load–displacement curves for bare, gypsum- and SaveBOARD-sheathed wall subassemblies.

4.3.1. Comparison with bare frame

The bare CFS frame exhibited the lowest axial capacity and the earliest onset of local and distortional buckling. The load–displacement curve shows rapid stiffness degradation following initial instability.

The addition of sheathing panels significantly enhanced both initial stiffness and ultimate load capacity. This confirms that sheathing provides lateral and rotational restraint to stud flanges, delaying buckling initiation.

The relative increase in peak load compared with the bare frame provides a quantitative measure of composite restraint efficiency.

The results in Table 4-1 show that all sheathed specimens achieved higher axial capacity than the bare frame. The bare CFS frame reached an ultimate axial resistance of 14.80 kN with an initial stiffness of 2.303 kN/mm. The gypsum-sheathed specimen reached 20.25 kN, corresponding to a 36.8% strength increase. The EPL specimen reached 18.80 kN, corresponding to a 27.0% increase, while the PIL specimen reached 20.20 kN, corresponding to a 36.5% increase.

Table 4-1 Comparison of axial stiffness and ultimate load for all wall configurations.

Panel type	The ultimate axial resistance P_u (kN)	The initial stiffness K_i (kN/mm)	Strength increases vs bare
Bare	14.80	2.303	–
Gypsum	20.25	2.933	+36.8%
EPL	18.80	2.508	+27.0%
PIL	20.20	2.267	+36.5%

It should be noted that the PIL specimen showed an initial stiffness of 2.267 kN/mm, which is slightly lower than the bare frame value of 2.303 kN/mm. This small difference should not be interpreted as a loss of sheathing effectiveness. Initial stiffness is sensitive to early-stage seating, screw slip, panel–frame contact mobilisation, local deformation at the screw connections and measurement range used for stiffness calculation. The more important observation is that the PIL specimen-maintained restraint during the subsequent nonlinear stage and achieved an ultimate axial resistance of 20.20 kN, compared with 14.80 kN for the bare frame.

Therefore, the axial contribution of PIL sheathing is reflected more clearly in the ultimate load and delayed buckling response than in the initial stiffness value alone. This supports the interpretation that SaveBOARD sheathing contributes through

sustained connection-mediated restraint rather than purely through initial elastic stiffness.

These results indicate that SaveBOARD sheathing can provide meaningful axial restraint to slender CFS studs. However, the results should be interpreted carefully. The PIL specimen achieved an axial strength enhancement comparable to the gypsum-sheathed specimen, whereas the EPL specimen provided a smaller but still significant enhancement. Therefore, the axial results support the conclusion that SaveBOARD sheathing can be structurally effective, but they do not justify a general statement that all SaveBOARD products exceed gypsum performance under axial compression.

The critical observation is that axial capacity enhancement is not governed only by the elastic modulus of the sheathing panel. Although gypsum has higher stiffness than PIL and EPL, the PIL specimen achieved a similar strength increase to gypsum. This suggests that the effectiveness of sheathing restraint depends on the combined stiffness of the panel, the screw connection response and the ability of the sheathing–connection system to restrain flange displacement and delay local or distortional buckling.

4.3.2. Influence of sheathing type

Although gypsum panels possess higher elastic modulus than SaveBOARD, the axial strength enhancement provided by the PIL specimen was comparable to the gypsum specimen, while the EPL specimen provided a lower but still substantial enhancement relative to the bare frame. The axial load–displacement curves in Figure 4-2 and the

values summarised in Table 4-1 show that gypsum, EPL and PIL increased the ultimate axial resistance by 36.8%, 27.0% and 36.5%, respectively.

This suggests that axial capacity enhancement is not governed solely by panel stiffness, but by the ability of the sheathing–connection system to restrain flange displacement and redistribute local compressive stresses.

The SaveBOARD specimens exhibited lower initial stiffness than the gypsum specimen, but this did not directly correspond to lower ultimate axial capacity. In particular, the PIL specimen achieved an ultimate axial resistance comparable to the gypsum specimen despite its lower initial stiffness. This indicates that the sheathing contribution should be evaluated using both initial stiffness and peak capacity, together with observed buckling mode and post-initial restraint behaviour.

4.3.3. Effect of stud thickness

Increasing stud thickness is expected to increase axial capacity because thicker CFS studs have greater cross-sectional stiffness and reduced susceptibility to local and distortional buckling. Conversely, thinner studs are more stability-sensitive and are therefore expected to benefit more from lateral and rotational restraint provided by attached sheathing. This interpretation is consistent with thin-walled stability theory, where the influence of restraint becomes more significant as member slenderness increases (Schafer, 2002).

In the present thesis, the axial compression results demonstrate that sheathing attachment increased ultimate axial resistance relative to the bare frame. However,

because the main axial results are not presented as a fully replicated thickness-by-thickness comparison, the influence of stud thickness is interpreted mechanistically rather than used to establish a general quantitative trend. Additional axial tests using paired bare and sheathed specimens for each stud thickness would be required to quantify the restraint effect as a function of slenderness.

4.4. Buckling mode and composite restraint mechanism

The observed failure modes under axial compression provide insight into the stabilising role of sheathing attachment. Representative deformation patterns at ultimate load are shown in Figure 4-3.

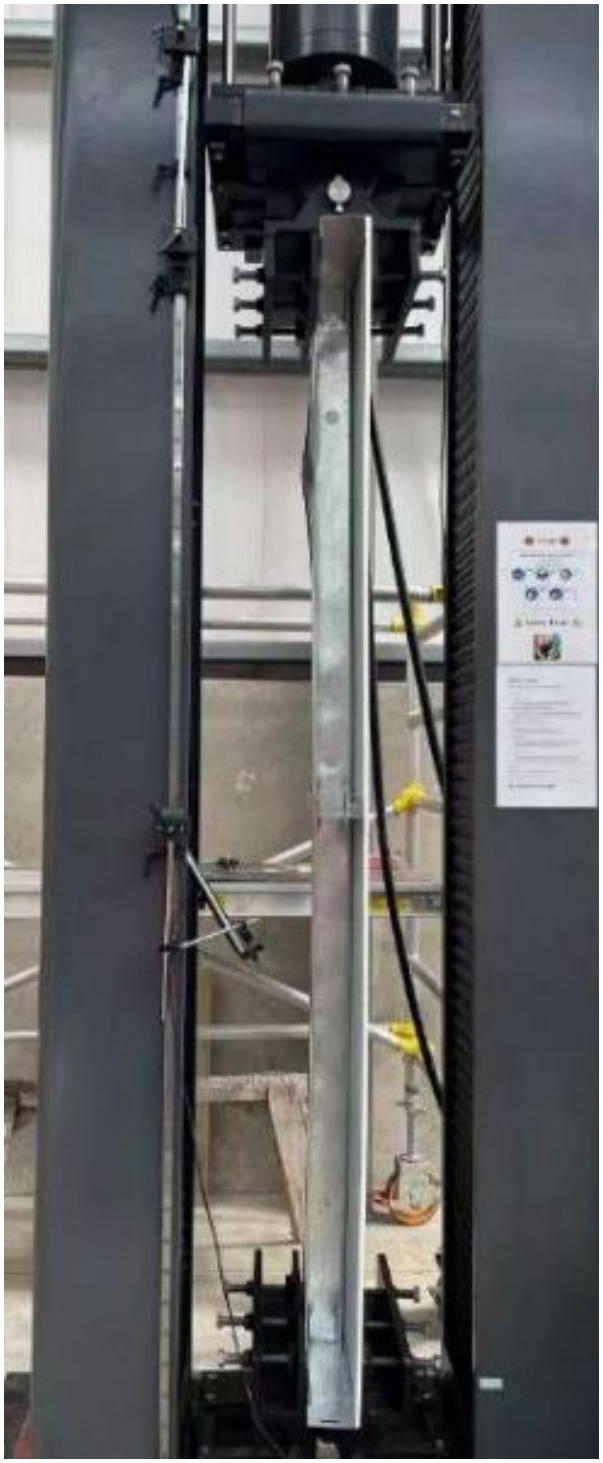
The buckling modes shown in Figure 4-3 are presented as representative visual evidence of the deformation patterns observed during the axial compression tests. The interpretation of local and distortional buckling was not based solely on the photographs, but also on the measured axial load–displacement response, visual observations during testing and post-test inspection of the stud and sheathing connection regions. The photographs are therefore used to support the discussion of buckling mode development rather than to serve as the only evidence for failure classification.



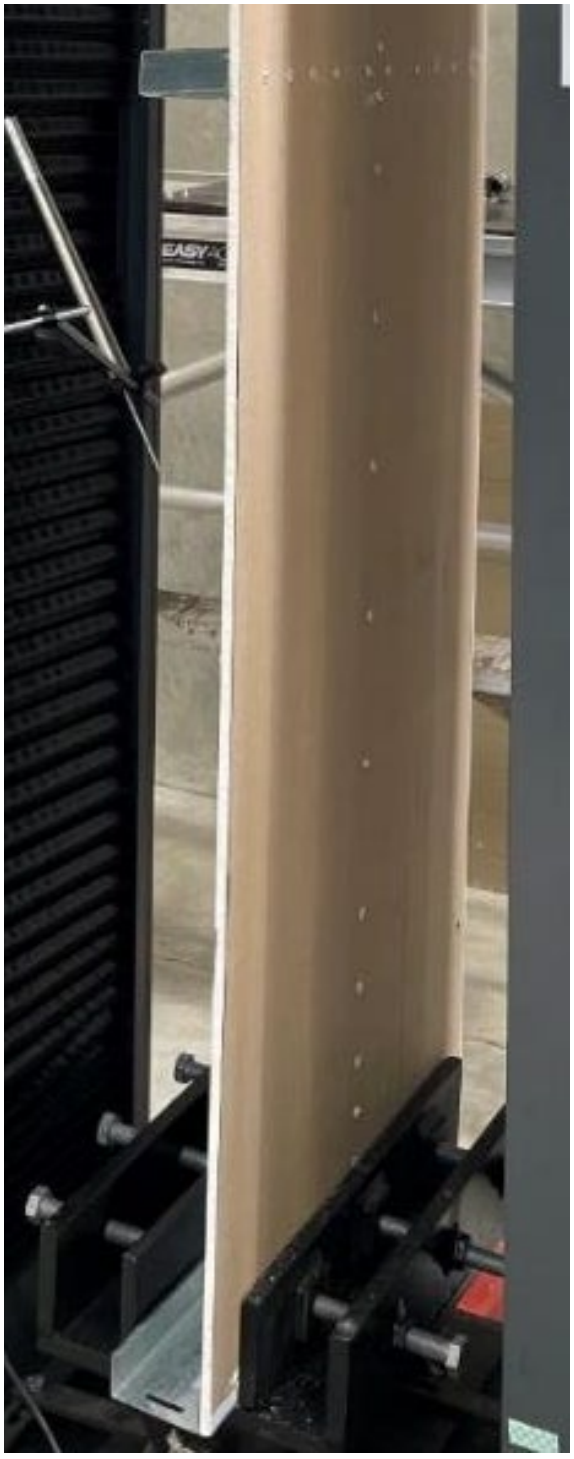
(a) Early-stage flange–web interaction and onset of distortional buckling.



(b) Large-amplitude post-buckling deformation of intermediate stud at ultimate stage.



(c) Gypsum-sheathed panel showing mid-height inward buckling of stud behind the sheathing.



(d) Sheathing cracking and screw-line crushing observed near ultimate load.



(e) Initial deformation of the EPL-sheathed panel with full sheathing engagement (The local indentation of the CFS flange).



(f) PIL-sheathed wall showing mid-height distortional buckling while sheathing remains attached.



(g) Controlled bearing indentation in the PIL board near ultimate load.

Figure 4-3 Representative local and distortional buckling modes observed in bare and sheathed axial compression specimens.

The bare frame showed earlier and more pronounced local flange deformation and distortional rotation. In contrast, the sheathed specimens-maintained attachment between the board and CFS framing during the main loading stage, which delayed

visible buckling deformation and modified the post-buckling response. Although the photographs provide only representative views of the deformed specimens, they support the measured trend that sheathing attachment increased axial resistance relative to the bare frame.

4.4.1. Bare frame behaviour

The bare CFS frames exhibited early local buckling of the compression flange, followed by distortional deformation involving flange–lip rotation. The absence of lateral restraint allowed flange displacement to develop freely, resulting in rapid stiffness degradation.

This behaviour is consistent with thin-walled stability theory, where local and distortional modes dominate in slender cold-formed sections (Hancock and Rasmussen, 1996; Schafer, 2002).

4.4.2. Sheathing-restrained behaviour

In contrast, the sheathed specimens demonstrated delayed buckling initiation because the attached panels provided restraint to the CFS stud along its height. This restraint limited flange out-of-plane displacement, provided rotational restraint at discrete screw locations, and distributed the stabilising effect along the stud rather than concentrating it at a single point.

The connection behaviour identified in Chapter 3 plays a critical role here. Progressive bearing deformation around screw holes allows limited local rotation while maintaining load transfer, thereby preventing immediate loss of stability.

This distributed restraint mechanism modifies the effective boundary conditions of the stud, increasing its critical buckling stress.

4.4.3. Interaction between connection stiffness and stability

The effectiveness of sheathing restraint depends on connection stiffness and spacing. A stiffer connection provides stronger rotational restraint but may concentrate stress locally. Conversely, progressive bearing deformation allows redistribution of compressive stresses along the stud length.

This interaction explains why SaveBOARD-sheathed specimens, despite lower elastic modulus, achieved comparable axial strength enhancement to gypsum-sheathed specimens. Stability improvement is governed by restraint continuity rather than by panel stiffness alone.

4.4.4. Implications for design

The findings suggest that:

1. Sheathing restraint significantly enhances axial stability in slender CFS wall panels, consistent with established instability theory for thin-walled members.
2. While slenderness sensitivity is a well-recognised characteristic of sheathing-braced CFS systems, the present results demonstrate that sustainable composite boards exhibiting progressive bearing behaviour can sustain distributed restraint even in highly slender studs.

3. The durability of restraint provided by SaveBOARD panels allows stability enhancement to be maintained beyond initial local deformation, highlighting the importance of post-buckling compatibility rather than initial stiffness alone.

These observations indicate that sustainable composite boards such as SaveBOARD are not merely stiffness-based alternatives to gypsum, but may provide structurally viable restraint mechanisms particularly in instability-governed axial load applications.

4.5. Structural interpretation and effectiveness of SaveBOARD sheathing

The experimental results reveal that the axial enhancement provided by sheathing is not governed solely by panel elastic stiffness. Although gypsum exhibits a substantially higher elastic modulus than the sustainable composite boards, the axial results did not show a direct proportional relationship between panel stiffness and ultimate axial resistance. The PIL-sheathed specimen achieved an ultimate axial resistance of 20.20 kN, corresponding to a 36.5% increase relative to the bare frame, which was comparable to the 20.25 kN and 36.8% increase achieved by the gypsum-sheathed specimen. In contrast, the EPL-sheathed specimen reached 18.80 kN, corresponding to a lower but still substantial increase of 27.0%.

This indicates that axial capacity enhancement in slender CFS wall panels is primarily controlled by sustained flange restraint and progressive screw-bearing interaction rather than by bending stiffness of the sheathing panel.

In the bare frame, axial failure was dominated by distortional buckling localised at mid-height, with rapid post-peak degradation. The addition of sheathing introduced

distributed rotational restraint along the stud length, modifying the instability mode from concentrated distortional buckling to a more distributed deformation pattern.

For gypsum panels, high initial stiffness provided strong early-stage restraint; however, brittle cracking reduced the effectiveness of restraint once local damage initiated. In contrast, SaveBOARD panels exhibited progressive bearing deformation at screw locations, enabling continued load transfer even after local yielding of the stud flange. This mechanism allowed composite action to be sustained beyond initial buckling, resulting in comparable ultimate capacity with improved deformation tolerance.

From a structural mechanics perspective, the effectiveness of SaveBOARD sheathing lies in its compatibility with thin-walled instability behaviour. The lower elastic modulus reduces initial stiffness slightly, but the enhanced tensile capacity and ductile bearing behaviour promote stable post-buckling load redistribution.

This suggests that, for slender CFS studs, the durability of restraint is more critical than the magnitude of initial stiffness.

The influence of stud thickness is interpreted in relation to thin-walled stability behaviour. Thinner studs are more susceptible to local and distortional buckling, and therefore the same level of sheathing restraint is expected to produce a greater relative stability benefit than in thicker studs. The present results support the broader mechanism that sheathing attachment delays buckling and increases axial resistance, but the available axial test matrix is not sufficient to establish a general quantitative relationship between stud thickness and restraint efficiency.

The axial compression results also show that initial stiffness and ultimate axial resistance should not be interpreted as identical indicators of sheathing restraint. Initial stiffness reflects the early elastic response of the test assembly and may be influenced by contact seating, screw slip and minor imperfections. Ultimate axial resistance, however, depends on whether the sheathing–screw system can continue to restrain flange displacement and rotation as buckling develops. This distinction explains why the PIL specimen could exhibit an initial stiffness similar to, or slightly lower than, the bare frame while still achieving a substantial increase in ultimate axial capacity.

Collectively, the results indicate that SaveBOARD sheathing can provide structurally effective buckling restraint within the tested axial configurations. The PIL specimen achieved ultimate axial capacity comparable to the gypsum-sheathed specimen, while the EPL specimen still provided a clear improvement relative to the bare frame. These observations suggest that the effectiveness of SaveBOARD sheathing arises from progressive composite interaction and deformation compatibility, rather than elastic rigidity alone.

4.6. Chapter summary

This chapter investigated the axial compression behaviour of full-height single-stud CFS wall subassemblies and evaluated the stabilising contribution of attached sheathing. Relative to the bare reference specimen, the addition of sheathing increased ultimate axial resistance by providing distributed lateral and rotational restraint to the slender CFS stud. The gypsum-, EPL- and PIL-sheathed specimens increased the ultimate axial resistance by 36.8%, 27.0% and 36.5%, respectively. Within the tested configurations,

the PIL specimen therefore achieved axial strength enhancement comparable to the gypsum reference, whereas EPL provided a lower but still substantial increase relative to the bare specimen.

The results also demonstrate that initial axial stiffness and ultimate axial resistance should not be interpreted as equivalent measures of sheathing effectiveness. Although gypsum provided the highest initial stiffness, PIL achieved a similar ultimate resistance despite its substantially lower panel elastic modulus. This indicates that axial stability depends not only on initial material stiffness but also on the ability of the sheathing–screw system to maintain lateral and rotational restraint as local and distortional buckling develops.

The observed deformation patterns further showed that sheathing attachment modified the buckling response of the CFS stud by reducing concentrated flange displacement and promoting a more distributed deformation pattern. The connection mechanisms identified in Chapter 3 provide a physical explanation for this response: progressive screw-bearing deformation allows load transfer and restraint to remain active after local deformation has initiated.

These findings address RQ1 by demonstrating that sustainable composite sheathing can provide structurally meaningful buckling restraint within the tested axial subassembly configurations. The results should not, however, be interpreted as complete multi-stud wall capacities because the tests were designed to isolate the response of a single repeated stud–sheathing–fastener unit.

Chapter 5 Cyclic lateral behaviour and axial–cyclic interaction of SaveBOARD-sheathed CFS walls

5.1. Role of connection mechanics in cyclic wall behaviour

While axial compression behaviour provides insight into instability restraint mechanisms, the structural performance of sheathed CFS wall systems under seismic and wind-induced loading demands is governed primarily by cyclic lateral response, as discussed in Chapter 1. Under reversed loading, degradation mechanisms at screw connections, progressive damage accumulation in sheathing, and redistribution of stresses along panel edges control global hysteretic behaviour.

As established in Chapter 3, connection behaviour in SaveBOARD panels is characterised by progressive bearing deformation rather than abrupt brittle fracture. This distinction is expected to influence cyclic hysteresis stability, stiffness degradation and energy dissipation characteristics at wall scale.

Furthermore, Chapter 4 demonstrated that sheathing attachment modifies stability behaviour through distributed restraint. Under cyclic loading, however, additional factors such as pinching, strength degradation and damage localisation must be considered.

This chapter addresses Research Questions RQ2–RQ4 by quantifying the cyclic load–displacement behaviour of the wall specimens, evaluating stiffness degradation and energy dissipation, examining the influence of screw spacing configuration, and assessing the effect of combined axial compression and cyclic lateral loading.

The experimental results presented herein integrate the connection-level findings of Chapter 3 with the stability mechanisms identified in Chapter 4.

5.2. Subassembly-level cyclic reference programme

5.2.1. Purpose and specimen configuration

A supplementary series of cyclic lateral tests was conducted on full-height single-stud CFS wall subassemblies to isolate the interaction between the central CFS stud, sheathing board and screw fasteners under reversed lateral deformation. The specimens had an overall height of 2400 mm and width of 600 mm and were sheathed on one side. These specimens should be interpreted as subassembly-level representations of a repeated stud–sheathing–fastener unit rather than complete multi-stud shear walls.

The subassembly cyclic programme included gypsum, EPL and PIL sheathing and examined the influence of screw spacing and framing thickness. The tested configurations included S1-PIL-50, S1-PIL-100, S1-PIL-150, S1-PIL-DE, S2-EPL-DE, S2-PIL-DE and S2-GYP-DE. The programme provided an intermediate experimental scale between the local screw-connection tests and the subsequent full-scale cyclic wall tests.

5.2.2. Loading protocol and data reduction

The cyclic subassembly tests were conducted using a horizontal reaction frame with the bottom horizontal member fixed and lateral displacement applied to the top member through a hydraulic actuator. A free-top boundary condition was adopted, allowing in-plane translation and rotation of the top member. This condition was selected to isolate

the stud–sheathing–fastener interaction rather than reproduce the diaphragm restraint of a complete building system.

Lateral displacement was applied under displacement control following Method B of ASTM E2126-19 at a loading rate of 2 mm/s. Single fully reversed cycles were applied at displacement amplitudes of 1.25, 2.5, 5, 7.5 and 10 mm, followed by three fully reversed cycles at each displacement level from 20 mm to 180 mm in increments of 20 mm. No constant axial load was applied during the subassembly cyclic tests.

5.2.3. Cyclic response and failure mechanisms

The cyclic subassemblies exhibited asymmetric hysteretic behaviour because of the free-top boundary condition and progressive damage accumulation. The gypsum-sheathed specimen exhibited high initial stiffness but pronounced pinching and rapid strength degradation following cracking along the screw lines. In contrast, EPL and PIL specimens generally showed more progressive bearing, crushing and tearing around the fasteners, allowing load transfer to be maintained over a larger deformation range.

Within the PIL subassembly series, screw spacing influenced both strength mobilisation and damage progression. The 50 mm spacing delayed connection damage and produced the strongest response within the tested spacing series, whereas the 150 mm spacing exhibited earlier panel separation and more pronounced cyclic degradation. These results established screw density as an important connection-level/system-transition variable and motivated the subsequent full-scale investigation of screw-spacing effects.

5.2.4. Role of the subassembly tests in the full-scale programme

The subassembly cyclic tests were not intended to replace full-scale wall testing. Instead, they provided a controlled intermediate scale for identifying the influence of sheathing type, connection density and framing characteristics on cyclic degradation. The subsequent full-scale cyclic wall programme therefore extended these observations to complete 1200 mm × 2400 mm wall specimens incorporating multiple studs, practical wall framing and a broader range of sustainable composite-board configurations.

5.3. Experimental programme and test matrix

To evaluate the cyclic lateral behaviour of SaveBOARD-sheathed CFS wall panels, a series of full-scale quasi-static reversed cyclic tests was conducted. The test programme was designed to systematically investigate the influence of sheathing type, screw spacing configuration and axial load condition on global hysteretic response.

All specimens were tested using a displacement-controlled loading protocol consistent with ASTM E2126-19. A free-top boundary condition was adopted, in which the top track was allowed to translate laterally and rotate in-plane without rotational restraint from a diaphragm.

5.3.1. Test setup

Lateral displacement was applied under displacement control following Method B of ASTM E2126-19 at a loading rate of 2 mm/s. The protocol comprised single fully reversed cycles at displacement amplitudes of 1.25, 2.5, 5, 7.5 and 10 mm, followed by

three fully reversed cycles at each displacement level from 20 mm to 180 mm in 20 mm increments.

The experimental setup is illustrated in Figure 5-1.

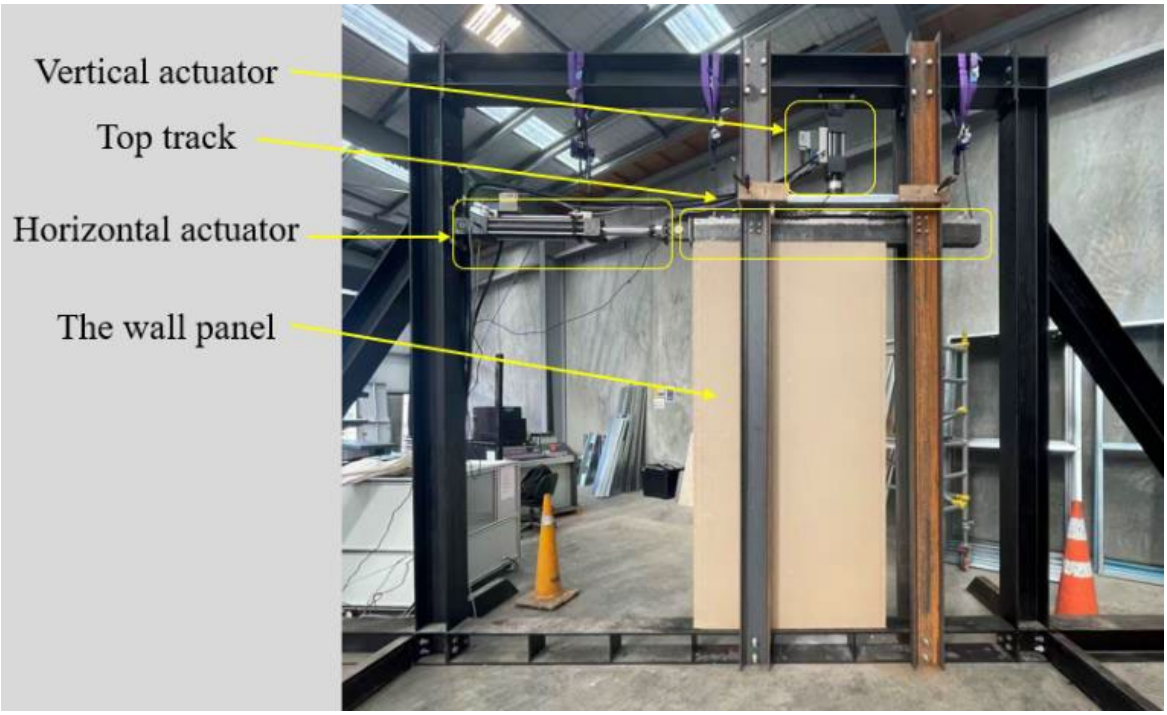


Figure 5-1 Cyclic lateral loading test setup.

The horizontal actuator applied cyclic displacement at the top track of the wall panel, while the bottom track was anchored to a rigid foundation beam. Out-of-plane bracing was provided to prevent global overturning unrelated to in-plane behaviour.

5.3.2. Loading protocol

Lateral displacement was applied under displacement control following Method B of ASTM E2126-19. The protocol consisted of single fully reversed cycles at amplitudes of 1.25, 2.5, 5, 7.5 and 10 mm, followed by three fully reversed cycles at each displacement amplitude from 20 mm to 180 mm in 20 mm increments. The loading rate

was maintained at 2 mm/s. Except for specimen S1-PIL-200-V, which was subjected to a constant axial load of 12 kN, the cyclic wall specimens were tested without additional axial compression.

5.3.3. Sheathing and framing variables

The cyclic test matrix included SaveBOARD-sheathed walls using the relevant EPL, PIL and RAB variants, together with gypsum-sheathed reference walls and specimens with different stud thicknesses. These configurations allowed the cyclic response of composite and conventional sheathing systems to be compared under identical loading conditions.

5.3.4. Screw spacing configuration

Screw spacing was selected as a primary variable to examine its influence on cyclic stiffness, strength, energy dissipation and damage localisation. The full-scale cyclic wall programme included uniform screw spacings of 100 mm, 150 mm and 200 mm, together with a densified-edge (DE) configuration. The 200 mm spacing was adopted as the reference configuration, while the 150 mm and 100 mm spacings were used to investigate the effect of increasing fastener density. The DE configuration was included to assess whether concentrating fasteners in high-demand edge and corner regions could improve load transfer and delay local connection damage without uniformly increasing fastener density across the wall.

The rationale for including densified-edge layouts is based on the connection-level findings in Chapter 3, where stress concentration and bearing behaviour were shown to

influence deformation stability. Screw spacing configurations including densified-edge arrangement in Appendix D.

5.3.5. Axial load application

One specimen was subjected to combined axial compression and cyclic lateral loading to provide preliminary insight into axial–cyclic interaction effects.

A constant axial load of 12 kN was applied to one specimen to provide a preliminary and indicative assessment of axial–cyclic interaction. The purpose of this single test was not to establish statistical trends, but to qualitatively examine how axial compression influences cyclic stiffness degradation, strength asymmetry and damage progression.

Although limited in scope, the results provide useful mechanistic observations regarding interaction between buckling restraint and connection-driven cyclic degradation.

Table 5-1 Summary of cyclic wall specimens and test parameters.

Parameter	Levels investigated	Relevance to practice
Sheathing type	GYP, PLY, RAB1, RAB2, PIL, EPL	Conventional vs sustainable alternatives
Stud thickness	0.75 mm and 1.05 mm nominal thicknesses in the cyclic wall programme	Representative thin-gauge and thicker light-gauge framing used to assess slenderness sensitivity
Screw spacing	100, 150, 200 mm; DE	Common installation ranges
Axial load	0 kN; 12 kN (single specimen)	Indicative gravity load effect

5.3.6. Instrumentation and data collection

During each cyclic test, the applied horizontal load and top displacement were recorded continuously. Local panel damage progression and screw deformation patterns were

also monitored through visual observation during and after loading. The measured load–displacement data were then used to derive hysteresis loops, from which the main response parameters, including initial stiffness, peak lateral strength, energy dissipation and ductility factor, were calculated.

5.3.7. EEEP idealisation and characteristic parameters

To provide a consistent quantitative comparison of the measured cyclic responses, the experimental envelope curves were idealised using an Equal Energy Elastic–Perfectly Plastic (EEEP) representation. Because the measured responses exhibited directional asymmetry, the positive and negative loading directions were evaluated separately.

For each loading direction, an experimental envelope was obtained by connecting the peak load at each imposed displacement amplitude. The peak load and corresponding displacement were then identified. The ultimate load was defined as 80% of the peak load on the descending branch, and the corresponding displacement was taken as the ultimate displacement. Where the measured response did not decrease to 80% of the peak load within the imposed displacement range, the displacement of the last completed cycle was adopted as the ultimate displacement.

The yield load and yield displacement were determined by enforcing equal energy between the measured envelope and the idealised elastic–perfectly plastic response up to the ultimate displacement. Initial stiffness was calculated from the resulting yield load and yield displacement, and ductility was evaluated from the ratio of ultimate

displacement to yield displacement. The same procedure was applied consistently to all specimens.

5.4. Hysteretic behaviour and load–displacement response

The full cyclic load–displacement responses are provided in Appendix E, and the complete characteristic parameters and failure photographs are provided in Appendices F and G. However, the key cyclic performance parameters are summarised in Table 5-2 so that the main experimental trends can be evaluated directly in this chapter.

Table 5-2 Representative cyclic performance parameters for selected wall specimens.

Specimen	Main variable represented	Peak lateral strength (kN)	Energy dissipation (kJ)	Main interpretation
S1-GYP-200	Gypsum reference, 200 mm screw spacing	4.25	0.22	Lowest strength and energy dissipation; brittle cracking and severe pinching
S1-PLY-200	Plywood reference, 200 mm screw spacing	11.10	0.65	Highest reference strength; strong but material-specific response
S1-PIL-200	PIL, 200 mm screw spacing	7.66	0.54	Stable composite-board response at reference screw spacing
S1-PIL-150	PIL, 150 mm screw spacing	9.35	0.63	Improved strength and energy dissipation relative to 200 mm spacing
S1-PIL-100	PIL, 100 mm screw spacing	10.26	0.51	Higher strength than 150 mm spacing but not proportional energy increase
S1-PIL-DE	PIL, densified-edge spacing	9.11	0.34	Densification improves local restraint but does not maximise energy dissipation
S1-RAB1-200	RAB1, 200 mm screw spacing	10.38	0.68	High strength and energy dissipation among SaveBOARD specimens
S1-RAB2-200	RAB2, 200 mm screw spacing	9.66	0.61	Stable response despite reduced board thickness
S1-EPL-200	EPL, 200 mm screw spacing	8.14	0.54	Comparable energy dissipation to PIL-200 with moderate strength
S1-PIL-200-V	PIL with 12 kN axial load	8.80	0.42	Indicative axial–cyclic interaction specimen; higher peak strength than PIL-200 but lower energy dissipation

This presentation of the results is intended to avoid unnecessary repetition while maintaining a clear link between the detailed experimental data and the interpretation developed in the main text. The appendix material provides the complete dataset and visual evidence for transparency and traceability, whereas Table 5-2 focuses on the parameters most relevant to comparing sheathing type, screw spacing configuration and axial-load condition. Therefore, the discussion in this chapter is based on the representative quantitative trends shown in Table 5-2, supported by the complete load–displacement curves, characteristic values and failure observations reported in the appendices.

5.4.1. Global hysteresis characteristics

All sheathed specimens exhibited stable hysteretic response up to peak load, followed by progressive stiffness degradation. However, distinct differences were observed between sheathing types.

Gypsum-sheathed specimens displayed noticeable pinching behaviour, abrupt stiffness degradation after peak load and localised cracking near the panel edges. In contrast, the SaveBOARD-sheathed specimens exhibited more gradual stiffness reduction, reduced pinching severity and more distributed damage progression. These differences are consistent with the connection-level observations in Chapter 3, where the composite boards demonstrated progressive bearing deformation around screw connections rather than brittle fracture.

5.4.2. Envelope curves

Backbone, or envelope, curves derived from the hysteresis loops are shown in Figure 5-2. These curves are used to compare the key lateral response characteristics of the tested wall specimens, including initial lateral stiffness, peak lateral capacity and post-peak softening behaviour. Although the gypsum-sheathed specimens exhibited slightly higher initial stiffness, the SaveBOARD-sheathed specimens achieved comparable peak lateral strength. This indicates that global shear capacity is not solely dependent on panel elastic modulus, but is also strongly influenced by screw connection behaviour and the ability of the sheathing–fastener interface to maintain load transfer during cyclic loading.

The curves in Figure 5-2 are experimental envelope curves extracted from the measured hysteresis loops. They should not be interpreted as smoothed analytical backbone curves. For each displacement amplitude, the peak load reached in the positive and negative loading directions was identified and connected to describe the evolution of lateral resistance.

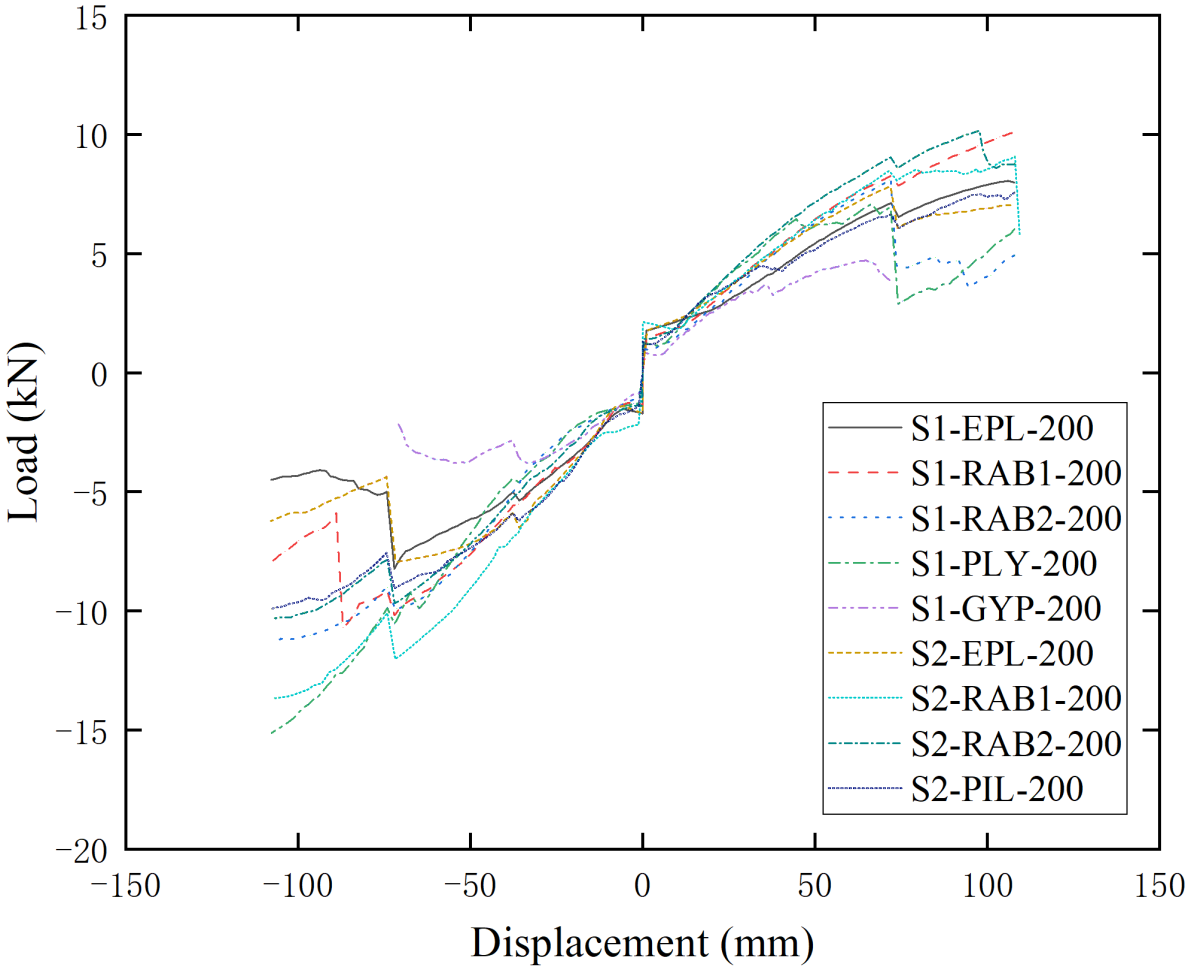


Figure 5-2 Experimental envelope curves derived from the measured cyclic hysteresis loops. (The curves connect the peak response points at successive displacement amplitudes and therefore retain the effects of experimentally observed damage progression and connection degradation.)

Therefore, local changes or sudden drops in the plotted response reflect experimentally observed damage events, such as screw slip, local bearing deformation, panel cracking or connection degradation. These features are retained in the figure because they represent the actual cyclic degradation behaviour of the tested wall specimens.

5.4.3. Energy dissipation

Energy dissipation per cycle, calculated as the area enclosed by each hysteresis loop, is illustrated in Figure 5-3. The derived and normalised lateral performance parameters for all sheathed CFS wall specimens are summarised in Appendix H.

Composite board specimens exhibited stable cumulative energy dissipation across increasing drift levels. This behaviour is associated with reduced pinching severity and sustained load transfer through progressive screw-bearing mechanisms.

In gypsum-sheathed walls, brittle cracking along screw lines resulted in abrupt stiffness degradation and limited force recovery during load reversal. Severe pinching reduced the enclosed hysteresis loop area by restricting reloading resistance, thereby diminishing cumulative energy absorption.

In contrast, the composite boards demonstrated distributed tearing and bearing deformation around fasteners, enabling continued shear transfer even after local damage initiation. This progressive mechanism preserved loop width at higher drift levels and delayed rapid energy deterioration.

The results suggest that energy dissipation in sheathed CFS walls is governed not only by peak lateral resistance but by the durability of composite action under cyclic degradation. Consequently, the enhanced cyclic stability observed in the tested sustainable composite-board specimens is attributed primarily to progressive screw-bearing deformation, distributed damage development and sustained load transfer, rather than to their lower elastic modulus.

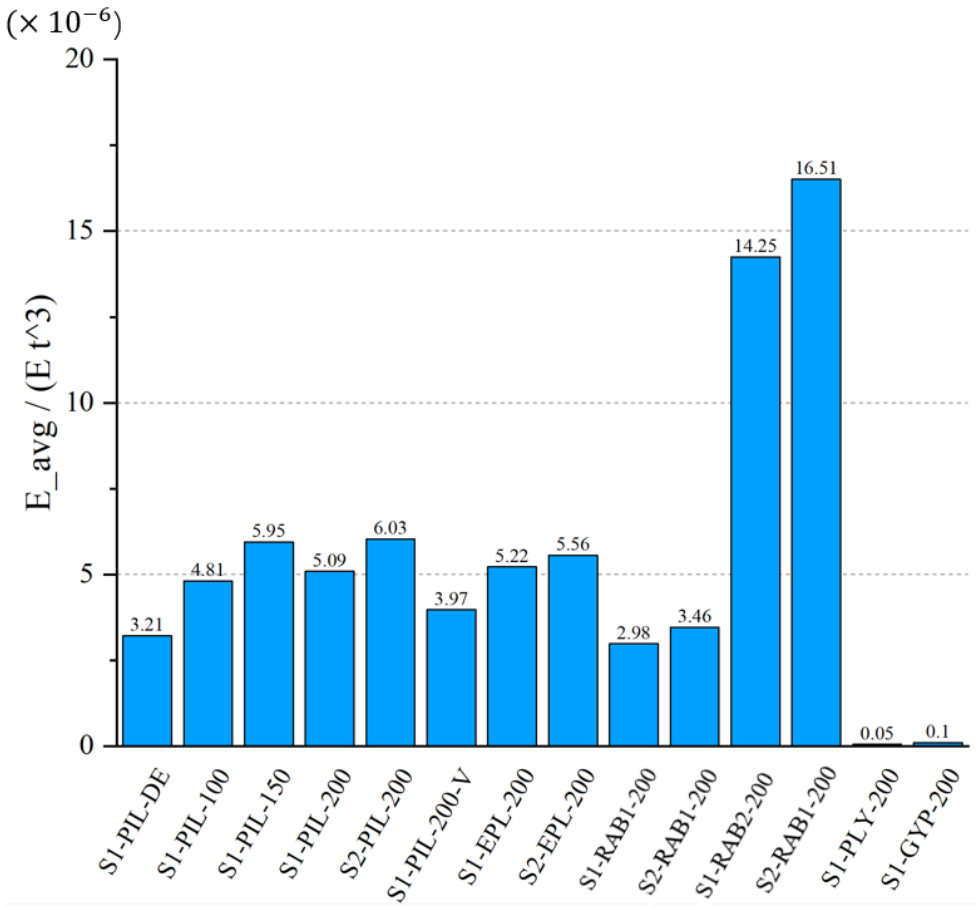


Figure 5-3 Energy dissipation comparison between sheathing types.

5.5. Influence of screw spacing and densified-edge configuration

Screw spacing plays a critical role in governing cyclic stiffness, strength and degradation behaviour of sheathed CFS wall systems. As identified in Chapter 3, connection behaviour determines rotational restraint and progressive damage accumulation. At wall scale, the spatial distribution of these discrete restraints directly influences hysteretic response.

5.5.1. Effect of uniform screw spacing

Representative backbone curves for different uniform screw spacing configurations are presented in Figure 5-4.

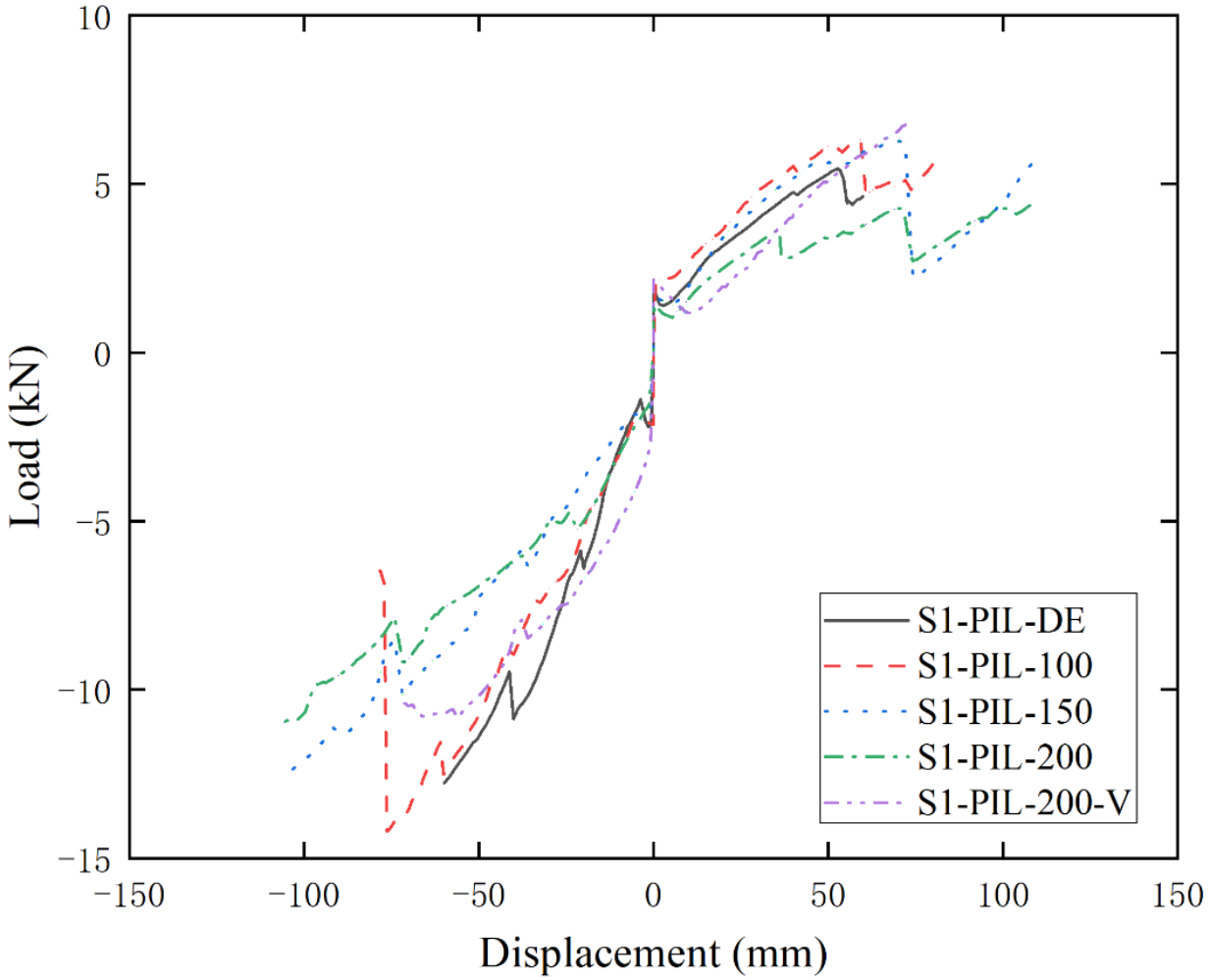


Figure 5-4 Backbone curves for different uniform screw spacing configurations.

Specimens with reduced screw spacing generally exhibited higher initial stiffness, increased peak lateral strength and lower inter-storey drift at equivalent load levels. This indicates that increasing fastener density improved load transfer between the sheathing and the CFS framing. However, the improvement was not proportional as screw spacing became closer, and diminishing returns were observed beyond a certain threshold. Although the number of active connections increased, stress concentration near the panel edges also intensified, which accelerated local damage progression and limited further gains in cyclic performance.

This indicates that cyclic performance enhancement through densification is nonlinear and influenced by local bearing capacity of the sheathing material.

5.5.2. Densified-edge configuration

Densified-edge layouts improved initial lateral stiffness, peak load capacity and the stability of hysteresis loops by increasing restraint in high-demand regions near the panel boundaries, where shear forces are concentrated. Unlike uniform densification across the entire panel, this edge-focused reinforcement strategy improves structural efficiency by strengthening the critical load-transfer regions without requiring excessive fastener use throughout the wall panel.

5.5.3. Mechanistic interpretation

The influence of screw spacing can be interpreted using the distributed spring model introduced in Chapter 4. Increasing fastener density effectively increases the lateral spring stiffness along the stud–panel interface.

However, if local bearing capacity is limited, excessive fastener density may lead to earlier damage localisation rather than improved global ductility.

The progressive bearing behaviour observed in SaveBOARD connections (Chapter 3) mitigates abrupt failure even under densified configurations, allowing stable hysteretic response across a range of spacing conditions.

This suggests that optimal screw spacing is material-dependent and cannot be directly transferred from gypsum-based detailing rules.

5.5.4. Design implications

The findings demonstrate that:

1. Screw spacing strongly influences cyclic pinching severity.
2. Moderate spacing provides a balance between stiffness and ductility.
3. Densified-edge detailing improves efficiency by targeting critical stress regions.
4. Composite boards may tolerate spacing variation better than brittle panels due to progressive crushing mechanisms.

These observations directly address **Research Question RQ3** and highlight the importance of connection-level mechanics in defining wall-scale cyclic performance.

5.6. Axial–cyclic interaction effects

To evaluate the influence of combined axial compression and cyclic lateral loading, selected wall specimens were subjected to constant vertical load during cyclic testing. The objective was to investigate how axial demand modifies hysteretic response, damage progression and stiffness degradation.

5.6.1. Global hysteretic response under combined loading

Representative hysteresis loops for specimens tested with and without axial compression are shown in Figure 5-4.

The presence of axial load increased the initial lateral stiffness, which can be attributed to enhanced friction and contact between framing components. However, beyond moderate drift levels, the specimens subjected to axial compression showed earlier

stiffness degradation, accelerated damage accumulation near the panel corners and slightly reduced deformation capacity. This behaviour indicates that axial load alters stress redistribution within the wall system by increasing compression demand in the framing members and accelerating local connection and panel damage under cyclic lateral loading.

5.6.2. Damage localisation and failure mode transition

Under combined loading, the compressive stress in the studs increased flange demand and modified the interaction between local buckling and lateral shear deformation. Failure observations showed greater damage concentration near the panel–stud interface at the lower corners, increased screw rotation in the compression zones, and earlier onset of local buckling compared with specimens subjected to purely lateral cyclic loading. This indicates that axial compression intensified local instability demand and accelerated connection-related damage in critical regions of the wall.

Figure 5-5 provides representative visual observations of damage progression in the cyclic-only and combined axial–cyclic specimens. The photographs are used as qualitative support for the measured cyclic response rather than as the sole basis for comparing damage severity. Because both specimens developed connection-dominated damage around the sheathing–fastener interface, the overall visual appearance of the two walls is similar. The main difference is interpreted from the combination of photographic observations, hysteresis response, stiffness degradation and energy dissipation trends.



(a) Comparison under cyclic-only loading.

(b) Comparison under axial–cyclic loading.

Figure 5-5 Representative damage progression observed in the cyclic-only and combined axial–cyclic PIL wall specimens. (The photographs provide qualitative visual evidence of connection-dominated damage and are interpreted together with the measured hysteresis response, stiffness degradation and energy dissipation results.)

The combined axial–cyclic specimen did not show a fundamentally different visual failure mode from the cyclic-only specimen. Instead, the effect of axial compression was reflected mainly in the progression of cyclic degradation and deformation capacity. This is consistent with the interpretation that the axial load modified the stability reserve of the CFS framing and accelerated damage accumulation, rather than creating a completely new failure mechanism. Because only one combined axial–cyclic specimen was tested, this comparison is treated as indicative mechanistic evidence.

5.6.3. Mechanistic interpretation

The observed behaviour can be interpreted as the coupling between axial compression-induced reduction in buckling reserve capacity and cyclic shear-induced progressive connection degradation. Under axial loading, the stud operates closer to its critical buckling state. When cyclic shear is superimposed, local rotation and bearing deformation at screw locations reduce the effective restraint stiffness provided by the sheathing–fastener system. As a result, the stabilising mechanism identified in Chapter 4 becomes progressively weakened under repeated cyclic deformation, leading to earlier stiffness degradation and more concentrated damage development under combined axial–cyclic loading.

However, SaveBOARD-sheathed specimens maintained relatively stable hysteresis despite axial load. This is attributed to the progressive crushing mechanism identified in Chapter 3, which allows redistribution of stresses rather than abrupt loss of restraint.

5.6.4. Implications for design and seismic performance

The axial–cyclic interaction results indicate that moderate axial load can enhance initial stiffness while reducing ultimate drift capacity. Under combined loading, stability–connection interaction becomes increasingly important, while the progressive bearing behaviour of the composite boards can mitigate abrupt degradation. Slender framing systems are nevertheless more sensitive to axial–cyclic coupling effects. These findings address Research Question RQ4 and highlight the importance of evaluating combined

loading conditions when assessing sustainable composite sheathing in structural applications.

5.7. Quantitative justification of key cyclic performance statements

This section provides a quantitative comparison of the principal cyclic performance trends using peak lateral strength, energy dissipation and the normalised performance measures introduced in the subsequent synthesis. The purpose is to relate the observed hysteretic and damage characteristics to measurable response parameters and to distinguish material effects from the influence of screw spacing and framing configuration. The aim is to demonstrate that the observed trends are supported by measurable differences in peak strength, energy dissipation and structural efficiency, rather than qualitative interpretation alone.

Like-for-like comparison of peak strength and energy dissipation. To distinguish the effect of sheathing material from the influence of screw spacing, material comparisons were made using specimens with the same framing series and nominal screw spacing. For the S1 specimens with a uniform 200 mm screw spacing, the gypsum-sheathed reference specimen S1-GYP-200 achieved a peak lateral strength of 4.25 kN and an energy dissipation of 0.22 kJ. Under the same nominal spacing, S1-PIL-200 achieved 7.66 kN and 0.54 kJ, S1-EPL-200 achieved 8.14 kN and 0.54 kJ, S1-RAB1-200 achieved 10.38 kN and 0.68 kJ, and S1-RAB2-200 achieved 9.66 kN and 0.61 kJ.

Within these tested configurations, the sustainable composite-board specimens therefore developed greater measured lateral resistance and energy dissipation than the

gypsum reference specimen under the same nominal framing series and screw spacing. These results support a configuration-specific comparison, rather than a general claim that sustainable composite boards universally outperform gypsum sheathing.

The observed differences are interpreted together with the measured hysteretic response and failure progression. The gypsum specimen exhibited localised cracking and pronounced pinching following damage initiation, whereas the sustainable composite boards generally developed more progressive bearing, crushing and distributed connection damage. This allowed load transfer to be maintained over a larger deformation range in the tested specimens.

Normalised structural efficiency and the “plywood dominance” issue. Direct comparison of absolute strength can be misleading because plywood has inherently higher elastic modulus. Once performance is normalised by stiffness potential (e.g., using the adopted stiffness-normalisation framework), the apparent dominance of plywood reduces substantially, and sustainable composite boards become competitive or superior in efficiency.

This can be illustrated by the stiffness-normalised energy dissipation indicator (Appendix H / Table 5): S1-RAB2-200 reaches 14.25 (stiffness-normalised energy index), and S2-RAB2-200 reaches 16.51, whereas S1-PLY-200 yields only 0.05 under the same normalisation basis.

Therefore, statements implying “SaveBOARD outperforms plywood” should be interpreted as efficiency in mobilising connection-based deformation and energy absorption, not as a claim that the raw absolute capacity of plywood is always lower.

Mechanistic linkage to pinching and damage progression. The quantitative trends above are consistent with the observed failure hierarchy: gypsum systems exhibit localised brittle cracking leading to rapid stiffness loss and severe pinching, while composite boards demonstrate progressive bearing deformation and more distributed panel participation. This distributed mechanism sustains load transfer and maintains broader hysteresis loops, which directly increases energy dissipation and reduces pinching severity.

Accordingly, the improved cyclic stability of sustainable composite boards in this study is best explained by **connection deformation stability and damage distribution**, rather than by panel elastic modulus alone.

Axial–cyclic interaction (scope-limited but defensible). A single specimen subjected to 12 kN axial compression provides preliminary insight into axial–cyclic interaction: compared with its non-axially-loaded counterpart, axial load increased initial stiffness and lateral resistance (partly by suppressing uplift and increasing frictional restraint), while reducing deformation capacity due to earlier local damage demand in the framing–sheathing system. This observation should be treated as indicative rather than generalisable, given the single-specimen scope.

5.8. Chapter summary

This chapter investigated the cyclic lateral behaviour of SaveBOARD-sheathed CFS wall systems and examined the influence of sheathing type, screw spacing, framing configuration and combined axial–cyclic loading. The cyclic results demonstrate that the global response is strongly governed by the evolution of the sheathing–fastener interface. Within the tested configurations, the sustainable composite-board specimens generally exhibited more gradual stiffness degradation and more distributed damage progression than the gypsum reference, consistent with the progressive bearing and crushing mechanisms identified at connection level.

Like-for-like comparisons also showed that the sustainable composite boards could develop substantial lateral resistance and energy dissipation despite their relatively low elastic modulus. For the S1 specimens with 200 mm screw spacing, the gypsum reference achieved a peak lateral strength of 4.25 kN and energy dissipation of 0.22 kJ, whereas the corresponding PIL specimen achieved 7.66 kN and 0.54 kJ. These results support the conclusion that cyclic performance is governed not only by panel stiffness but also by the ability of the connection system to maintain load transfer during progressive damage.

Screw spacing significantly affected strength mobilisation, energy dissipation and damage localisation. Within the PIL series, reducing spacing from 200 mm to 150 mm increased both peak resistance and energy dissipation, while further reduction to 100 mm increased peak strength without a proportional increase in energy dissipation. The densified-edge configuration further demonstrated that increasing fastener density in

critical regions can modify local restraint and damage progression, although the results do not establish a universal optimum screw spacing.

The combined axial–cyclic test provided preliminary evidence that sustained compression modifies the lateral response of the wall. The specimen subjected to 12 kN axial compression developed higher peak lateral resistance but lower energy dissipation than its cyclic-only counterpart, indicating that increased initial engagement may be accompanied by accelerated degradation and reduced deformation capacity. Because this conclusion is based on a single combined-loading specimen, it is interpreted as indicative rather than generalisable.

Collectively, the findings address RQ2–RQ4 and demonstrate that cyclic response in the tested CFS wall systems is controlled by the interaction between connection degradation, sheathing restraint, framing stability and fastener detailing. These results provide the experimental basis for the cross-scale synthesis and design-oriented interpretation developed in Chapter 6.

Chapter 6 Synthesis of experimental findings and design implications

6.1. Introduction

This chapter synthesises the experimental findings across the connection scale (Chapter 3) and wall scale (Chapters 4–5) to establish a mechanism-based interpretation of how sustainable composite sheathing modifies the structural response of CFS stud wall systems. Rather than restating results, the objective is to (i) clarify the hierarchy of governing mechanisms, (ii) explain why specific trends were observed under axial and cyclic loading, and (iii) translate those mechanisms into design-relevant detailing guidance for walls sheathed with sustainable composite boards.

The synthesis is structured around a "load path" perspective: load transfer in sheathed walls is mediated by screw connections, which mobilise the sheathing to provide restraint to stud instability under axial compression and to provide racking resistance under cyclic lateral loading. The test results show that sustainable composite boards do not simply behave as weaker substitutes for plywood or gypsum; instead, they shift the controlling mechanism towards distributed, progressive connection deformation and away from brittle panel fracture, which has direct implications for robustness and cyclic degradation.

The analytical expressions presented in this chapter are introduced as simplified conceptual or proportional relationships to assist interpretation of the experimental results. They are not intended as closed-form theoretical derivations, but rather as

physically motivated representations consistent with established stability and hysteretic response theory.

To avoid repeating the same numerical results throughout the synthesis chapter, the main experimental values used for cross-scale interpretation are summarised in Table 6-1. Later sections refer to this table when discussing the hierarchy of mechanisms, stability–connection coupling and design implications.

Table 6-1 Key experimental results used for synthesis and cross-scale interpretation.

Scale / comparison	Specimen or material	Key result	Interpretive purpose in Chapter 6
Axial compression	Bare frame	Ultimate axial resistance = 14.80 kN; initial stiffness = 2.303 kN/mm	Baseline axial response without sheathing restraint
Axial compression	Gypsum-sheathed specimen	Ultimate axial resistance = 20.25 kN; strength increase = 36.8%; initial stiffness = 2.933 kN/mm	Conventional sheathing reference for axial restraint
Axial compression	PIL-sheathed specimen	Ultimate axial resistance = 20.20 kN; strength increase = 36.5%; initial stiffness = 2.267 kN/mm	SaveBOARD axial restraint comparison with gypsum
Cyclic lateral, same spacing	S1-GYP-200	Peak lateral strength = 4.25 kN; energy dissipation = 0.22 kJ	Gypsum cyclic reference at 200 mm screw spacing
Cyclic lateral, same spacing	S1-PIL-200	Peak lateral strength = 7.66 kN; energy dissipation = 0.54 kJ	PIL cyclic response at the same 200 mm screw spacing
Cyclic lateral, screw spacing effect	S1-PIL-100	Peak lateral strength = 10.26 kN; energy dissipation = 0.51 kJ	Combined effect of PIL sheathing and increased fastener density
Combined axial–cyclic	S1-PIL-200-V	12 kN axial load; peak lateral strength = 8.80 kN; energy dissipation = 0.42 kJ	Indicative axial–cyclic interaction specimen

The values in Table 6-1 are used as representative synthesis data. They are not intended to replace the complete test datasets reported in the experimental chapters and appendices.

6.2. Hierarchy of structural mechanisms governing sheathed CFS walls

The experimental evidence obtained in this thesis indicates that, within the tested configurations, the structural behaviour of sheathed CFS wall systems was governed by a hierarchical interaction of mechanisms acting at multiple scales. This hierarchy can be quantitatively demonstrated rather than qualitatively inferred.

Table 6-2 Synthesis of experimental evidence and governing mechanisms across scales.

Scale	Experimental evidence	Observed mechanism	Implication for CFS wall behaviour	Design relevance
Connection scale	RAB and PIL screw connection tests showed progressive bearing deformation, screw tilting and local crushing around screw holes. Strength and displacement capacity increased with improved edge distance.	Local screw–sheathing interaction controls the onset of nonlinear deformation. SaveBOARD response is governed by progressive bearing and crushing rather than abrupt brittle fracture.	Connection degradation controls the durability of sheathing restraint and the severity of cyclic pinching.	Connection detailing, edge distance and screw placement should be treated as primary design variables for recycled composite sheathing.
Axial compression scale	Sheathed axial subassemblies achieved higher ultimate axial resistance than the bare frame. PIL achieved axial enhancement comparable to gypsum, while EPL provided a lower but meaningful improvement.	Sheathing–screw attachment provides lateral and rotational restraint to slender CFS studs and delays local or distortional buckling.	Axial capacity enhancement depends on sustained restraint during buckling development, not initial elastic stiffness alone.	SaveBOARD may be considered as a restraint-contributing sheathing material within the tested axial configurations, but complete wall design capacity requires further verification.
Cyclic wall scale	Within the tested configurations, SaveBOARD-sheathed specimens generally exhibited more gradual hysteretic degradation than the gypsum reference, supported by the measured strength, energy dissipation and observed damage progression.	Cyclic response is governed by progressive connection deformation, damage redistribution and fastener-density effects.	Wall-level strength and energy dissipation depend on both material-specific damage mode and screw spacing configuration.	Screw spacing should be optimised for the composite board rather than directly transferred from gypsum or plywood detailing practice.
Combined axial–cyclic scale	The single 12 kN axial–cyclic specimen indicated increased peak resistance but reduced energy dissipation compared with the corresponding cyclic-only specimen.	Axial load modifies stability reserve and accelerates cyclic damage progression without necessarily changing the basic connection-dominated failure hierarchy.	Axial compression may reduce deformation capacity even when peak lateral resistance increases.	Axial–cyclic interaction should be treated conservatively until additional axial load ratios and replicate specimens are tested.

The synthesis in Table 6-2 shows that the governing behaviour of SaveBOARD-sheathed CFS walls is controlled by the interaction between local connection damage, sheathing restraint and thin-walled framing stability.

6.2.1. Connection behaviour as the primary nonlinear trigger

At cyclic wall scale, degradation trends should be interpreted by separating material effects from fastener-density effects wherever possible. For like-for-like comparison at the same 200 mm screw spacing, the gypsum reference specimen S1-GYP-200 achieved a peak lateral strength of 4.25 kN and energy dissipation of 0.22 kJ, while the PIL specimen S1-PIL-200 achieved a peak lateral strength of 7.66 kN and energy dissipation of 0.54 kJ. Because both specimens used the same nominal screw spacing, this comparison more directly reflects differences in sheathing material response and connection degradation mechanism.

The PIL specimen showed higher lateral resistance and greater energy dissipation than the gypsum reference under the same spacing condition. This suggests that the cyclic response was influenced not only by the elastic modulus of the sheathing material, but also by the local screw–sheathing damage mechanism. The gypsum specimen was more strongly affected by brittle cracking and pinching, whereas the PIL specimen developed progressive bearing deformation and local crushing around screw connections.

The S1-PIL-100 specimen, which reached 10.26 kN, is used separately to discuss the additional influence of reduced screw spacing. It should not be interpreted as evidence of material effect alone because the comparison includes both material type and fastener density. This distinction separates material-related connection behaviour from the additional influence of fastener density on load-transfer capacity.

For the specimens tested in this study, global hysteretic stability was governed more strongly by connection deformation mode and damage progression than by panel elastic stiffness alone.

This suggests that the dominant nonlinear trigger in the tested wall specimens was local screw–sheathing interaction rather than frame yielding.

6.2.2. Sheathing restraint as axial stability modifier

The axial tests demonstrated that sheathing attachment can substantially modify the stability response of slender CFS studs, but the magnitude of the improvement was not proportional to initial panel stiffness. In particular, the similar ultimate resistance achieved by the PIL- and gypsum-sheathed specimens, despite their substantially different elastic properties, indicates that sustained connection-mediated restraint during nonlinear deformation is a key contributor to axial stability. This finding links the connection-level bearing behaviour observed in Chapter 3 with the wall-subassembly response reported in Chapter 4.

6.2.3. Framing slenderness as amplifier

Framing slenderness is interpreted as an amplifier of sheathing restraint effectiveness. According to thin-walled stability theory (Schafer, 2002), members with higher slenderness are more sensitive to changes in lateral and rotational restraint because their local and distortional buckling resistance is lower. Therefore, a given level of restraint provided by sheathing and screw connections is expected to have a greater relative influence on thinner studs than on thicker studs.

In this thesis, the experimental results show that sheathing attachment increased axial resistance relative to the bare frame. However, the available axial dataset is not used to derive a general quantitative relationship between stud thickness and restraint efficiency. Instead, slenderness is included in the hierarchical interpretation as a mechanics-based factor that controls the sensitivity of the CFS stud to connection-mediated sheathing restraint.

The hierarchy is therefore interpreted as follows: connection mechanism controls the durability of restraint, while framing slenderness controls the sensitivity of the stud to that restraint.

6.2.4. Unified hierarchical model

Based on the experimental linkage, wall performance may be conceptualised as:

$$\text{Wall Response} = f(\text{Connection Mechanism, Restraint Stiffness, Stud Slenderness, Load Combination}) \quad (2)$$

In this hierarchical model, the connection mechanism defines the degradation path of the wall system, while restraint stiffness controls the delay of local and distortional buckling. Framing slenderness then amplifies the influence of restraint loss, and the applied load combination modifies how demand is distributed between the CFS framing, sheathing panels and screw connections. This model provides a unified explanation for the major experimental trends observed across Chapters 3 to 5.

The unified mechanism can be summarised as the following load-transfer sequence:

external axial or lateral demand → CFS framing deformation → screw–sheathing load transfer → local bearing and crushing around screw holes → redistribution of restraint along the panel boundary → modification of stud buckling or cyclic hysteretic response.

This sequence explains why the structural response of SaveBOARD-sheathed CFS walls cannot be interpreted from sheathing elastic modulus alone. The recycled composite board contributes through connection-mediated restraint and progressive local deformation, which allows the sheathing to remain engaged during nonlinear wall response.

6.3. Stability–connection coupling mechanism

The experimental results demonstrate that axial stability and cyclic degradation are not independent phenomena in sheathed CFS wall systems. Instead, they are coupled through the evolution of connection stiffness and restraint effectiveness.

This section develops a unified interpretation of how connection deformation, buckling susceptibility, and load combination interact.

6.3.1. Axial restraint depends on connection rotational stiffness

From Chapter 4, axial capacity enhancement arises because sheathing restrains flange rotation and out-of-plane displacement. This restraint can be idealised as a distributed rotational spring system along the stud height.

The effective critical buckling load of a restrained stud may be expressed conceptually as:

$$P_{cr,restrained} = P_{cr,bare} \cdot \left(1+\alpha \frac{k_\theta}{k_{ref}}\right) \quad (3)$$

Where, k_θ = effective rotational stiffness provided by screw connections, k_{ref} = reference rotational stiffness, α= slenderness-dependent amplification factor.

As summarised in Table 6-X, both gypsum and PIL increased ultimate axial resistance by approximately 36% relative to the bare frame. This similarity in peak axial resistance, despite differences in initial stiffness and material properties, supports the interpretation that sustained connection-mediated restraint during buckling development is more important than initial elastic stiffness alone.

This suggests that axial strength enhancement is governed not by initial elastic stiffness alone, but by the ability of the screw–sheathing system to retain rotational restraint near peak load. In other words, sustained restraint during the critical buckling stage is more important than the initial stiffness measured at small deformation.

6.3.2. Cyclic loading progressively reduces rotational stiffness

Under cyclic lateral loading, screw connections experience progressive bearing indentation and rotation (Chapter 3). This reduces effective rotational stiffness $k_\theta$with increasing drift.

The hysteresis results illustrate this degradation effect. The gypsum-sheathed specimen S1-GYP-200 reached a peak lateral strength of 4.25 kN and dissipated 0.22 kJ of energy, whereas the PIL-sheathed specimen S1-PIL-100 reached a substantially higher peak lateral strength of 10.26 kN and dissipated 0.51 kJ of energy. This comparison indicates that the progressive bearing behaviour of PIL helped maintain more stable cyclic load

transfer and reduced the severity of degradation relative to the gypsum reference specimen.

Gypsum loses effective connection stiffness rapidly after cracking, causing pinching and accelerated degradation. In contrast, PIL maintains gradual bearing deformation, preserving partial rotational restraint during cyclic reversal.

Thus, cyclic degradation may be interpreted as:

$$k_\theta(\Delta) = k_{\theta,0} - \beta \cdot D(\Delta) \quad (4)$$

Where, $D(\Delta)$ = accumulated local damage as function of drift, β = degradation coefficient dependent on material fracture mode. For brittle panels (gypsum), β is high.

For progressive composite panels (PIL/EPL), β is lower.

6.3.3. Coupling under combined axial and cyclic loading

When axial compression is present during cyclic loading, the stud operates closer to its buckling threshold:

$$P_{applied} \rightarrow P_{cr,restrained} \quad (5)$$

Simultaneously, cyclic shear reduces k_θ via connection degradation.

Thus, two interacting processes occur: axial compression reduces the available stability margin of the CFS framing, while cyclic damage progressively reduces the rotational restraint provided by the screw–sheathing connections. Their interaction accelerates instability localisation and explains why combined loading reduced deformation capacity even when the initial lateral stiffness increased.

This coupling accelerates instability localisation and explains why combined loading reduced deformation capacity even when initial lateral stiffness increased. Mechanistically, the axial load increases compressive stress in the stud flanges, while cyclic rotation progressively reduces the local restraint provided by the screw–sheathing connections. As this restraint weakens, the effective buckling threshold of the CFS stud is reduced, causing instability to localise earlier under combined axial–cyclic loading. However, because the composite boards degrade progressively rather than catastrophically, the loss of restraint occurs gradually rather than abruptly. This explains why the SaveBOARD-sheathed specimens were still able to retain relatively stable hysteretic behaviour even under combined loading.

6.3.4. Unified coupling interpretation

The combined experimental evidence suggests the following coupled relationship:

$$\text{Wall Capacity} = f(P_{cr}(k_\theta), k_\theta(\Delta), \text{Stud Slenderness}, P_{axial}) \quad (6)$$

Where, P_{cr} increases with initial restraint stiffness, $k_\theta(\Delta)$ decreases with cyclic damage, Slenderness amplifies sensitivity, Axial load reduces stability reserve.

This formulation explains several key experimental observations. It clarifies why axial capacity enhancement can be similar for gypsum and PIL despite their differences in initial stiffness, because peak axial performance depends strongly on the retention of rotational restraint near the critical buckling stage. It also explains why cyclic pinching severity differs significantly between materials, as different sheathing materials exhibit different connection degradation and damage progression mechanisms. In addition, the

formulation accounts for the diminishing returns observed in densified screw layouts, where increased fastener density improves load transfer but also intensifies local stress concentration. Finally, it explains why axial–cyclic interaction reduces ductility by increasing stability demand while cyclic damage progressively weakens restraint. The key insight is that connection degradation modifies stability, while stability demand also modifies connection damage accumulation. These two mechanisms are therefore inseparable at the wall scale.

e.

6.4. Normalised performance and structural efficiency interpretation

Raw structural performance indicators such as peak lateral strength, initial stiffness and cumulative energy dissipation remain the primary basis for comparing the tested wall specimens. These absolute values are essential because they represent the direct structural demand that a wall can resist. However, absolute comparison alone may favour materials with inherently higher elastic modulus or greater thickness, without indicating how effectively a material–connection system mobilises its available mechanical capacity.

For this reason, normalised performance indicators are used in this section as secondary interpretive tools. They do not replace the absolute experimental results, and they are not intended to prove general superiority of one sheathing material over another. Instead, they provide an additional way to discuss how efficiently the tested sheathing–

connection systems mobilised strength, deformation capacity and energy dissipation within the specific configurations examined in this thesis.

6.4.1. Need for normalisation

The cyclic results provide a useful comparison of the selected specimens. The gypsum-sheathed specimen S1-GYP-200 achieved a peak lateral strength of 4.25 kN and dissipated 0.22 kJ of energy. In comparison, the PIL-sheathed specimen S1-PIL-100 achieved a peak strength of 10.26 kN and an energy dissipation of 0.51 kJ, while the plywood-sheathed specimen S1-PLY-200 reached 11.10 kN and 0.65 kJ. These results show that plywood achieved the highest absolute strength and energy dissipation among the selected specimens, while the PIL specimen also demonstrated substantial cyclic resistance despite the lower stiffness of the recycled composite board.

If interpreted solely by peak strength, plywood achieved the highest lateral resistance among the selected reference specimens, followed by PIL and then gypsum. This absolute comparison is important and should not be discounted. However, plywood also possesses substantially higher elastic modulus and stiffness potential than the recycled composite boards. Therefore, a secondary normalised comparison can help indicate whether the lower-stiffness composite boards mobilised their available material and connection capacity efficiently relative to their mechanical properties.

6.4.2. Thickness-normalised strength

Let the thickness-normalised lateral strength be defined as:

$$F_{norm,t} = \frac{F_{peak}}{t_{panel}} \quad (7)$$

This metric reduces the influence of panel thickness and provides a secondary indication of strength mobilised per unit panel thickness. Under this interpretation, the tested composite boards showed competitive thickness-normalised performance in selected configurations. This does not imply that thickness-normalised strength should replace absolute lateral resistance, but it suggests that the wall response was influenced by distributed connection deformation and damage progression, rather than by panel thickness alone.

6.4.3. Stiffness-normalised mobilisation efficiency

A more revealing metric is stiffness-normalised performance:

$$\eta_s = \frac{F_{peak}}{K_0} \quad (8)$$

Where, F_{peak}= peak lateral load, K_0= initial stiffness.

This ratio represents the drift capacity required to mobilise peak strength.

From Appendix H, S1-GYP-200 shows: $F_{peak} = 4.25$kN, $K_0 = 1.195$kN/mm.

Whereas S1-PIL-100 shows: $F_{peak} = 10.26$kN,$K_0 = 2.411$kN/mm.

For stiffness-normalised interpretation, like-for-like comparisons are made using specimens with the same screw spacing wherever possible. Therefore, S1-PIL-200 is compared with S1-GYP-200 when discussing material-related mobilisation efficiency. The S1-PIL-100 specimen is discussed separately as evidence of fastener-density effect, because reducing screw spacing from 200 mm to 100 mm changes the number of load-transfer points and therefore cannot be attributed to material behaviour alone.

Although PIL showed higher lateral resistance than gypsum in the selected comparison, its response should be interpreted in terms of gradual connection deformation rather than superior stiffness conversion. The stiffness-normalised ratio indicates that the tested composite-board system mobilised strength through a more progressive nonlinear response, while the gypsum reference was more strongly affected by brittle cracking and earlier degradation.

6.4.4. Energy efficiency index

Energy dissipation per unit strength may be defined as:

$$\eta_E = \frac{E_{total}}{F_{peak}} \tag{9}$$

Using Appendix H: Gypsum: $0.22/4.25 \approx 0.052$ kJ/kN, PIL-100: $0.51/10.26 \approx 0.050$kJ/kN, PLY-200: $0.65/11.10 \approx 0.059$kJ/kN.

While plywood exhibits slightly higher energy per unit strength, PIL achieves comparable efficiency despite lower intrinsic modulus and thickness.

This suggests that, within the selected cyclic wall configurations, sustainable composite boards were able to mobilise connection deformation into energy absorption effectively. However, this should be interpreted as a configuration-specific efficiency observation rather than a general conclusion that all SaveBOARD-sheathed CFS walls will outperform conventional systems.

6.4.5. Integrated efficiency interpretation

Combining the axial and cyclic results provides useful mechanistic insight, but the interpretation must remain limited to the tested configurations. The PIL axial specimen achieved an axial strength enhancement of approximately 36.5% relative to the bare frame, while the S1-PIL-100 cyclic specimen reached a peak lateral strength of approximately 10.26 kN. These results indicate that PIL was able to provide axial restraint and cyclic resistance in the tested wall configurations.

The combined interpretation suggests that the recycled composite board contributed through two linked mechanisms: restraint of CFS stud instability under axial compression, and progressive screw-bearing deformation under cyclic loading. However, these observations should not be interpreted as a universal efficiency ranking. They provide evidence that SaveBOARD can be structurally effective within the tested arrangements, while further testing is required before general design efficiency factors can be proposed.

6.4.6. Implications of normalised interpretation

Without normalisation, high-modulus panels may appear dominant in terms of absolute strength and stiffness, while lower-modulus composite boards may appear less effective. However, when performance is normalised against relevant material or structural parameters, the tested composite boards demonstrate competitive efficiency within the investigated configurations. This indicates that the observed performance differences are mechanism-driven rather than stiffness-driven alone. In particular, ductility,

damage progression, energy dissipation and connection deformation stability should be considered together with peak strength when comparing sustainable composite boards with conventional sheathing systems. This normalised framework therefore provides a rational basis for interpreting sustainable composite boards in performance-based design contexts.

It should also be noted that the normalised indices used in this section are interpretive rather than codified design parameters. They are sensitive to the selected normalisation basis, including panel thickness, elastic modulus, initial stiffness and energy dissipation definition. Therefore, the normalised results are used only to support mechanistic discussion of material utilisation and connection mobilisation. They should not be used independently to rank sheathing materials for design without considering absolute strength, stiffness, deformation capacity, failure mode and the limited number of specimens tested in this thesis.

6.5. Design implications for load-bearing CFS wall systems with sustainable composite sheathing

The experimental findings across connection, axial and cyclic loading scales provide several design-relevant insights for the application of sustainable composite boards such as SaveBOARD in load-bearing CFS wall systems.

The following implications are derived from the tested configurations and should be treated as preliminary guidance rather than design rules. They indicate how

SaveBOARD-sheathed CFS walls may be detailed and evaluated in future design development.

6.5.1. Connection detailing as a primary design parameter

The experimental findings indicate that connection detailing should be treated as a primary design parameter for CFS wall systems incorporating sustainable composite sheathing. Across the connection and wall-level tests, the global response was strongly influenced by the ability of the screw connections to transfer load between the sheathing and the CFS framing. Therefore, screw spacing, screw edge distance and local bearing behaviour should not be regarded only as construction details, but as variables that directly influence strength mobilisation, damage progression and cyclic degradation.

At connection scale, the edge-distance tests showed that local screw–sheathing response was governed by bearing deformation, screw rotation, local crushing and, in some cases, tearing near the loaded edge. Larger edge distances generally provided a greater surrounding material area for bearing deformation and stress redistribution, while smaller edge distances increased the likelihood of premature edge tearing or pull-through. This implies that adequate edge distance is important not only for local connection strength, but also for maintaining distributed restraint along the wall boundary under cyclic loading.

At wall scale, screw spacing influenced lateral strength, initial stiffness and hysteretic stability. Reducing screw spacing increased the number of load-transfer points between the sheathing and framing, but the benefit was not proportional to fastener density. The

PIL spacing series showed that reducing spacing from 200 mm to 150 mm increased both peak lateral strength and energy dissipation. However, further reduction to 100 mm increased peak strength but did not produce a proportional improvement in energy dissipation. This indicates that closer screw spacing can improve strength mobilisation, but excessive densification may concentrate local bearing damage and reduce the efficiency of cyclic energy dissipation.

The densified-edge configuration also supports this interpretation. Targeted increase of fastener density near high-demand edge regions can improve local restraint without uniformly increasing the number of fasteners over the whole wall. However, the results should be interpreted as preliminary because only selected configurations were tested. The practical implication is that screw detailing for SaveBOARD-sheathed CFS walls should aim to promote progressive bearing-dominated deformation rather than premature edge tearing. Detailing rules developed for brittle gypsum systems or stiffness-dominated wood-based systems should not be transferred directly to recycled composite boards without material-specific verification.

6.5.2. Axial load-bearing applications

The axial compression results show that sustainable composite sheathing can contribute to the axial stability of slender CFS wall subassemblies by providing lateral and rotational restraint through the screw-connected sheathing–frame interface. In the tested axial configurations, the bare frame reached an ultimate axial resistance of 14.80 kN. The gypsum-sheathed specimen reached 20.25 kN, corresponding to a 36.8%

increase relative to the bare frame. The EPL and PIL specimens reached 18.80 kN and 20.20 kN, corresponding to increases of 27.0% and 36.5%, respectively.

These results indicate that SaveBOARD sheathing can provide meaningful buckling restraint within the tested axial configurations. In particular, the PIL specimen achieved ultimate axial resistance comparable to the gypsum-sheathed specimen, while the EPL specimen provided a lower but still substantial improvement relative to the bare frame. Therefore, the axial performance of SaveBOARD should not be assessed only by comparing elastic modulus values with conventional sheathing materials. Although SaveBOARD has lower elastic stiffness than gypsum or plywood, its contribution to axial resistance depends on whether the sheathing–screw system can maintain restraint as local and distortional buckling develops.

The initial stiffness results should also be interpreted carefully. The gypsum specimen showed the highest initial stiffness, while the PIL specimen had an initial stiffness similar to, and slightly lower than, the bare frame. This does not negate the axial restraint contribution of PIL, because initial stiffness is sensitive to early seating, contact mobilisation, screw slip and the selected displacement range used for stiffness calculation. Ultimate axial resistance, post-initial restraint and observed buckling behaviour provide a more complete assessment of sheathing effectiveness.

For design interpretation, SaveBOARD sheathing may therefore be considered as a restraint-contributing material within the scope of the tested axial wall subassemblies. However, the axial specimens were full-height single-stud subassemblies rather than

complete multi-stud walls. The results should therefore be used to interpret the restraint mechanism of SaveBOARD sheathing, rather than to define complete wall design capacity. Further tests on complete multi-stud walls, different axial load ratios, different boundary conditions and additional replicate specimens are required before general axial design guidance can be established.

6.5.3. Cyclic and seismic performance considerations

The cyclic test results indicate that sustainable composite sheathing can provide stable lateral response when the screw–sheathing interface develops progressive bearing deformation rather than abrupt brittle fracture. For material comparison, specimens with the same screw spacing should be compared. At the same 200 mm screw spacing, the gypsum reference specimen S1-GYP-200 achieved a peak lateral strength of 4.25 kN and energy dissipation of 0.22 kJ, while the PIL specimen S1-PIL-200 achieved a peak lateral strength of 7.66 kN and energy dissipation of 0.54 kJ. This like-for-like comparison suggests that the PIL-sheathed wall mobilised greater lateral resistance and energy dissipation than the gypsum reference within the tested configuration.

The improved cyclic response is interpreted as a consequence of the progressive connection damage mechanism observed at connection scale. Gypsum-type brittle cracking tends to cause pinching and rapid stiffness degradation after local damage initiates. In contrast, SaveBOARD specimens developed more gradual local crushing and bearing deformation around the screws, allowing load transfer to be maintained over a larger deformation range. This mechanism is important for seismic and wind-

related cyclic performance because wall response is governed not only by peak strength, but also by the stability of hysteresis loops, resistance to pinching and the ability to redistribute local damage.

The screw spacing comparison further shows that detailing has a strong influence on cyclic performance. For the PIL specimens, reducing the screw spacing from 200 mm to 150 mm increased peak strength from 7.66 kN to 9.35 kN and increased energy dissipation from 0.54 kJ to 0.63 kJ. Further reducing the spacing to 100 mm increased peak strength to 10.26 kN, but energy dissipation decreased to 0.51 kJ. This indicates that closer screw spacing improves strength, but does not necessarily maximise energy dissipation or overall cyclic efficiency. Therefore, excessive fastener densification should not automatically be assumed to improve seismic performance.

Within the tested PIL configurations, the 150–200 mm screw spacing range provided a balanced response between strength mobilisation and distributed damage progression, while the 100 mm spacing increased peak resistance without proportional energy-dissipation benefit. This observation should be treated as preliminary and configuration-specific, not as a codified screw spacing recommendation. For future seismic design development, SaveBOARD-sheathed CFS walls should be assessed using peak strength, stiffness degradation, energy dissipation, deformation capacity and damage localisation together, rather than by peak strength alone.

6.5.4. Combined axial–cyclic loading

The combined axial–cyclic test provides preliminary evidence that gravity load can modify cyclic damage progression in SaveBOARD-sheathed CFS wall systems. In the test programme, one PIL wall specimen was subjected to a constant axial load of 12 kN during cyclic lateral loading. This specimen, S1-PIL-200-V, reached a peak lateral strength of 8.80 kN and energy dissipation of 0.42 kJ. Compared with the corresponding cyclic-only specimen S1-PIL-200, which reached 7.66 kN and 0.54 kJ, the combined axial–cyclic specimen showed higher peak strength but lower energy dissipation.

This behaviour suggests that axial compression may increase initial engagement of the CFS framing and temporarily increase lateral resistance, but may also reduce deformation capacity and accelerate cyclic degradation at larger drift levels. Mechanistically, the presence of axial load reduces the available stability reserve of the CFS stud. At the same time, cyclic loading progressively damages the screw–sheathing interface and reduces the effective restraint provided by the sheathing. The combined effect is a coupling between framing instability demand and connection degradation.

For design interpretation, axial load should therefore not be assumed to be beneficial simply because it may increase peak lateral resistance. In load-bearing seismic wall applications, the combined action of gravity load and cyclic lateral displacement may reduce ductility, energy dissipation and post-peak stability. Connection detailing becomes more important under combined demand because the sheathing–screw system must maintain restraint while the stud is simultaneously subjected to compression and lateral deformation.

However, the axial–cyclic conclusion must be treated cautiously because it is based on a single combined loading specimen. The result provides useful mechanistic evidence, but it does not establish a general axial–cyclic interaction rule. Additional tests with different axial load ratios, wall geometries, sheathing materials, screw spacing configurations and replicate specimens are required before design-level recommendations can be proposed.

6.5.5. Material selection and sustainability considerations

The results of this thesis indicate that SaveBOARD should not be evaluated simply as a lower-stiffness substitute for gypsum or plywood. Its structural contribution arises from a different mechanism. Rather than matching the elastic stiffness of conventional sheathing materials, SaveBOARD contributes through progressive screw-bearing deformation, local crushing around fasteners, distributed damage development and sustained connection-mediated restraint to CFS framing. This distinction is central to the design interpretation of recycled composite sheathing in CFS wall systems.

From a material selection perspective, plywood still provides high absolute strength and stiffness, while gypsum remains a widely used conventional reference material. However, the tested SaveBOARD specimens demonstrated that lower elastic modulus does not necessarily prevent a sheathing material from contributing to axial restraint and cyclic lateral resistance. The PIL specimen achieved axial strength enhancement comparable to gypsum in the tested axial configuration, and the cyclic tests showed that

SaveBOARD-sheathed walls can achieve stable hysteretic response through progressive connection deformation.

The design relevance of SaveBOARD should therefore be assessed using a combined set of performance criteria. These include peak strength, initial stiffness, deformation capacity, energy dissipation, damage progression, screw connection behaviour and buckling restraint. A stiffness-only comparison may underestimate the structural usefulness of recycled composite boards, while a peak-strength-only comparison may overlook differences in damage tolerance and cyclic degradation behaviour.

The sustainability motivation also remains important. SaveBOARD is manufactured from recycled packaging and soft plastics and is commercially available in New Zealand construction practice. Its use in CFS wall systems therefore has potential value not only as a structural sheathing option, but also as part of a broader circular-economy approach to building materials. The findings of this thesis support the structural feasibility of SaveBOARD sheathing within the tested configurations, but further work is required before broader design application can be recommended.

Future material selection should therefore consider both structural and environmental performance. Structurally, additional testing is required to verify long-term durability, moisture effects, fire performance, construction tolerance and behaviour under different wall configurations. Environmentally, the recycled content and local availability of SaveBOARD provide a practical reason to continue developing sustainable CFS wall systems. The main implication is that sustainable composite boards should be evaluated

through their actual sheathing–connection–framing interaction, rather than rejected solely on the basis of lower elastic modulus.

6.5.6. Scope of application

The design implications presented in this chapter are derived from the specific experimental and numerical configurations investigated in this thesis and should therefore be interpreted as mechanistic and preliminary guidance rather than codified design recommendations. The tested configurations represent selected CFS framing sections, sustainable composite board products, fastener arrangements, wall geometries, loading conditions and boundary conditions. A consolidated discussion of the experimental and numerical limitations of the research, together with recommendations for future work, is provided in Section 7.4.

6.5.7. Methodological implications

The modelling attempts highlight a broader methodological challenge in simulating sheathed CFS wall systems:

Accurate representation of connection-dominated degradation requires detailed contact and fracture modelling, yet full-scale wall models contain hundreds of discrete fastener interactions, leading to prohibitive computational demand.

This limitation suggests that future numerical work may require a more explicitly multi-scale modelling approach. In particular, connection-level calibrated spring elements may be needed to represent screw–sheathing deformation and degradation more efficiently, while hybrid modelling frameworks could combine detailed local models

with reduced-order global wall models. Although the modelling effort in this thesis did not produce a fully converged predictive wall-scale simulation, it provides valuable insight into the computational complexity inherent in connection-dominated structural systems.

6.6. Original contribution of the synthesis

The original contribution of this synthesis is the identification of SaveBOARD-sheathed CFS walls as connection-mediated composite systems rather than simple stiffness-based replacements for conventional sheathing. The experimental evidence shows that the recycled composite boards modify the governing wall response by promoting progressive screw-bearing deformation, distributed damage development and sustained restraint to thin-walled CFS framing.

This mechanism distinguishes SaveBOARD from brittle cracking-dominated gypsum systems and from stiffness-dominated wood-based comparisons. It explains why a lower-modulus recycled composite board can still provide meaningful axial restraint and cyclic resistance within the tested configurations. The thesis therefore contributes a mechanistic framework in which material properties, screw connection behaviour and framing stability are interpreted together, rather than as separate isolated parameters

6.7. Chapter summary

This chapter integrated the connection-, axial- and cyclic-scale findings into a unified interpretation of the structural behaviour of CFS wall systems incorporating sustainable composite sheathing. The synthesis identifies the screw–sheathing connection as the

principal mechanism through which the board becomes structurally engaged with the CFS framing. Connection deformation governs the transfer and redistribution of force, while the resulting restraint modifies the stability response of slender studs under axial compression and the degradation pathway of the wall under reversed cyclic loading.

The combined evidence indicates that the structural contribution of sustainable composite sheathing cannot be assessed using panel elastic modulus alone. Progressive bearing and crushing around screw connections allow restraint and load transfer to be maintained after local deformation begins, explaining why lower-modulus composite boards can provide meaningful axial restraint and cyclic resistance within the tested configurations. Framing slenderness, screw density and axial compression modify this response by changing the demand placed on the connection-mediated restraint system.

The normalised performance assessment provides a secondary means of interpreting how effectively different sheathing systems mobilise their available material and connection characteristics. These indices are used as interpretive tools rather than design parameters, and the absolute experimental strengths, stiffnesses, deformation capacities and failure modes remain the primary basis for structural comparison.

From a design perspective, the results indicate that sustainable composite sheathing should be treated as part of an interacting sheathing–connection–framing system. Connection detailing, edge distance, screw spacing and framing stability are therefore important design variables rather than secondary installation details. However, the

proposed implications remain preliminary and configuration-specific because the experimental database does not yet support codified design rules.

The principal contribution of this synthesis is therefore a mechanism-based framework that links local screw-bearing behaviour to wall-level axial stability and cyclic degradation. This framework provides the basis for the final conclusions in Chapter 7, where the findings are assessed directly against the research questions and the overall contributions and limitations of the thesis are established.

Chapter 7 Conclusions

7.1. Overview and research context

This thesis investigated the structural performance of cold-formed steel (CFS) wall systems incorporating sustainable composite sheathing, with specific reference to SaveBOARD panels used in New Zealand construction. The study was motivated by the need to evaluate whether recycled composite boards can provide structurally meaningful sheathing action in load-bearing CFS wall systems, rather than being considered only as non-structural lining or cladding-related products.

A multi-scale experimental framework was adopted to link material behaviour, screw connection response, axial compression behaviour and cyclic lateral wall performance. This framework allowed the global response of SaveBOARD-sheathed CFS walls to be interpreted through the interaction between local screw-bearing deformation, sheathing restraint and the stability sensitivity of thin-walled CFS studs. Within the tested configurations, the results indicate that SaveBOARD panels can contribute to axial restraint and cyclic lateral resistance through progressive connection-dominated deformation mechanisms. However, the conclusions are limited to the specimen geometries, screw details, boundary conditions, material products and loading conditions examined in this thesis.

7.2. Conclusions in relation to the research questions

The conclusions of this thesis are summarised below in relation to the four research questions defined in Chapter 1. This structure is used to maintain a direct link between the research gap, the experimental evidence and the final conclusions.

RQ1 asked how SaveBOARD sheathing influences the axial compression behaviour and buckling restraint of full-height single-stud CFS wall subassemblies compared with conventional sheathing systems. The axial compression tests showed that sheathing attachment increased the axial capacity of slender CFS wall specimens relative to the bare frame. The improvement was associated with distributed lateral and rotational restraint provided by the sheathing–screw system along the stud height. Within the tested axial configurations, the PIL specimen achieved axial strength enhancement comparable to the gypsum-sheathed specimen, while the EPL specimen achieved a lower but still meaningful improvement relative to the bare frame. These results indicate that SaveBOARD sheathing can provide effective buckling restraint, although the degree of improvement depends on the specific board product and specimen configuration.

The axial results also showed that restraint effectiveness is not governed by sheathing elastic modulus alone. Although SaveBOARD panels have lower elastic modulus than conventional gypsum or plywood materials, their progressive screw-bearing deformation allowed load transfer to be maintained after local deformation initiated. This suggests that, for slender CFS studs, the durability of restraint and connection deformation compatibility are important contributors to axial capacity enhancement.

Therefore, RQ1 is answered by concluding that SaveBOARD can act as a structurally effective sheathing restraint within the tested axial wall configurations, but further testing is required before general axial design recommendations can be established.

RQ2 asked to what extent the cyclic lateral response of SaveBOARD-sheathed CFS walls is governed by connection behaviour, and how this compares with conventional sheathing materials. The connection tests and cyclic wall tests together showed that the wall response was strongly influenced by local screw–sheathing interaction. SaveBOARD specimens generally exhibited progressive bearing deformation around screw connections, whereas brittle reference materials such as gypsum were more prone to abrupt local cracking and severe pinching. At wall scale, this connection behaviour contributed to more stable hysteretic response and more distributed damage progression in the tested SaveBOARD-sheathed specimens compared with the gypsum reference specimen.

The results therefore support the interpretation that the cyclic performance of SaveBOARD-sheathed CFS walls is connection-dominated. The governing mechanism is not simply the elastic stiffness of the sheathing panel, but the ability of the screw connection zone to sustain bearing deformation, redistribute local damage and maintain load transfer under repeated displacement reversals. RQ2 is answered by concluding that connection behaviour was a primary mechanism controlling cyclic response in the tested walls, and that SaveBOARD's progressive bearing-dominated response provided a more gradual degradation pathway than brittle panel fracture.

RQ3 asked how screw spacing configuration, including densified-edge detailing, interacts with composite board properties to influence strength, stiffness and energy dissipation. The cyclic wall tests showed that reducing screw spacing generally increased lateral strength and initial stiffness by increasing the number of active load-transfer points between the sheathing and CFS framing. However, the improvement was not proportional to fastener density. The comparison between different PIL screw spacing configurations indicated diminishing returns when screw spacing was reduced beyond a certain level. This behaviour suggests that closer spacing can improve load transfer, but excessive fastener density may concentrate local bearing damage and does not necessarily maximise energy dissipation.

Densified-edge detailing provided a further means of concentrating restraint in regions of high connection demand without uniformly increasing fastener density throughout the wall. However, the results also indicate that optimum screw spacing is material-dependent and should not be transferred directly from gypsum, plywood or steel-sheet sheathing systems to recycled composite boards without verification. RQ3 is answered by concluding that screw spacing is a primary design variable for SaveBOARD-sheathed CFS walls, but its effect must be interpreted through the interaction between fastener density, local bearing deformation and panel damage progression.

RQ4 asked how the combination of axial compression and cyclic lateral loading affects damage progression and deformation capacity in SaveBOARD-sheathed CFS wall systems. The single combined axial–cyclic specimen indicated that axial compression may increase initial lateral resistance by engaging the CFS framing more strongly, but

may also accelerate degradation and reduce deformation capacity at larger drift levels. This behaviour is consistent with the interaction between reduced stability reserve in the compressed stud and progressive degradation of screw connections under cyclic loading.

Because only one combined axial–cyclic specimen was tested, the RQ4 conclusion must be treated as indicative rather than generalisable. The test provides useful mechanistic evidence that axial load can modify the distribution and progression of cyclic damage, but it does not provide a sufficient statistical basis for design-level axial–cyclic interaction rules. RQ4 is therefore answered by concluding that axial compression influenced the cyclic damage pathway in the tested specimen, but additional tests with different axial load ratios, wall geometries and replicate specimens are required to establish general conclusions.

7.3. Contributions of the thesis

The main contribution of this thesis is the development of a multi-scale experimental understanding of SaveBOARD-sheathed CFS wall systems. The study provides material, connection, axial and cyclic wall-level evidence for a sustainable recycled composite board that has not been widely represented in peer-reviewed CFS wall databases. By linking screw connection behaviour to axial restraint and cyclic hysteresis, the thesis shows that the structural contribution of recycled composite sheathing cannot be assessed only through elastic stiffness or material strength. Instead, the governing response depends on the interaction between panel deformation, screw-bearing behaviour and the stability sensitivity of thin-walled CFS framing.

A second contribution is the identification of progressive bearing-dominated connection behaviour as a favourable mechanism for maintaining distributed load transfer. This mechanism helps explain why lower-stiffness composite boards can still provide meaningful axial and cyclic wall performance within the tested configurations. A third contribution is the demonstration that screw spacing and edge detailing should be considered material-dependent design parameters, because fastener density affects both strength mobilisation and damage localisation.

Overall, the thesis provides experimental evidence and mechanistic interpretation that can support future development of performance-informed design guidance for CFS walls incorporating sustainable composite sheathing.

7.4. Limitations and future research

The findings and conclusions of this thesis should be interpreted within the scope of the experimental and numerical programmes undertaken. Although the study provides a multi-scale investigation spanning material characterisation, screw connection behaviour, axial compression response and cyclic wall performance, the experimental database represents a defined range of CFS sections, SaveBOARD products, fastener details, wall geometries, loading protocols and boundary conditions. The results therefore establish behaviour and mechanisms for the tested configurations rather than universally applicable design relationships.

At the connection level, the experiments demonstrated clear effects of edge distance and sheathing type on connection strength, deformation capacity and failure

progression. However, screw installation torque and pre-tension were not directly measured or controlled beyond standard practical installation procedures. Consequently, any contribution from local clamping and friction could not be isolated from the bearing-dominated connection response. In addition, the tested ranges of board thickness, screw geometry and edge distance do not encompass all practical connection configurations. Future connection-level studies should include controlled screw installation torque, direct measurement of fastener pre-tension where practicable, additional board thicknesses and fastener types, and repeated specimens to quantify experimental variability and develop statistically supported connection models.

The axial compression programme was based on full-height single-stud wall subassemblies rather than complete multi-stud wall systems. This configuration was appropriate for isolating the restraint provided by the sheathing–screw system to an individual CFS stud, but it does not reproduce load sharing, boundary-stud effects or system-level interaction within a complete wall. The axial results should therefore be interpreted as evidence of sheathing restraint and buckling modification rather than as direct design capacities for complete walls. Further research should extend the axial programme to complete multi-stud walls, additional CFS section thicknesses and slenderness ratios, different sheathing configurations, alternative boundary conditions and replicated specimens. Such tests would allow the restraint contribution of sustainable composite sheathing to be quantified more generally and provide a stronger basis for design-oriented stability models.

The cyclic wall programme was conducted using a specific full-scale wall geometry under quasi-static reversed cyclic loading with selected screw-spacing configurations. Although the programme demonstrated the influence of sheathing type, framing thickness and fastener density, the conclusions are limited to the investigated specimen geometry, single-sided sheathing arrangement and free-top boundary condition. Dynamic and rate-dependent effects were not evaluated, and the response of walls with different aspect ratios, diaphragm restraint conditions, hold-down arrangements and alternative connection details remains to be established. Future work should therefore include repeated full-scale wall tests covering a wider range of geometries, restraint conditions and fastener layouts, together with dynamic or higher-rate loading where relevant to seismic performance.

The combined axial–cyclic investigation represents a particularly important limitation of the present study. Only one specimen was tested under a constant axial load of 12 kN. The resulting observations provide useful mechanistic evidence that axial compression can modify lateral resistance, deformation capacity and damage progression; however, they do not provide a sufficient basis for establishing a general axial-load interaction relationship. Future experimental programmes should investigate multiple axial load ratios, including repeated specimens at each load level, and should consider different framing slenderness levels, wall geometries and boundary conditions. This would allow the interaction between axial stability reserve, cyclic connection degradation and wall deformation capacity to be quantified systematically.

The numerical modelling programme also has defined limitations. The FE models were used primarily to support mechanistic interpretation rather than to provide a fully validated predictive design tool. The screw fasteners were represented explicitly using three-dimensional solid elements, which enabled local contact interaction to be considered but substantially increased contact complexity and computational demand. Fully detailed wall-scale simulations incorporating progressive board fracture, nonlinear contact and a large number of discrete fastener interactions encountered convergence and computational limitations. Mesh sensitivity was therefore assessed primarily at the level of deformation trends, and a fully converged predictive wall-scale fracture model was not achieved within the scope of the thesis.

Future numerical research should develop a calibrated multi-scale modelling framework in which experimentally derived screw connection laws are incorporated into computationally efficient wall-level models. Detailed local connection models could be used to establish nonlinear force–deformation and degradation relationships, which could then be represented using calibrated spring or connector elements at wall scale. Such an approach would provide a more practical route for conducting parametric studies of wall geometry, stud thickness, screw spacing and axial load interaction while retaining experimentally validated connection behaviour.

Finally, the present research focused primarily on short-term structural behaviour. Broader implementation of sustainable composite sheathing in load-bearing CFS wall systems will also require consideration of durability and service-environment effects. Moisture exposure, long-term material degradation, fire performance, construction

tolerances and installation variability were outside the scope of the present structural test programme. Future studies should investigate these factors alongside structural performance before general design recommendations or broader code-level implementation are proposed.

Overall, future research should progress from the controlled mechanistic experiments developed in this thesis towards larger and more statistically representative experimental databases, validated multi-scale numerical models and ultimately design-oriented assessment methods. Such work would allow the configuration-specific findings presented here to be extended towards reliable performance-based design guidance for CFS wall systems incorporating sustainable composite sheathing.

7.5. Closing statement

This thesis supports the structural feasibility of using sustainable composite sheathing in CFS wall systems within the tested configurations. The results indicate that SaveBOARD panels can contribute to axial restraint and cyclic lateral resistance through progressive screw-bearing deformation and distributed sheathing–frame interaction. Rather than acting as direct stiffness-based replacements for conventional gypsum or plywood, these recycled composite boards modify the degradation pathway of the wall system by promoting more gradual connection-dominated damage progression. With further testing and model development, the findings of this thesis can contribute to future performance-informed design approaches for sustainable sheathed CFS wall systems.

References

Abeysiriwardena, T., Peiris, M. and Mahendran, M. (2021). Local in-plane strength and stiffness of stud-to-sheathing fastener connections in LSF wall panels. *Thin-Walled Structures*, 160, 107383.

American Iron and Steel Institute (AISI) (2020). *North American standard for cold-formed steel framing—Lateral design (AISI S213)*. Washington, DC: AISI.

American Iron and Steel Institute (AISI) (2020). *North American standard for cold-formed steel structural framing (AISI S240-20)*. Washington, DC: AISI.

American Society for Testing and Materials (ASTM) (2017). *ASTM D790-17: Standard Test Methods for Flexural Properties of Unreinforced and Reinforced Plastics and Electrical Insulating Materials*. West Conshohocken, PA: ASTM International. Available at: https://www.astm.org/d0790-17.html (Accessed: 16 February 2026).

American Society for Testing and Materials (ASTM) (2019). *ASTM E2126-19: Standard test methods for cyclic (reversed) load test for shear resistance of vertical elements of the lateral force resisting systems for buildings*. West Conshohocken, PA: ASTM International.

American Society for Testing and Materials (ASTM) (2020). *ASTM D3500-20: Standard Test Methods for Structural Panels in Tension*. West Conshohocken, PA:

ASTM International. Available at: https://www.astm.org/d3500-20.html (Accessed: 16 February 2026).

Boudreault, F., Bruneau, M. and Tremblay, R. (2017). Cyclic behavior of composite board-sheathed cold-formed steel walls. *Journal of Structural Engineering (ASCE)*, 143(9), 04017052.

Brière, V., Becque, J. and Rogers, C.A. (2018). Cold-formed steel centre-sheathed (mid-ply) shear walls. *Engineering Structures*, 168, pp. 36–47.

Chen, B.Y. and Tay, T.E. (2017). Progressive damage in fibre-reinforced composites: Towards more accurate and efficient computational modelling and analysis. In: Beaumont, P., Soutis, C. and Hodzic, A. (eds.) *The Structural Integrity of Carbon Fiber Composites*. Cham: Springer, pp. 303–328.

Chen, J., Li, Q. and Schafer, B.W. (2015). Failure mechanisms of sheathing-to-cold-formed steel connections. *Thin-Walled Structures*, 94, pp. 112–123.

Chen, W., Ye, J. and Chen, T. (2016). Design of cold-formed steel screw connections with gypsum sheathing at ambient and elevated temperatures. *Applied Sciences*, 6(9), 248.

Cold-Formed Steel Engineers Institute (CFSEI) (2008) *Technical Note: Cold-Formed Steel Wall Systems*. Washington, DC: CFSEI. Available at: https://cfsei.memberclicks.net (Accessed: 16 February 2026).

DaBreo, J. and Rogers, C.A. (2014). Steel-sheathed cold-formed steel shear walls under combined loading. *Thin-Walled Structures*, 74, pp. 232–245.

Dujmović, D., et al. (2021). Application of failure criteria on plywood under bending. *Polymers*, 13(24), 4449.

EcoChoice Aotearoa (2025) *Eco Choice Aotearoa Certification – SaveBOARD*. Auckland: Eco Choice Aotearoa. Available at: https://www.ecochoiceaotearoa.org.nz (Accessed: 16 February 2026).

EPD Australasia (2025). *Environmental Product Declaration (EPD-IES-0014116:001) – saveBOARD Paperfaced Internal Wall and Ceiling Lining*. EPD-Australasia, valid 05 Jan 2025–05 Jan 2030.

Federal Emergency Management Agency (FEMA) (2000). *Prestandard and commentary for the seismic rehabilitation of buildings (FEMA 356)*. Washington, DC: FEMA.

Federal Emergency Management Agency (FEMA) (2005). *Improvement of nonlinear static seismic analysis procedures (FEMA 440)*. Washington, DC: FEMA.

Filiatrault, A. and Folz, B. (2002). Performance-based seismic design of woodframe buildings. I: Seismic demand analysis. *Journal of Structural Engineering (ASCE)*, 128(1), pp. 39–47.

Fiorino, L., Iuorio, O. and Landolfo, R. (2012). Seismic analysis of sheathing-braced cold-formed steel structures. *Engineering Structures*, 34, pp. 538–547.

Folz, B. and Filiatrault, A. (2001). *SAWS version 1.0—A computer program for seismic analysis of woodframe structures*. CUREE–Caltech Woodframe Project, SSRP-2001/09. La Jolla, CA: University of California, San Diego.

Fülöp, L.A. and Dubina, D. (2004). Performance of wall-stud cold-formed shear panels under monotonic and cyclic loading. *Thin-Walled Structures*, 42(2), pp. 321–338.

Fülöp, L.A. and Dubina, D. (2006a). Influence of fastener spacing on cold-formed steel shear walls. *Thin-Walled Structures*, 44(2), pp. 130–143.

Fülöp, L.A. and Dubina, D. (2006b). Seismic performance of cold-formed steel walls under combined loading. *Thin-Walled Structures*, 44(3), pp. 350–365.

Hancock, G.J. and Rasmussen, K.J.R. (1995). Design of cold-formed steel structures. *Thin-Walled Structures*, 23(1–4), pp. 1–19.

Hancock, G.J. and Rasmussen, K.J.R. (1996). Design of cold-formed steel columns. *Journal of Structural Engineering (ASCE)*, 122(12), pp. 1385–1393.

Huang, K., Roy, K., Hudd, R., Wang, W. and Lim, J.B.P. (2025). Structural behaviour of sustainable composite board and cold-formed steel connections: Experimental study. *Journal of Building Engineering*, 111, 113383.

Ibarra, L.F., Medina, R.A. and Krawinkler, H. (2005). Hysteretic models that incorporate strength and stiffness deterioration. *Earthquake Engineering & Structural Dynamics*, 34(12), pp. 1489–1511.

Kyvelou, P., Gardner, L. and Nethercot, D.A. (2017). Testing and analysis of composite cold-formed steel and wood-based flooring systems. *Journal of Structural Engineering (ASCE)*, 143(11), 04017146.

Landolfo, R., Della Corte, G. and Fiorino, L. (2006). Seismic behavior of sheathed cold-formed structures. *Journal of Structural Engineering (ASCE)*, 132(4), pp. 570–581.

Li, Q., Wang, Z. and Tian, Y.S. (2017). Experimental investigation of cold-formed steel shear walls with edge fastener variations. *Engineering Structures*, 150, pp. 52–66.

Li, Y. and Schafer, B.W. (2016). System-level behavior of cold-formed steel shear walls. *Journal of Constructional Steel Research*, 122, pp. 357–369.

Moen, C.D. and Schafer, B.W. (2008). Direct strength method for cold-formed steel members. *Thin-Walled Structures*, 46(7–9), pp. 741–760.

Mourad, S.A., Gendy, B.L. and Elsaied, R.M. (2026). Effect of connection type on the behaviour of cold-formed steel sheathed shear walls under monotonic loading. *Civil and Environmental Engineering*, 22(1), 0044.

Mulford Plastics (2023) *SaveBOARD Panel Product Information*. Auckland: Mulford Plastics. Available at: https://www.mulfordplastics.co.nz (Accessed: 16 February 2026).

Peck, Q., Rogers, C.A. and Serrette, R. (2012). Cold-formed steel framed gypsum shear walls: In-plane response. *Journal of Structural Engineering (ASCE)*, 138(7), pp. 932–941.

Pehlivan, B.M., et al. (2025). Seismic behavior of cold-formed steel framed multi-panel shear wall systems. *Bulletin of Earthquake Engineering*.

Peterman, K.D., Nakata, N. and Schafer, B.W. (2014). Hysteretic characterization of cold-formed steel stud-to-sheathing connections. *Journal of Constructional Steel Research*, 101, pp. 254–264.

Ringas, N. and Becque, J., 2023. Experimental characterisation of connection behaviour for sheathed cold-formed steel shear walls. *ce/papers*, 6(3–4), pp.135–144.

Rizk, R. (2018). Higher strength cold-formed steel framed steel shear walls for mid-rise construction. *American Iron and Steel Institute Research Report RP17-4*, July 2018.

Rogers, C.A. and Hancock, G.J. (1999). Screw-fastened connections in cold-formed steel construction. *Journal of Structural Engineering (ASCE)*, 125(9), pp. 961–970.

Rogers, C.A. and Fülöp, S., 2006. Influence of sheathing-to-frame connections on cyclic behaviour of cold-formed steel shear walls. *Thin-Walled Structures*, 44(12), pp.1258–1268.

SaveBOARD (2022) *SaveBOARD Technical Information and Product Data Sheet*. Auckland: saveBOARD Ltd. Available at: https://www.saveboard.nz (Accessed: 16 February 2026).

SaveBOARD (2024) *Environmental Product Declaration (EPD) – SaveBOARD Structural Board*. Auckland: saveBOARD Ltd. Available at: https://www.saveboard.nz/sustainability (Accessed: 16 February 2026).

Schafer, B.W. (2002). Local, distortional, and Euler buckling interaction in thin-walled members. *Journal of Structural Engineering (ASCE)*, 128(3), pp. 289–299.

Schafer, B.W. (2008). Review: The direct strength method of cold-formed steel member design. *Journal of Constructional Steel Research*, 64(7–8), pp. 766–778.

Serrette, R.L. (2003). *Estimating the response of cold-formed steel frame shear walls*. Research Report RP03-7. Washington, DC: American Iron and Steel Institute / Steel Framing Alliance.

Serrette, R.L. and Encalada, J.A. (1998). Static racking behavior of light-gauge steel stud walls. *Journal of Structural Engineering (ASCE)*, 124(8), pp. 919–925.

Serrette, R.L., Encalada, J., Juadines, M. and Nguyen, H. (1997). Static racking behavior of plywood, OSB, gypsum, and fiberboard walls with metal framing. *Journal of Structural Engineering (ASCE)*, 123(8), pp. 1079–1086.

Shamim, I. and Rogers, C.A. (2013). Steel-sheathed cold-formed steel shear walls under dynamic loading. *Thin-Walled Structures*, 71, pp. 57–71.

Standards Australia (2010). *AS 1720.1-2010: Timber structures*. Sydney: Standards Australia.

Telue, Y. and Mahendran, M. (2004). Behaviour and design of cold-formed steel wall frames lined with plasterboard on both sides. *Engineering Structures*, 26(5), pp. 567–579.

Tian, Y.S., Wang, J., Lu, T.J. and Barlow, C.Y. (2004). An experimental study on the axial behaviour of cold-formed steel wall studs and panels. *Thin-Walled Structures*, 42(4), pp. 557–573.

Tian, Y.S. and Wang, Y.C. (2008). Behavior of screw connections under cyclic loading. *Thin-Walled Structures*, 46(10), pp. 1219–1232.

Tian, Y.S. and Wang, Y.C. (2011). Axial load effects on cold-formed steel shear walls. *Engineering Structures*, 33(4), pp. 1100–1112.

Vieira, L.C.M. and Schafer, B.W. (2012). Lateral stiffness and strength of sheathing-braced cold-formed steel stud walls. *Engineering Structures*, 37, pp. 205–213.

Wu, H., Chao, S., Li, Y. and Sang, L. (2020). Experimental investigation of strengthened screw connection and application in CFS shear walls. *Journal of Constructional Steel Research*, 168, 105870.

Xu, L. and Martinez, J. (2006). Strength and stiffness determination of shear wall panels in cold-formed steel framing. *Thin-Walled Structures*, 44(10), pp. 1084–1095.

Zhang, B. and Xu, L. (2016). Cyclic behavior of cold-formed steel shear walls sheathed with wood-based panels. *Thin-Walled Structures*, 101, pp. 64–75.

Zhang, Z., Eladly, M., Rogers, C.A. and Schafer, B.W. (2024). Cold-formed steel framed shear wall test database. *Journal of Structural Engineering (ASCE)*, 150(10), 04024153.

Appendix A

Summary of mean tensile displacement and connection strength data of the RAB board (adapted from Huang et al., 2025).

The horizontal distances of screw to edge H (mm)	The vertical distances of screw to edge V (mm)	Mean tensile displacement l (mm)	Mean connection strengths P_{Exp} (kN)
25	10	5.21	1.64
	15	6.91	2.04
	20	7.81	2.60
	25	6.60	3.22
	30	7.89	3.38
	35	9.03	3.51
	40	10.13	3.30
60	10	3.16	1.52
	20	5.73	2.38
	30	7.42	2.98
	40	11.58	3.53
	50	15.50	4.07
40	40	11.12	3.25
45	45	13.50	3.45
50	50	21.51	4.26
55	55	20.43	4.61
60	60	19.20	4.69

Summary of mean tensile displacement and connection strength data of the PIL board (adapted from Huang et al., 2025).

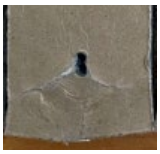
The horizontal distances of screw to edge H (mm)	The vertical distances of screw to edge V (mm)	Mean tensile displacement l (mm)	Mean connection strengths P_{Exp} (kN)
25	10	5.12	1.64
	15	7.52	2.04
	20	9.39	2.60
	25	8.68	3.22
	30	9.36	3.38
	35	11.25	3.51
20	50	8.18	1.52
30		11.58	2.38
40		13.38	2.98
50		18.13	3.53
60		20.17	4.07
30	30	11.50	3.10
35	35	11.84	3.25
40	40	15.59	3.83
45	45	16.44	3.77

Summary of mean tensile displacement and connection strength data of the PLY board (adapted from Huang et al., 2025).

The horizontal distances of screw to edge H (mm)	The vertical distances of screw to edge V (mm)	Mean tensile displacement l (mm)	Mean connection strengths P_{Exp} (kN)
25	10	3.29	1.67
	15	6.28	2.29
	20	8.74	2.81
	25	12.91	2.48
	30	15.59	2.57

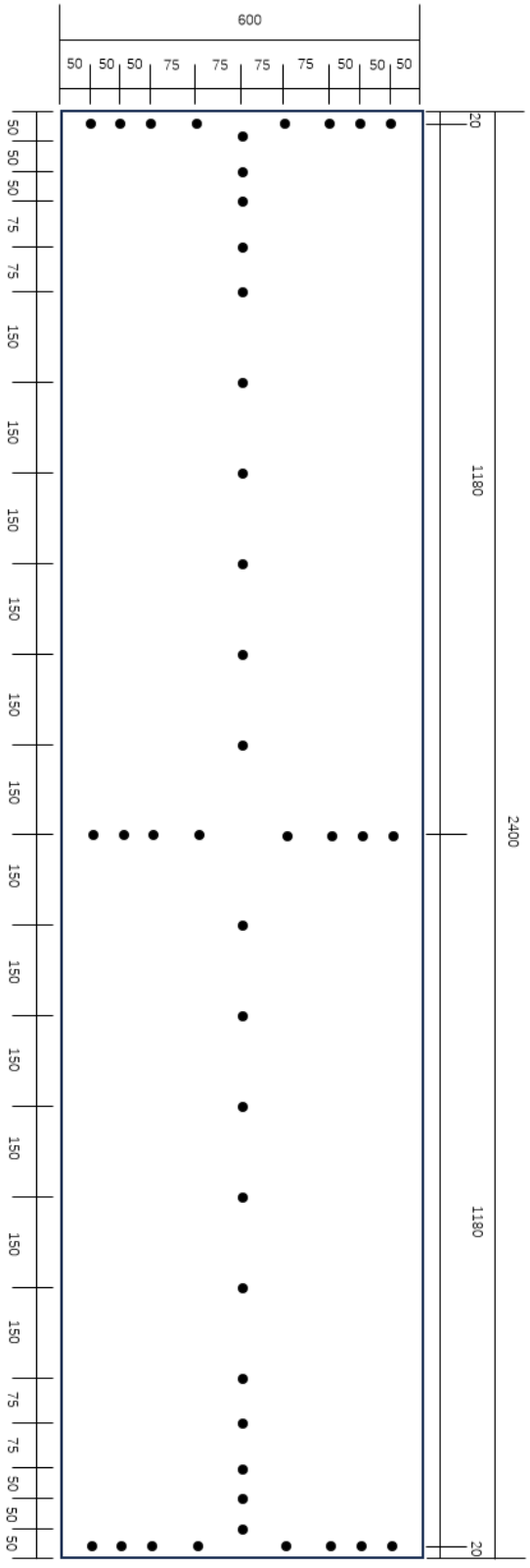
Appendix B

The comparison results (adapted from Huang et al., 2025).

				
RAB-H25-V10 *S*、*Tear*	RAB-H25-V15 *S*、*C*、*Tear*	RAB-H25-V20 *S*、*C*、*Tear*	RAB-H25-V25 *T*、*C*、*Tear*	RAB-H25-V30 *T*、*C*
				
RAB-H25-V35 *T*、*C*	RAB-H25-V40 *S*、*C*	RAB-H60-V10 *S*、*C*、*Tear*	RAB-H60-V20 *S*、*C*、*Tear*	RAB-H60-V30 *S*、*C*、*Tear*
				
RAB-H60-V40 *S*、*C*、*Tear*	RAB-H60-V50 *C*、*Tear*	RAB-H60-V60 *C*	RAB-H40-V40 *T*、*C*、*Tear*	RAB-H45-V45 *T*、*C*、*Tear*
				
RAB-H50-V50 *C*	PIL-H55-V55 *C*	PIL-H25-V10 *S*、*Tear*	PIL-H25-V15 *S*、*C*、*Tear*	PIL-H25-V20 *S*、*C*、*Tear*
				
PIL-H25-V25 *T*、*S*、*C*、*Tear*	PIL-H25-V30 *T*、*C*	PIL-H25-V35 *T*、*C*	PIL-H20-V50 *T*、*C*	PIL-H30-V50 *T*、*C*
				
PIL-H40-V50 *T*、*C*	PIL-H50-V50 *C*	PIL-H60-V50 *C*	PIL-H30-V30 *T*、*S*、*C*、*Tear*	PIL-H35-V35 *T*、*S*、*C*、*Tear*
				
PIL-H40-V40 *T*、*S*、*C*、*Tear*	PIL-H45-V45 *C*			

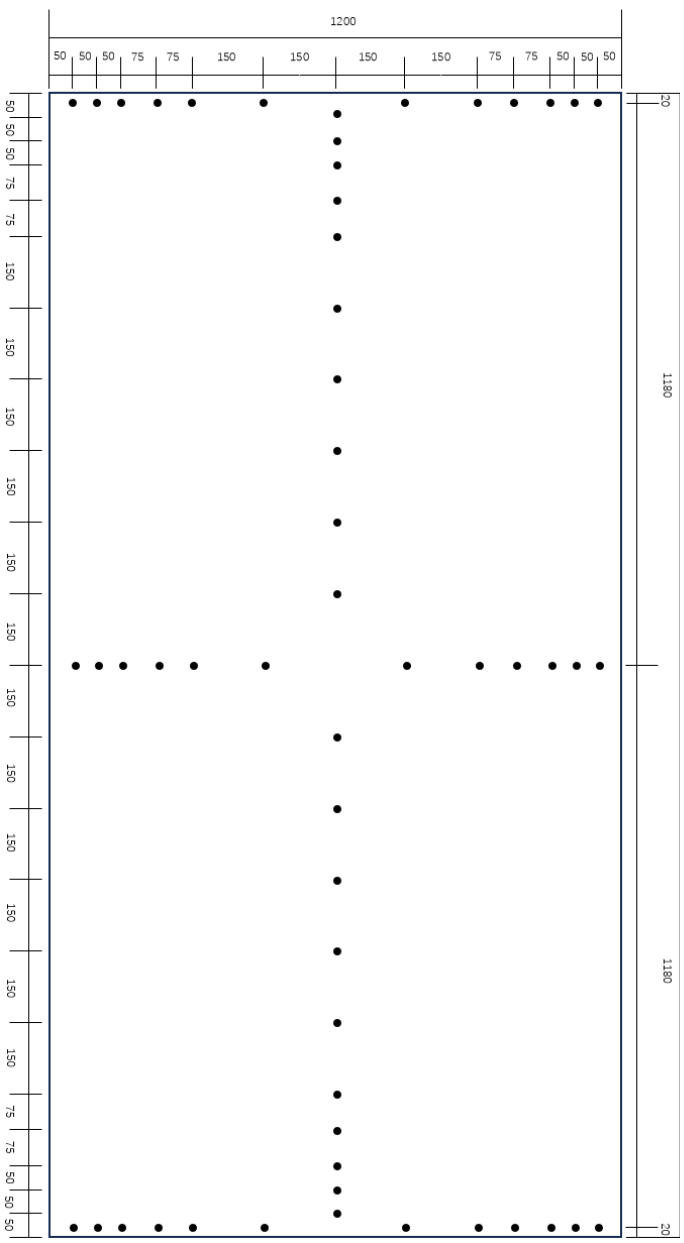
Appendix C

Summary of axial wall test specimens and spacing of screws.

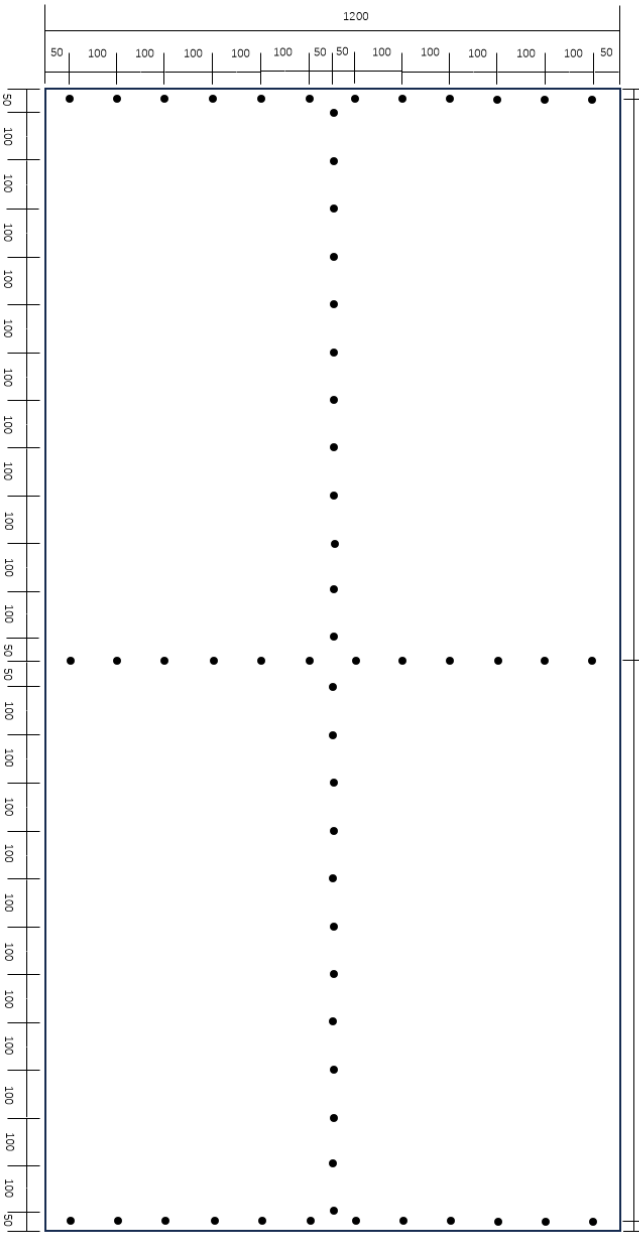


Appendix D

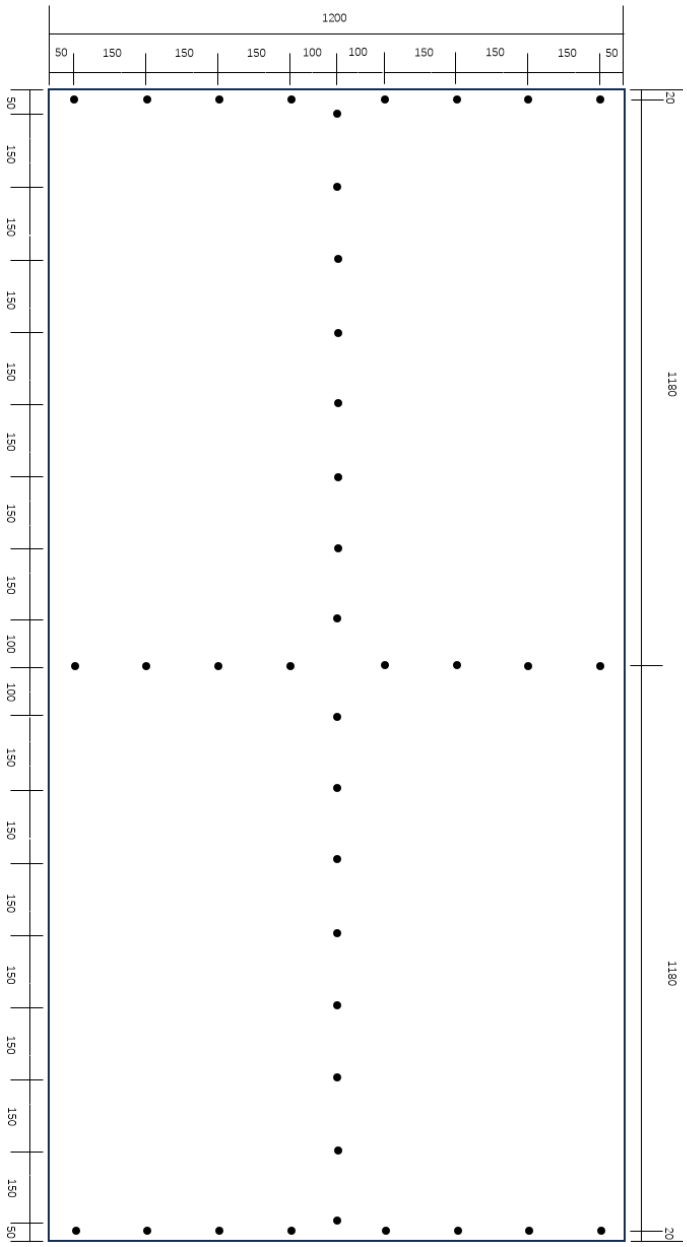
Screw spacing configurations adopted in the tests.



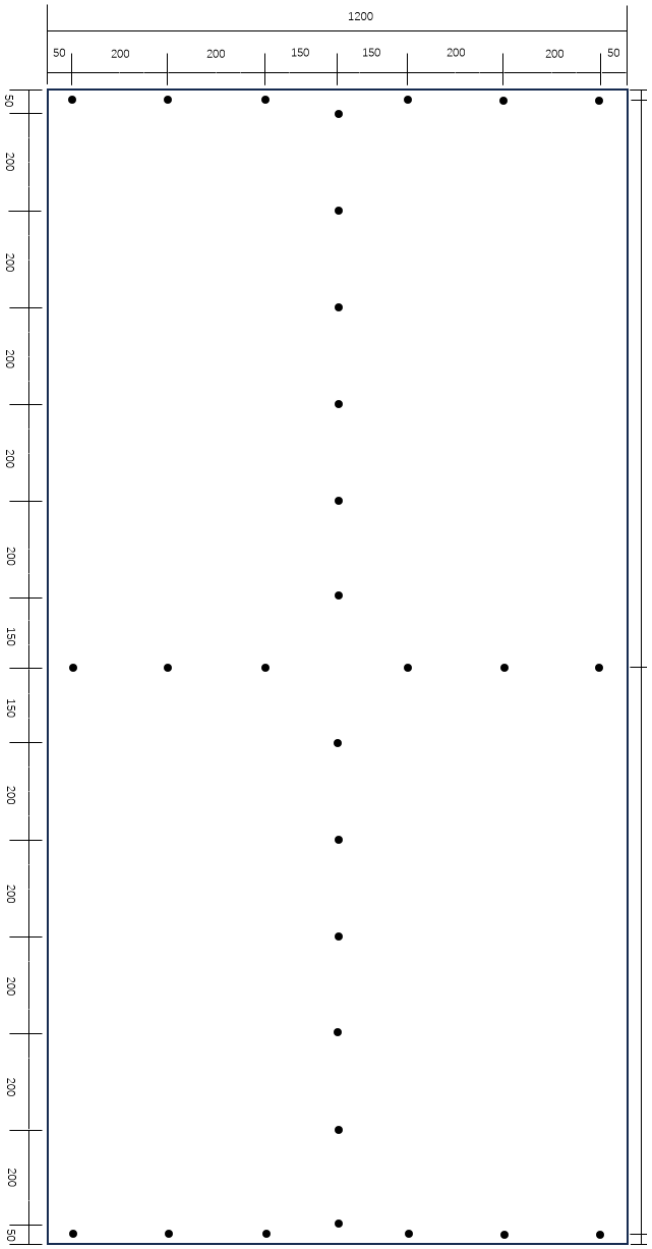
(c) The DE spacing of screws



(d) The 100mm spacing of screws



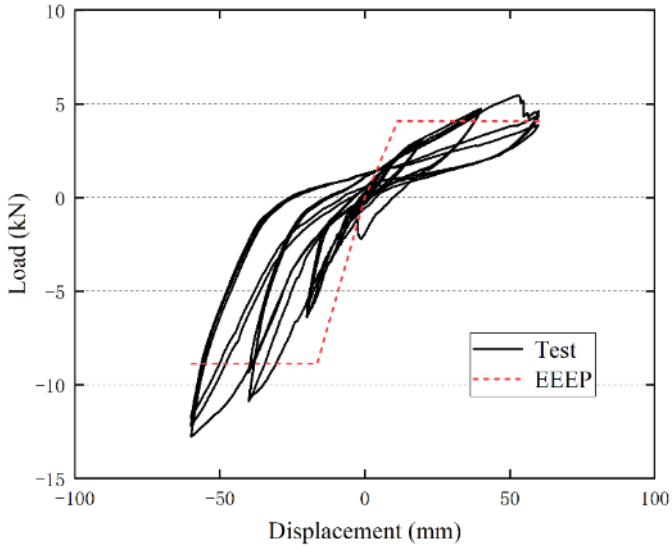
(e) The 150mm spacing of screws



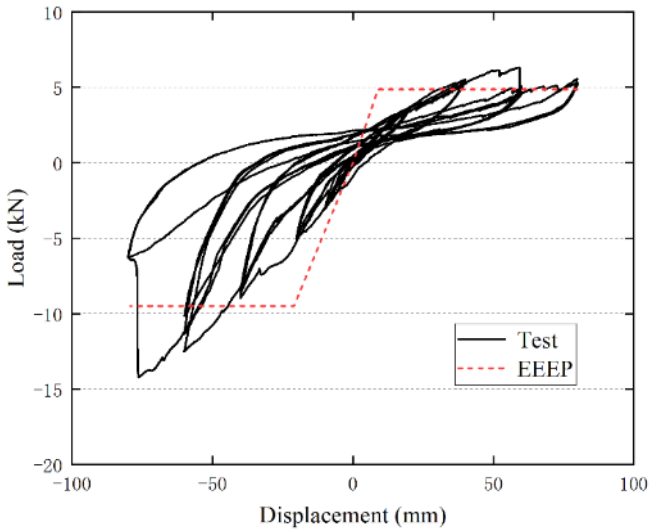
(f) The 200mm spacing of screws

Appendix E

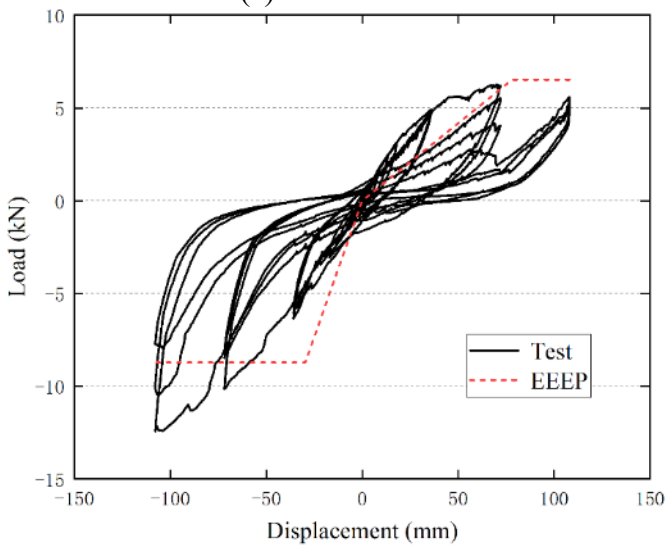
Hysteresis responses and corresponding EEEP idealisations of all tested specimens, illustrating the influence of sheathing type, screw spacing and framing thickness.



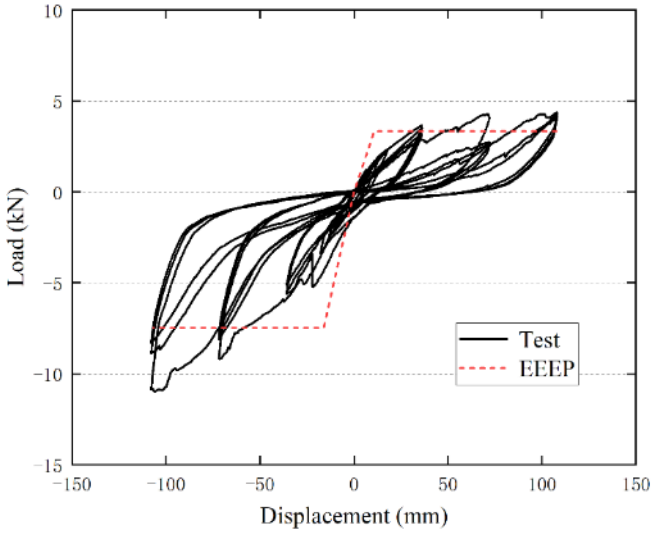
(a) S1-PIL-DE



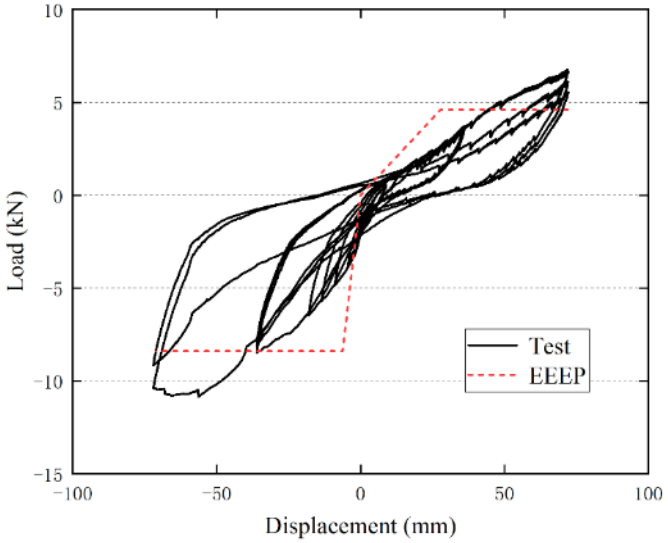
(b) S1-PIL-100



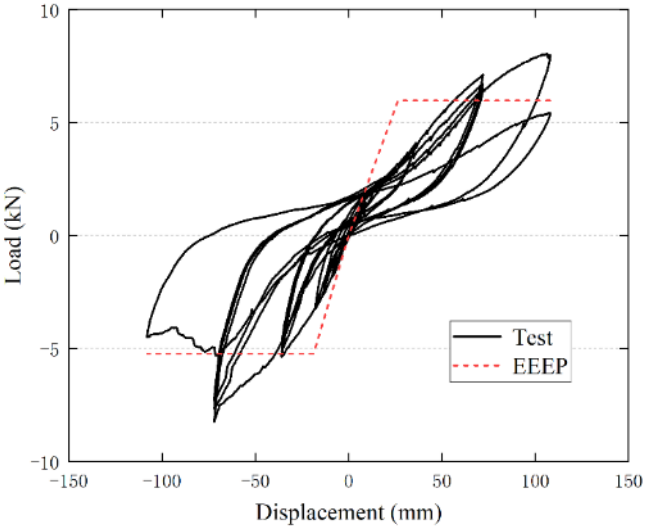
(c) S1-PIL-150



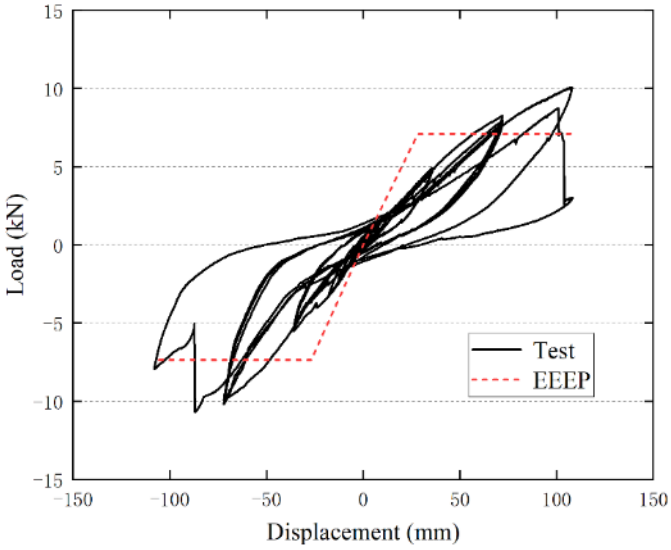
(d) S1-PIL-200



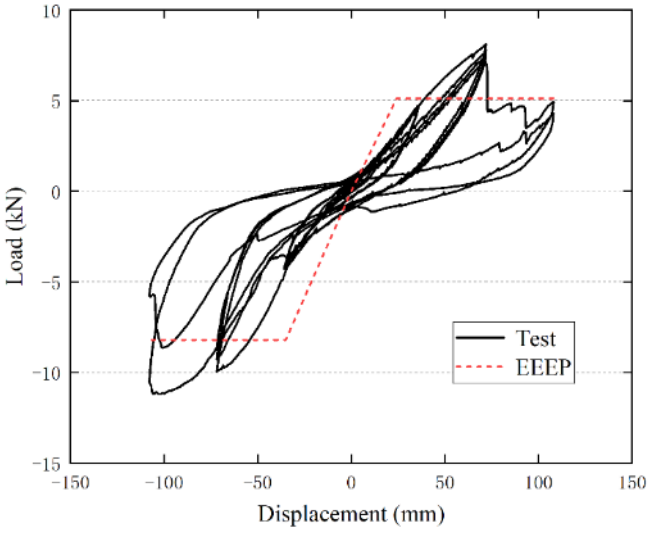
(e) S1-PIL-200-V



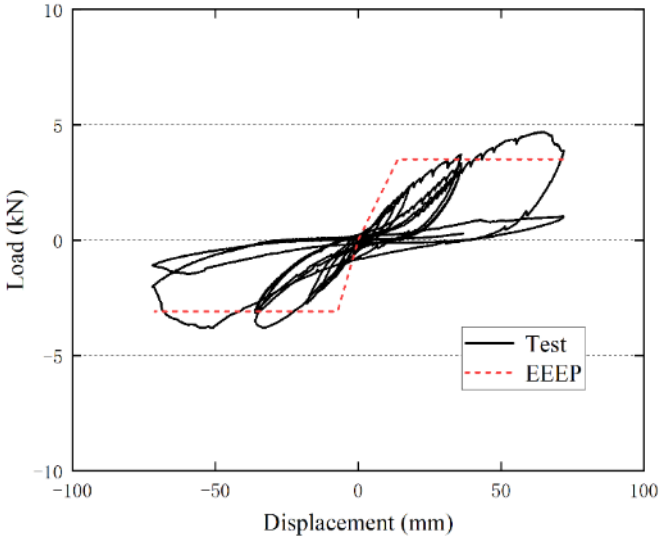
(f) S1-EPL-200



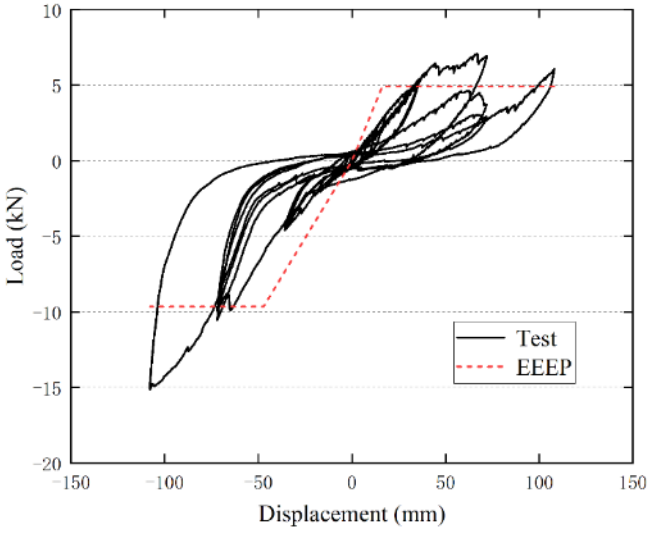
(g) S1-RAB1-200



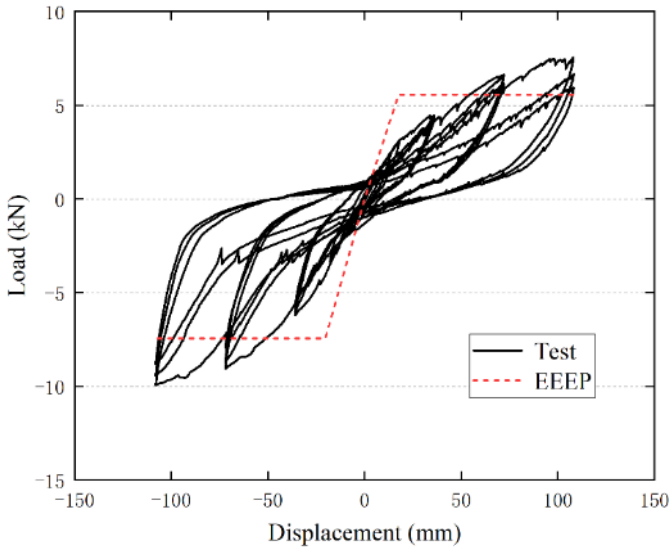
(h) S1-RAB2-200



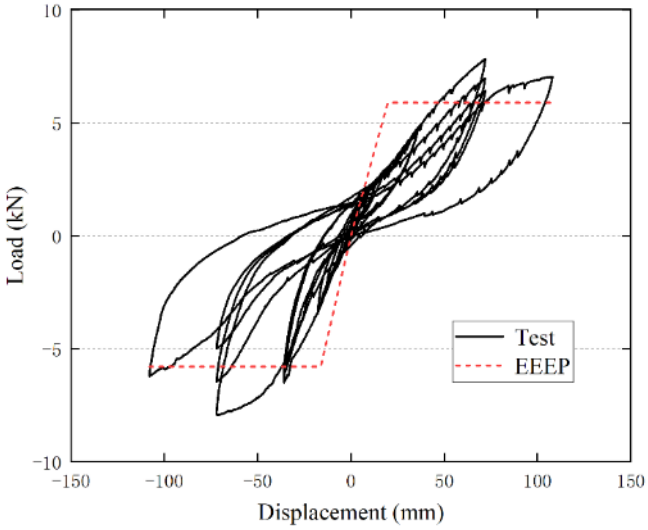
(i) S1-GYP-200



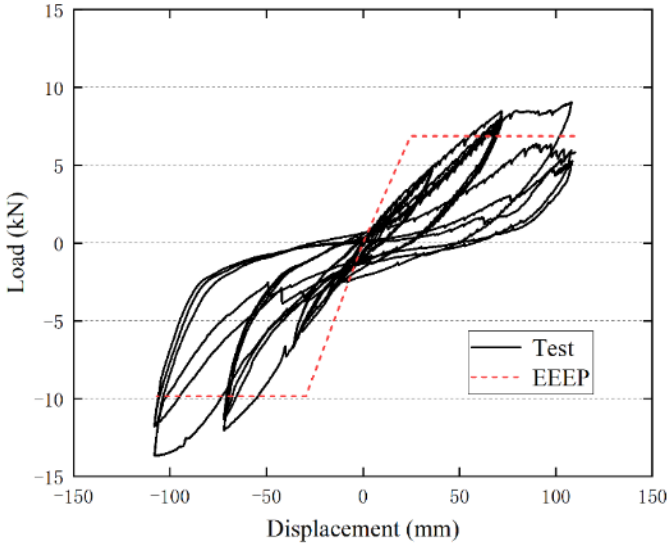
(j) S1-PLY-200



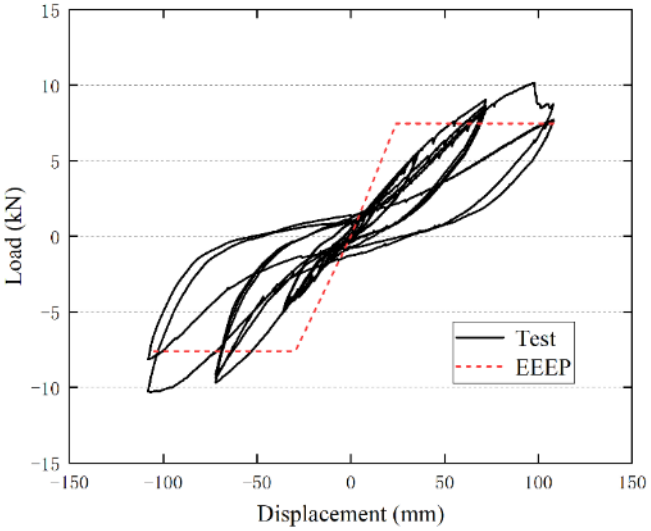
(k) S2-PIL-200



(l) S2-EPL-200



(m)S2-RAB1-200



(n) S2-RAB2-200

Appendix F

A summary of all characteristic parameters under cyclic loading.

Specimen	Direction	P_y (kN)	Δ_y (mm)	Δ_u (mm)	P_{max} (kN)	Δ_{max} (mm)	P_u (kN)	K_0 (kN/mm)	E_d (kJ)	E_{sum} (kJ)
S1-PIL- DE	Push	4.07	60.01	60.01	5.45	52.81	4.36	0.07	0.22	0.68
	Pull	-8.88	-16.47	-59.82	-12.76	-59.82	-10.21	0.54	0.46	
S1-PIL-100	Push	4.86	79.91	79.91	6.32	59.26	5.06	0.06	0.37	1.02
	Pull	-9.50	-20.99	-79.15	-14.20	-76.31	-11.36	0.45	0.65	
S1-PIL-150	Push	6.53	108.09	108.09	6.27	70.31	5.02	0.06	0.45	1.26
	Pull	-8.72	-29.61	-107.89	-12.43	-107.89	-9.94	0.29	0.81	
S1-PIL-200	Push	3.34	107.76	107.76	4.36	107.76	3.49	0.03	0.34	1.08
	Pull	-7.47	-16.05	-106.76	-10.96	-105.76	-8.77	0.47	0.74	
S1-PIL-200-V	Push	4.61	72.15	72.15	6.75	72.15	5.40	0.06	0.27	0.84
	Pull	-8.39	-6.22	-71.18	-10.84	-56.18	-8.67	1.35	0.57	
S1-RAB1-200	Push	7.09	107.26	107.26	10.06	107.26	8.05	0.07	0.66	1.36
	Pull	-7.36	-26.88	-107.99	-10.69	-87.00	-8.55	0.27	0.70	
S1-RAB2-200	Push	5.12	107.95	107.95	8.12	72.00	6.50	0.05	0.49	1.22
	Pull	-8.21	-35.02	-106.57	-11.20	-102.36	-8.96	0.23	0.73	
S1-EPL-200	Push	5.97	107.89	107.89	8.05	106.09	6.44	0.06	0.57	1.08
	Pull	-5.23	-18.83	-107.88	-8.23	-72.09	-6.58	0.28	0.51	
S1-GYP-200	Push	3.51	71.66	71.66	4.70	64.99	3.76	0.05	0.23	0.44
	Pull	-3.09	-7.21	-71.29	-3.80	-33.54	-3.04	0.43	0.21	
S1-PLY-200	Push	4.92	107.91	107.91	7.07	66.61	5.66	0.05	0.49	1.30
	Pull	-9.65	-47.19	-107.76	-15.13	-107.76	-12.10	0.20	0.81	
S2-PIL-200	Push	5.56	107.91	107.91	7.55	107.91	6.04	0.05	0.55	1.28
	Pull	-7.43	-20.26	-107.91	-9.92	-107.91	-7.94	0.37	0.73	
S2-RAB1-200	Push	6.87	109.45	109.45	9.07	108.09	7.26	0.06	0.67	1.57
	Pull	-9.85	-29.63	-106.76	-13.66	-106.76	-10.93	0.33	0.91	
S2-RAB2-200	Push	7.47	108.02	108.02	10.15	97.77	8.12	0.07	0.72	1.42
	Pull	-7.60	-29.60	-106.76	-10.31	-106.56	-8.25	0.26	0.70	
S2-EPL-200	Push	5.89	106.74	106.74	7.82	71.95	6.26	0.06	0.57	1.15
	Pull	-5.79	-16.15	-107.92	-7.93	-70.76	-6.34	0.36	0.58	

Appendix G

Representative failure modes under cyclic loading.



(a) Localised cracking along the bottom edge of gypsum board

(b) Bottom-edge fracture and fastener-related damage in gypsum board

(c) Localised bottom-edge damage in plywood sheathing

Figure G-1 Localised failure modes in gypsum- and plywood-sheathed walls.



(a) RAB1 stud buckling and screw failure

(b) PIL stud and tensile corner damage

(c) Frame bottom screw pull-out

Figure G-2 Frame- and connection-dominated failure modes in selected sheathed CFS wall specimens.



(a) Distributed panel deformation in RAB2 sheathing



(b) Progressive panel deformation in PIL sheathing



(c) Panel deformation without connection failure in RAB1 sheathing



(d) Corner tearing associated with panel deformation in EPL sheathing



(e) Global panel bending in RAB1 sheathing



(f) Distributed surface deformation in PIL sheathing

Figure G-3 Panel deformation–dominated failure modes in sustainable composite sheathing.



(a) Localised connection separation in plywood sheathing

(b) Localised separation near fasteners in RAB1 sheathing board

(c) Progressive connection separation in PIL sheathing

(d) Connection separation and panel detachment in EPL sheathing

Figure G-4 Connection-dominated separation in plywood and sustainable composite sheathing.

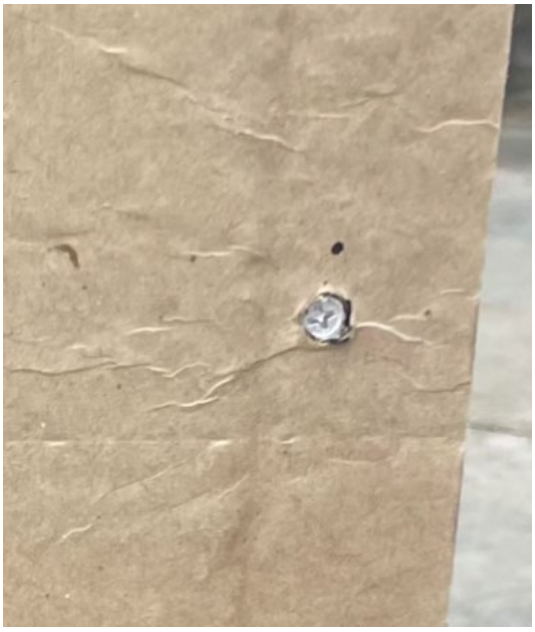
Appendix H

Derived and normalised lateral performance parameters of sheathed CFS wall specimens.

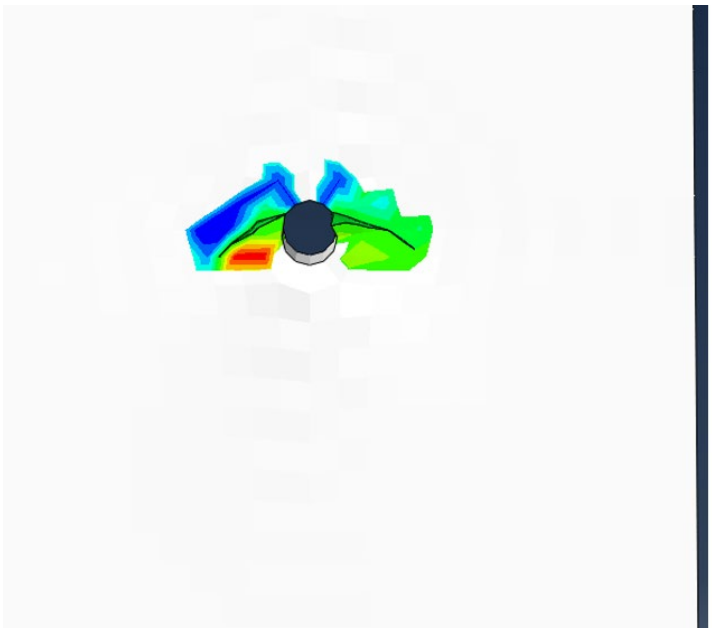
Specimen	$P_{\max_avg}$ (kN)	E_{avg} (kJ)	$\frac{P_{\max_avg}}{t}$	$\frac{K_0}{t}$	$\frac{E_{avg}}{t}$	$\frac{P_{\max_avg}}{Et^3}$ $(\times 10^{-6})$	$\frac{K_0}{Et^3}$ $(\times 10^{-6})$	$\frac{E_{avg}}{Et^3}$ $(\times 10^{-6})$
S1-PIL- DE	9.11	0.34	0.91	0.0068	0.0340	85.90	0.64	3.21
S1-PIL-100	10.26	0.51	1.03	0.0061	0.0510	96.79	0.57	4.81
S1-PIL-150	9.35	0.63	0.94	0.0060	0.0631	88.21	0.57	5.95
S1-PIL-200	7.66	0.54	0.77	0.0031	0.0540	72.26	0.29	5.09
S1-PIL-200-V	8.80	0.42	0.88	0.0064	0.0420	82.97	0.60	3.97
S1-RAB1-200	10.38	0.68	0.86	0.0055	0.0565	45.62	0.29	2.98
S1-RAB2-200	9.66	0.61	1.38	0.0068	0.0873	225.31	1.11	14.25
S1-EPL-200	8.14	0.54	0.81	0.0055	0.0541	78.65	0.54	5.22
S1-GYP-200	4.25	0.22	0.43	0.0049	0.0218	1.91	0.02	0.10
S1-PLY-200	11.10	0.65	0.93	0.0038	0.0543	0.80	0.00	0.05
S2-PIL-200	8.74	0.64	0.87	0.0052	0.0640	82.41	0.49	6.03
S2-RAB1-200	11.37	0.79	0.95	0.0052	0.0656	49.98	0.28	3.46
S2-RAB2-200	10.23	0.71	1.46	0.0099	0.1011	238.60	1.61	16.51
S2-EPL-200	7.88	0.58	0.79	0.0055	0.0575	76.09	0.53	5.56

Appendix I

Representative qualitative FE deformation patterns compared with experimental observations.



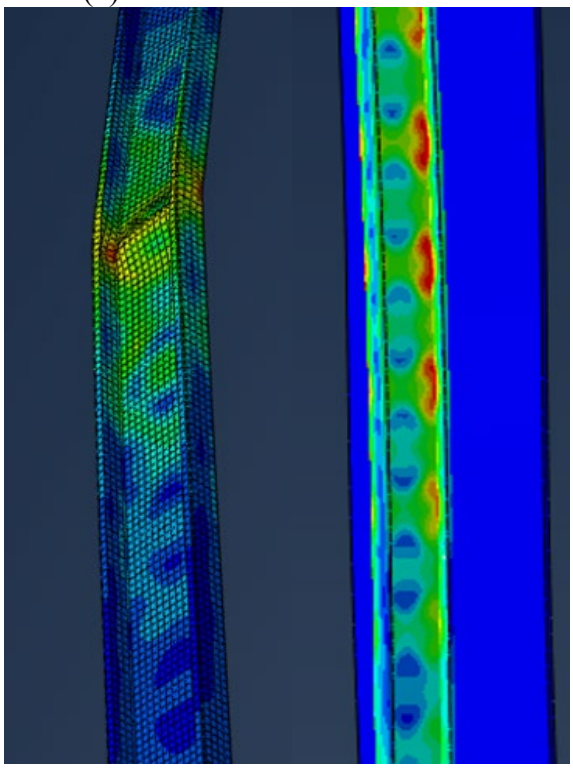
(a) Experimental screw connection results



(b) FE screw connection results

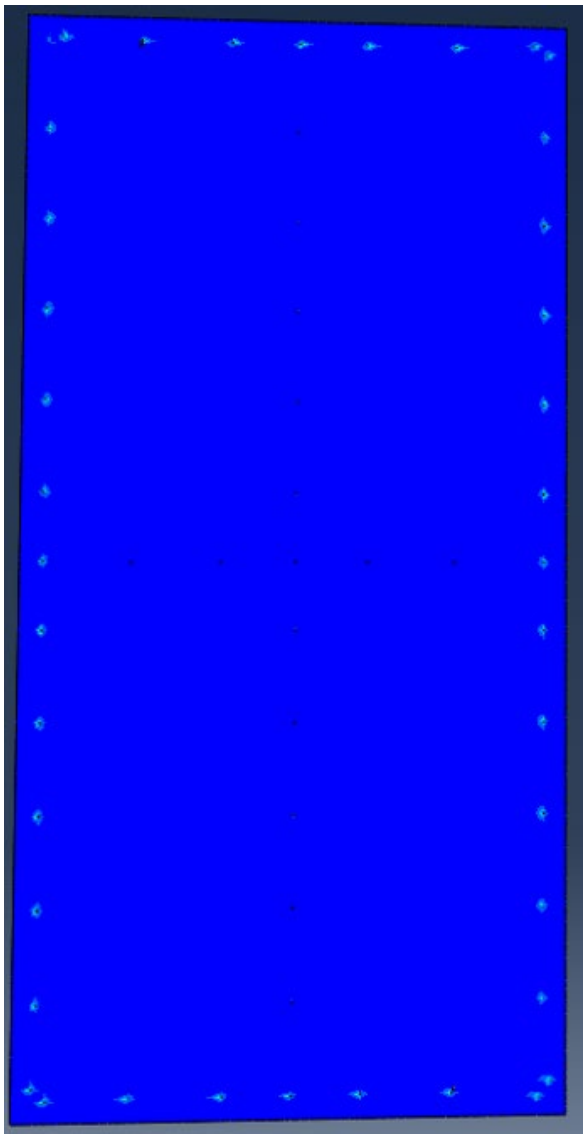


(c) Experimental vertically loaded results



(d) FE vertically loaded results





(e) Experimental cyclically loaded results (f) FE cyclically loaded results

Figure I -1 Representative qualitative comparisons of experimental observations and finite element deformation patterns under different loading conditions.